EFFECTS OF BACKMIXING ON CONCENTRATION PROFILES IN A PULSE COLUMN

By

BILL EDWARD CLAYBAUGH

Bachelor of Science

University of Tulsa

Tulsa, Oklahoma

1953

Master of Science

Oklahoma State University

Stillwater, Oklahoma

1959

Submitted to the faculty of the Graduate School of the
Oklahoma State University in partial fulfillment
of the requirements of the degree of
DOCTOR OF PHILOSOPHY
August, 1961

EFFECTS OF BACKMIXING ON

CONCENTRATION PROFILES

IN A PULSE COLUMN

Thesis Approved:

John B. West
Thesis Advisor

R. N. Maddox

Joseph M. Marchello

Wayne C. Edmister

Earl E. Marshall

Dean of the Graduate School

PREFACE

The interpretation of experimental mass-transfer data from vertical contacting towers has, in the past, been somewhat limited by inadequate representation of the concentration driving forces involved. In a McCabe-Thiele type diagram, these driving forces are indicated by distances between the operating line and the equilibrium distribution curve, the operating line being calculated or determined graphically from solubility relations (the binodal solubility curve) and operating conditions. The classic assumption in all cases is that both the raffinate and the extract phases pass through the vertical contactor in plug flow, i.e., there is no backmixing of either phase.

Recently, the mass transfer of large amounts of solute against the direction of bulk flow has been recognized, and the phenomena has been characterized by the use of eddy diffusivities. The backmixing in either or both phases causes a decrease in the concentration driving forces at all points in the vertical contactor and precludes the use of ordinary calculation methods.

A new calculation method that circumvents the above deficiency has been proposed recently by T. Miyauchi. The calculation method is based on a simplified mathematical model that describes concentration profiles within vertical contactors and utilizes eddy diffusivities to characterize the backmixing.

This investigation was initiated to study backmixing in a pulse

column and to ascertain the effect of backmixing on concentration profiles. The applicability of the concentration profile calculation techniques of Miyauchi was also to be investigated. In the initial portion of this study, backmixing in the continuous phase of five two-phase equilibrated systems was experimentally determined. A simplified mathematical backmixing model was developed to aid in the interpretation and the extrapolation of these data. The backmixing results were used to predict the concentration profiles during extraction on three ternary systems at diverse operating conditions.

A second simplified mathematical model was developed in this study to describe mass transfer at the column interface. The resulting boundary condition was used to improve the theoretical concentration profile calculations.

There are many to whom I am indebted for their aid and encouragement during the course of this study. Professors J. B. West, R. N. Maddox, W. C. Edmister, J. M. Marchello, D. Cornell, J. R. Norton, and L. M. Reed must be specifically recognized as materially aiding in the progress of this research and in the overall graduate program. It is impossible to express the value of the encouragement received from my fellow graduate students during this research program; I will simply give my deepest thanks to A. Amir-Yeganeh, R. E. Thompson, and D. M. Groves.

I am most grateful for the personal financial assistance received through Continental Oil Company Fellowships during the last two years of graduate study.

To my wife, Marian, I owe an unending debt for her assistance and understanding during these many years of study.

TABLE OF CONTENTS

TABLE OF CONTENTS (Continued)

LIST OF TABLES

LIST OF TABLES (Continued)

LIST OF ILLUSTRATIONS

LIST OF ILLUSTRATIONS (Continued)

CHAPTER I

INTRODUCTION

The field of mass transfer, and specifically the area of vertical liquid-liquid contacting towers, has received widespread investigation over many years. Despite this fervor, this area of investigation is still in the stages of infancy. The literature does contain numerous reports of commercial, pilot, and bench-scale extraction units and their operational characteristics, but, of necessity, these reports deal with specific systems under specific conditions. Generalization of the experimental information has been difficult if not impossible. Within this maze of information and technology lie very few reliable techniques which are directly applicable to column design or scale-up. This is especially true where uncommon liquid systems are involved.

One of the principal difficulties in the commonly-used calculation methods is in proper representation of the concentration driving forces within the column. A common method is to use a logarithmic mean concentration difference, analogous to the logarithmic mean temperature difference in the field of heat transfer. In this type calculation, only the initial and terminal stream concentrations are utilized. A second common method is the McCabe Thiele type graphical solution for the number of theoretical stages, in which the operating line is obtained graphically from a triangular plot of the binodal curve or is assumed to be linear. In either of these cases, slug flow of both streams is assumed.

The assumption of slug flow of both phases may apply reasonably well to gas-liquid systems where well-irrigated plates are utilized, but the extension of this concept to liquid-liquid systems may constitute a grave error. The over-all mass-transfer coefficients, number of transfer units, or number of theoretical stages which are calculated by this technique must absorb any of the error present in the assumed concentration profiles. The final result is extreme difficulty in equipment design or scale-up unless strong reliance is placed on previous experience.

It was not until 1952 that Newman (27) stated clearly the significance of backmixing within vertical contacting towers and its effect on concentration profiles. In 1957, Miyauchi (26), and then Sleicher (33), published very similar theoretical studies describing the effects of backmixing within vertical contacting towers. The theoretically-derived equations (based on simplified mathematical models) involved two turbulence parameters, the longitudinal eddy diffusivities of the continuous and of the dispersed phases. These parameters supposedly could account for backmixing within the phases and thus allow the resulting concentration gradients to be more nearly correct.

Backmixing in a pulse column, as characterized by longitudinal eddy diffusivities, has thus far received only superficial examination (23), (38), (39). These examinations were statistical or exploratory in nature and formed no real basis for the theoretical examination of backmixing.

The present investigation was undertaken to examine backmixing within a pulse column and to develop some understanding of the phenomenological occurrences that affect it. Fluid physical properties and

various conditions of pulsation and flow were examined. The experimental observations contained herein provide strong argument for a backmixing model that was developed in conjunction with the experimental examination.

The concentration profiles of both liquid phases were determined experimentally for ten mass-transfer runs involving three different three-component systems. Solute was transferred both to and from the continuous phase and operation was in both the mixer-settler and the emulsion regions. The experimental concentration profiles so obtained were compared with concentration profiles which were calculated from the simplified mathematical model of Miyauchi. The continuous phase eddy diffusivities which were determined in the initial phase of this study were utilized.

A mathematical model which describes mass transfer occurring at the pulse column interface was developed during this study; the resulting boundary condition was applied to the backmixing model of Miyauchi. Again, a direct comparison of the theoretical and experimental concentration profiles was possible. In the application of the mass-transfer boundary condition to the Miyauchi backmixing model, a redefinition of two dimensionless concentration ratios was made. This extended the utility of the equations to more concentrated solutions in which the linear equilibrium distribution curve had a non-zero intercept.

CHAPTER II

REVIEW OF THE LITERATURE

Axial Eddy Diffusion

Turbulent transport of material against the direction of bulk movement is termed backmixing. For a continuous phase flowing down an extraction column, this backmixing would be exemplified by axial or longitudinal mixing of solute up the column, against the direction of bulk flow. According to Sleicher (33), axial mixing is the result of two phenomena.

> The first is true turbulence and molecular diffusion in the axial direction.... Second, axial mixing is caused by non-uniform velocity and subsequent radial mixing, which is sometimes called Taylor's diffusion after G. I. Taylor's analysis of axial mixing in pipes.

As pointed out by Sleicher, the first of these effects can be determined by upstream measurements of a tracer material continuously discharged from a point source. The sum of the two effects is correctly determined by downstream measurement techniques such as the frequency response technique, the pulse injection method, and the step function method.

The effects of turbulent mass transport have for many years been treated in the manner found successful for molecular transport, i.e., by use of the eddy diffusion coefficient. An excellent article on mass transport and its analogous phenomenon in the field of heat and momentum transport is given by T. K. Sherwood (31). The Fick's-first-law statement for mass transfer in the longitudinal direction that involves both

molecular and eddy diffusion is

$$dn_L/dt = -(D_L + E_L)\, dc/dz \qquad (1)$$

For the radial direction, it is

$$dn_r/dt = -(D_r + E_r)\, dc/dr \qquad (2)$$

Where turbulence and diffusion are isotopic, $D_L = D_r$ and $E_L = E_r$. Several investigations of both axial and radial eddy diffusion have appeared in the past ten years.

The point source technique was used by Gilliland and Mason (17) in 1949 to study turbulence of gas in a fluidized bed. Gas samples (air with helium tracer) were taken axially and radially, both up and down stream from the point of injection. The upstream longitudinal backmixing data were correlated by the equation

$$\ln c/c_o = -(F_c/E_c)z + B \qquad (3)$$

where c = concentration of the tracer at any point, z

c_o = concentration of the effluent stream

F_c = superficial velocity of the continuous phase, ft./hr.

z = positive distance up from the point of tracer injection, ft.

E_c = eddy diffusivity for the continuous phase, $ft.^2/hr.$

B = the value of $\ln c/c_o$ at z equal to zero.

Equation (3) was obtained by integration of Equation (1) for constant superficial velocity, constant eddy diffusivity, and negligible molecular diffusivity. Experimental radial concentration data indicated a

very flat profile upstream. The downstream profile was markedly concentrated near the middle of the three inch diameter bed.

A second investigation by Gilliland and Mason (18) pointed out one primary objection to downstream measurements when using a point source in a gas-solid study. It was found that gases pass upward through the fluidized bed "...both in the form of bubbles and by flowing through voids between the solid particles." The gases flowing in the voids were the primary recipients of the injected tracer gas and were also the primary source of the gas which was sampled. The resulting downstream experimental concentration profiles were abnormally high in solute concentration.

The upstream longitudinal diffusivity data of Gilliland and Mason were free of the above described effect and were correlated by equations of the form

$$\ln E_c = b_1 \ln F_c \rho_b + b_2 \qquad (4)$$

where ρ_b was the fluidized bed density and b_1 and b_2 were dependent on the fluidized particles. The values of eddy diffusivities obtained ranged from 1.5 down to 0.1 ft.^{2}/hr.

The first examination of backmixing in a pulse column was by Swift and Burger (38), (39) in 1953. The point source technique was used in a two-inch-diameter pulse column, 27.5 inches in length. A kerosene-type material was dispersed in water and manganous sulfate was used as the tracer. Samples of the aqueous phase were siphoned from the column upstream from the tracer injection point. On the basis of seven runs under various plate spacings, flow rates, and pulsing conditions, these

investigators concluded that

Backmixing was found to be surprisingly insensitive to all of the above variables [pulse frequency, amplitude, plate spacing, volume flow ratio, and throughput] with the exception of pulse amplitude and continuous-phase flow rate, showing greatest dependence on the latter. Backmixing increased with decreasing continuous-phase flow rate and increased with pulse amplitude.

The data Swift and Burger are included in Table IX, Appendix B.

Marr and Babb (23) recently attempted to define and evaluate the variables affecting pulse-column backmixing by a statistical study involving seven variables. These were:

f, pulse frequency,	30 to 60 cycles/min.
a, pulse amplitude,	0.5 to 1.0 in.
F_c continuous-phase superficial velocity,	200 to 710 ml./min.
F_d dispersed-phase superficial velocity,	300 to 500 ml./min.
t, plate thickness,	0.032 to 0.125 in.
I, plate spacing,	3 to 6 in.
d, hole diameter,	0.0625 to 0.125 in.

One-eighth replicates were run on a 2^7 factorially-designed experiment on each of three systems [$(1/8) \times 2^7 \times 3 = 48$ total runs]. The three systems employed were hexane-water, benzene-water and carbon tetrachloride-water.

The pulse column used by Marr and Babb was two inches in diameter, five feet in length, and utilized three-inch borosilicate glass tees as column end-sections. Stainless-steel plates with 23 per cent free area were used. A point source of ferric nitrate tracer solution was injected midway in the column and samples were removed upstream by hypodermic needles inserted through polyethylene plate gaskets.

The data were correlated by evaluation of exponents in an equation

obtained by dimensional analysis. Equation (5) was reported to give eddy diffusivities that "...had an average deviation of 17% from experimental values."

$$\frac{E_c}{F_c\, d} = 0.17 \left[\frac{\mu_c}{\rho_c F_c t}\right]^{1.45} \left[\frac{t}{d}\right]^{0.70} \left[\frac{I}{t}\right]^{0.68} \left[\frac{F_d \rho_c t}{\mu_c}\right]^{0.30}$$

$$\left[\frac{\gamma \rho_c t}{\mu_c^2}\right]^{0.42} \left[\frac{f \rho_c t^2}{\mu_c}\right]^{0.36} \left[\frac{a}{t}\right]^{0.07} \qquad (5)$$

Equation (5) only applied to water as the continuous phase and hence was simplified to

$$E_c = K\, I^{0.68}\, F_d^{0.30}\, a^{0.07}\, d^{0.30}\, \gamma^{0.42}\, F_c^{-0.45}\, t^{-0.05}\, f^{0.38} \qquad (6)$$

The constant K is apparently equal to $0.17\, \mu_c^{-0.07}\, \rho_c^{0.37}\, t^{-0.01}$.

A few exploratory runs were also described by Marr and Babb and are of interest here. Four polyethylene plates were inserted in the pulse column just above the tracer injection point. These plates gave values of E_c almost twice those obtained with only stainless steel plates. Also, a twenty weight per cent aqueous solution of sucrose was used as continuous phase with hexane dispersed. Viscosity of the sugar solution was twice that of water. "The F_c/E_c values were 25% lower for the sucrose solutions than for pure water."

In a cursory examination of column geometry, perforated plates at 1.5- and 3.0-inch spacing were included in the same pulse column. The

plates contained holes of 0.0625 and 0.125 inches diameter, respectively. Eddy diffusivity values were found to be 3 to 4 times greater in the region of the wider plate spacing; however, no attempt was made to separate the effects of the two variables (plate spacing and hole diameter).

The majority of backmixing studies have dealt with packed columns. The frequency response technique has found widest application (8), (24), (35). More recently the pulse function (5), (8), and the step function, (4), (19), have been used. The recent article by Cairns and Prausnitz includes a comprehensive evaluation of much of the packed column data previously reported. The results of several investigators, including observations on both gases and liquids, were brought into reasonable agreement with a correlation similar to Equation (4) of Gilliland and Mason. Cairns and Prausnitz plotted ln E as a function of $\ln[4m(F/\epsilon)]$ where m is a hydraulic radius, ϵ is the fraction voids and F is superficial velocity. The hydraulic radius, m, is equal to the free volume of the fluid divided by the wetted area. The correlation might be represented for mental visualization by the equation

$$\ln E = 2 + 0.8 \ln[4m(F/\epsilon)] \qquad (7)$$

where E and $4m(F/\epsilon)$ have units of $cm.^2/sec.$

One point is of special interest here. Cairns and Prausnitz make the following statement, which is based on the experimental work of Ebach and White (8) and on the fact that no models or theories have postulated that eddy diffusivities, E, are viscosity dependent: "...it does not appear appropriate to plot eddy diffusivity versus Reynolds number since the eddy diffusivity is in no way dependent on the kinematic viscosity."

Concentration Profiles

The first published statements which recognized the effects of backmixing in liquid-liquid extraction columns were made by M. L. Newman (27) in 1952. At that time he proposed an alternate explanation for the experimental observations of Geankoplis and co-workers (15), (16).

Geankoplis and Hixson (15) obtained continuous-phase concentration profiles in a spray column 2.57 feet in length and 1.448 inches in diameter. The extraction system used was isopropyl ether-ferric chloride-aqueous hydrochloric acid, with transfer being from the continuous aqueous phase. Internal samples were withdrawn at 3.3 per cent of the continuous-phase rate by use of a five-millimeter glass tube inserted into the column from the top. The continuous-phase profile revealed a sharp decrease in the solute concentration just at the feed entrance. The apparent per cent of extraction taking place in the first 0.167 feet of column length often amounted to 70 per cent of the total. No concentration discontinuity was found at the dilute end of the column. Three different continuous-phase entrance nozzles were used, but all results were similar.

Geankoplis and Hixson demonstrated that changing the contact area of the column interface could not account for the observed discontinuity. Their final conclusions were as follows:

> It seems more than likely that the inlet effect is caused by the inherent turbulence effect of coalescence of bubbles at the interface. Possibly the rate of formation of the bubbles at the ether nozzle may exceed the normal rate at which the bubbles can coalesce. Furthermore, the inlet effect may be a function of interfacial tension and also a large amount of extraction.

Geankoplis, Wells, and Hawk (16) performed experiments similar to

those just described but with a 62.5-inch-long spray column of 3.75 inches diameter. The toluene-acetic acid-water system was used, solute being transferred from the dispersed toluene phase. This column geometry, direction of mass transfer, and the high interfacial tension system also gave a continuous-phase concentration discontinuity as was previously noted. Due to the reverse direction of mass transfer, this discontinuity was, of course, a rapid concentration increase.

A concentration profile for the dispersed raffinate phase was calculated and was based on the apparent amount of solute transferred to the continuous phase. These calculations indicated a sharp decrease in the solute concentration of the raffinate phase just at the point of coalescence.

Newman (27), in his correspondence through Industrial and Engineering Chemistry, suggested that Geankoplis et. al. "...failed to realize the true significance of the observations they had made." He suggested "vertical mixing" of the continuous phase as the probable explanation for the "end effects" noted. He also pointed out that the method used for calculation of the dispersed-phase concentration profile was invalid.

Recently, Eguchi and Nagata (10) measured continuous phase profiles in a pulse column. The methyl isobutyl ketone-acetic acid-water system was used; transfer was from the dispersed organic phase. The column was 5.8 cm. in diameter and 55 cm. in height. Nine plates of 8.1 per cent free area and holes of 1.5 mm. diameter were spaced at 5.2 cm. intervals. The column was operated at organic flow rates of 0.18 to 0.38 $cm.^3/sec. cm.^2$ and aqueous flow rates of 0.14 to 0.44 $cm.^3/sec. cm.^2$. Flow rate ratios, F_d/F_c, varied from 0.70 to 1.50. Pulse amplitudes ranged from

0.1 to 0.85 cm. with pulse frequencies from 30 to 200 cycles per minute.

The continuous phase was sampled with glass lines which were built into the glass spacers separating the plates. Samples were withdrawn near the column wall, just below and above each plate. The data indicated that a finite increase in concentration of the continuous phase occurred as it passed through a plate. The resulting plots of continuous-phase concentration as a function of column position were stair-step in appearance.

In 1957, Miyauchi (26) presented a simplified model from which equations were derived to express concentration profiles in continuous-flow vertical contactors. Longitudinal backmixing of both streams was expressed in terms of the respective eddy diffusivities. The basic equations constitute a continuity statement for the solute in a horizontal differential cross-section of the column. For steady state conditions, these were

$$\epsilon_x E_x \left(\frac{\partial^2 c_x}{\partial z^2}\right) - F_x \left(\frac{\partial c_x}{\partial z}\right) - K_x a\ (c_x - c_x^*) = 0 \qquad (8)$$

$$\epsilon_y E_y \left(\frac{\partial^2 c_y}{\partial z^2}\right) + F_y \left(\frac{\partial c_y}{\partial z}\right) + K_x a\ (c_x - c_x^*) = 0 \qquad (9)$$

In dimensionless form,

$$\left(\frac{\partial^2 C_x}{\partial Z^2}\right) - P_x B \left(\frac{\partial C_x}{\partial Z}\right) - N_{ox} P_x B\ (C_x - C_x^*) = 0 \qquad (10)$$

$$\left(\frac{\partial^2 C_y}{\partial Z^2}\right) + P_y B \left(\frac{\partial C_y}{\partial Z}\right) + N_{oy} P_y B\ (C_x - C_x^*) = 0 \qquad (11)$$

Dimensionless boundary conditions for the two streams at Z = 0 were given as

$$(\partial C_{xo}/\partial Z) = -P_xB(1-C_{xo}) \tag{12}$$

$$-(\partial C_{yo}/\partial Z) = 0 \tag{13}$$

and

$$C_x^0 = 1 \tag{14}$$

At the extract entrance, Z = 1, the boundary conditions were given as

$$-(\partial C_{y1}/\partial Z) = P_yB(C_{y1}-C_y^1) \tag{15}$$

and

$$-(\partial C_{x1}/\partial Z) = 0 \tag{16}$$

Equations (10) and (11) were solved analytically for one general and eleven special cases involving different combinations of infinite, finite, and zero backmixing of both phases. Special consideration was also given to cases where the absorption factor, Λ, was equal to unity. Two cases of interest in this study are treated in detail in Chapter III.

A supplement to the paper of Miyauchi was published in which concentration profiles for both streams were tabulated for numerous values of the four variables P_xB, P_yB, Λ, and N_{ox} (25). Concentrations at distances Z = 0.0, 0.05, 0.15, 0.50, 0.85, 0.95, and 1.0 are given for both phases.

Sleicher (33), just shortly after Miyauchi, published material balance and boundary condition equations equivalent to those given above.

A solution for the general case of finite backmixing in each phase was obtained using dimensionless ratios that were similar to those of Miyauchi.

Extraction Efficiency

A great many articles on pulse-column operation have appeared in the literature since the original unclassified publication of Cohen and Beyer (7). The majority of studies reported have dealt with extraction efficiency as a function of operating conditions. Efficiencies were expressed in terms of transfer units, theoretical plates, or over-all mass-transfer coefficients. In all cases, plug flow of both phases was assumed. A few of the more pertinent observations will be listed below.

Perhaps the most revealing and influential article to appear early in pulse column studies was by Sege and Woodfield (29). Data reported on the tributyl phosphate-uranyl nitrate-aqueous nitric acid system indicated two general trends in heights of transfer units (HTU). At constant flow rate sums, the HTU values decreased with an increase in the a-f product, went through a minimum and then rose slightly as emulsion flooding was approached. This same trend was noted by Cohen and Beyer (7) in an earlier study.

The second trend that appeared was the effect of the flow rate sum, G/L, on the HTU at a constant pulse volume velocity, $2V_p$. In general, the flow rate sum had little effect except at high or at low values, for which conditions the HTU increased slightly.

It is of interest to note that the HTU minimum at a constant flow rate sum was also observed by A. E. Karr (20) in a reciprocating plate

column. This column contained plates with 5/8-inch holes and a free area of 62.8 per cent. The methyl isobutyl ketone-acetic acid-water and the o-xylene-acetic acid-water systems were used. It was noted by Karr that this column exhibited no insufficient pulsation flooding due to the plate geometry employed.

A statistical evaluation of the effects of plate spacing, hole diameter and per cent free area on the $(HTU)_{oe}$ was conducted by Burkhart and Fahien (3). Two levels of each parameter, as well as two levels each of pulse amplitude and pulse frequency, were studied. Hole diameter (1/32 and 1/16 inch) was found to be significant at the 99 per cent confidence level for all levels of pulsation. Plate spacing (1 and 2 inches) was significant at low pulsing conditions, and plate free area (13 and 25 per cent) at high pulsing conditions. Extraction efficiency, as exemplified by the $(HTU)_{oe}$, was presented as a function of the amplitude-frequency product, (a-f). All eight of the curves presented by Burkhart and Fahien exhibited a marked HTU decrease at the lowest a-f value (which was in the mixer-settler region of pulse-column operation). HTU values in general increased, decreased, then increased again as the a-f product was increased.

Fahien and Burkhart explained the increase in the $(HTU)_{oe}$ with increased pulsation on the basis of backmixing. It was observed that contact area, a, increased with increasing pulsation. It was reasoned that the over-all mass-transfer coefficient increased with increasing pulsation due to decreased film thicknesses. If the interfacial area and the over-all mass-transfer coefficient both increased, then the concentration driving force must have decreased in order to have a net decrease in the

mass-transfer rate. The recycle-volume rate equation of Edwards and Beyer (19) was used to estimate the recycle rates present.

Flooding and Holdup

Two distinctly different types of pulse column flooding have been reported. The first type of flooding, that which is most easily described mathematically, is insufficient pulsation flooding. Claybaugh (6), Edwards and Beyer (9), and Swift (37) have derived theoretical equations expressing the flow rate sum in terms of pulsing conditions. The most useful expression is

$$G \neq L = 2\ Aaf \neq b \qquad (17)$$

Equation (18) is the theoretical equation of Swift, but with an intercept constant b added. Claybaugh found in one investigation that the constant b was approximately 14 per cent of the maximum operational value of the flow rate sum. It must be noted that Equation (17) applies only when the continuous phase is withdrawn at a uniform rate and the dispersed phase is continuously injected. Eight other special cases have been treated by Swift (37).

The second type of pulse column flooding, emulsion flooding, is due to excess pulsation. Careful scrutiny of emulsion flooding studies reveals two, or possibly three, definitions of emulsion flooding (6), (29), (40). In general, it can be said that emulsion flooding constitutes an inoperative region of pulse column operation due to excess pulsation.

There have been no purely-theoretical expressions published for emulsion flooding. The most accurate and reliable method of data

correlation is that of Swift (37).

$$\ln (F_c \neq F_d)S_1 = C_2 \neq C_1(af)S_2 \qquad (18)$$

where F_c = Superficial velocity of the continuous phase

F_d = Superficial velocity of the dispersed phase

S_1 = $F^{0.34}/d^{0.60}$

S_2 = $d^{0.28}/I^{0.32}F^{0.82}$

C_1 and C_2 = Empirical physical property terms

F = Plate free area

I = Plate Spacing

d = Plate hole diameter

For a single column and system, the values of S_1, S_2, C_1, and C_2 are fixed.

J. D. Thornton (40) attempted through dimensional analysis and experimentation to describe emulsion flooding in terms of physical properties and column geometry. A review of this work, plus correlation of other available emulsion-flooding data, was made by Smoot, Marr and Babb (34). The data correlation was presented as a nomograph based on the flooding equation of Thornton.

Fractional holdup of the dispersed phase in pulse column operation has been reported by several investigators (11), (21), (40). Holdup during extraction for a pulse column of geometry similar to that used in this study was reported by Eguchi and Nagata (10). Their data were correlated by plotting ln (F_h) as a function of ln $(af/F_d)(1 \neq F_d/F_c)$ yielding a single straight line of negative slope. Holdup values in the range of 2 to 20 per cent were measured.

CHAPTER III

THEORY

To aid in the interpretation and extrapolation of engineering information, it is often expedient, and sufficient, to describe complex physical phenomena by simplified mathematical models. Such a procedure appears necessary when dealing with a system as complex as that existing in a pulse column. The following discussion deals with two mathematical models. The first model describes backmixing occurring in the continuous phase within a pulse column, and the second model deals with mass transfer taking place at the column liquid-liquid interface.

The first model is utilized to predict the effect of pulse column geometric variables as well as operating variables on backmixing. The second model provides boundary conditions which, when applied to the equations of Miyauchi, improve the agreement between experimental and calculated concentration profiles.

Continuous Phase Backmixing Model

Backmixing within a pulse column shall be considered as the result of two interrelated mixing phenomena. The first is mixing within the section between two plates; the second is mixing between sections, through the plates. Eddy-diffusivity values which are derived from fluid samples taken from many sections of the pulse column will be considered the result of both these phenomena.

Turbulence is created within each section of the pulse column by continuous phase flow, dispersed phase droplets, and the applied pulse. The concentration gradients between the perforated plates are affected by the bulk flow of the continuous phase, and the continuous phase which is recycled through the perforated plates.

Recycle Rate

The recycle rate in a pulse column at insufficient-pulsation flooding is zero. Any amount of pulsation above this minimum value merely recycles fluids across the plates. Rewriting Equation (17) to reflect this fact gives

$$V_r = V_r' = V_p - (G \neq L)/2 \tag{19}$$

where V_r and V_r' are the volume rate of recycle, ml./min., across the plate for the down and the up strokes, respectively. Equivalent equations for the volume recycled were given by Claybaugh (6) as

$$V_r = V_p \cos \phi \neq \sqrt{(G - L)/2\pi}(2\phi - \pi) - L \tag{20}$$

and

$$V_r' = V_p \cos \phi \neq \sqrt{(G - L)/2\pi}(2\phi \neq \pi) - G \tag{21}$$

where

$$\phi = \text{arc sin } (G - L)/\pi V_p$$

The above three equations apply to the special case of steady dispersed-phase feed and continuous-phase removal. Equivalent expressions for other flow cases are available through the studies of Swift (38) and of

Claybaugh (6).

Effective Concentration

The concentration and quantity of the continuous phase passing through an arbitrary plate within the pulse column form the basis for the model development. The continuous-phase concentration will be expressed in terms of the apparent concentration profile as described by Equation (3A).

$$\ln c/c_o = -(F_c/E_c)z \tag{3A}$$

The average concentration of the material passing through the plate at point z will be taken as that value on the apparent concentration profile at some distance $z + \Delta z/2$ or $z - \Delta z/2$. These concentrations are

$$c_{z + \Delta z/2} = c_o \exp\left[-(L/A\ E_c)\ (z + \Delta z/2)\right] \tag{22}$$

and

$$c_{z - \Delta z/2} = c_o \exp\left[-(L/A\ E_c)(z - \Delta z/2)\right] \tag{23}$$

where L/A is equal to F_c. A positive z is measured up the column and upstream for the continuous phase; hence, Equation (22) applies to the materials pulsed down through a plate.

Solution for the Eddy Diffusivity

The apparent longitudinal eddy diffusivity of the continuous phase will be determined by a material balance for the tracer material across a plate. The volume of continuous phase passing down through a plate is the bulk flow rate, L, plus the volume recycled, V_r. The volume of continuous phase passing through the plate on the upstroke is equal to

V_r'. The steady state material balance is, thus,

$$(V_r \neq L)\ c_{z \neq \Delta z/2} = (V_r')\ c_{z - \Delta z/2} \tag{24}$$

Substituting Equations (19), (22), and (23) into Equation (24) and solving for E_c gives

$$E_c = L\,\Delta z/A \ln \left[(2V_p - G \neq L)/(2V_p - G - L)\right] \tag{25}$$

Substitution of Equations (20), (21), (22) and (23) into Equation (24) gives

$$E_c = \frac{L\Delta z}{A} \quad \frac{1}{\ln \left[\dfrac{V_p \cos \phi \neq \left(\frac{G-L}{\pi}\right) \phi - \left(\frac{G-L}{2}\right)}{V_p \cos \phi \neq \left(\frac{G-L}{\pi}\right) \phi - \left(\frac{G \neq L}{2}\right)} \right]} \tag{26}$$

For a flow rate ratio of unity, $G = L$, $\cos \phi = 1$, and $(G - L)\phi/\pi = 0$. Equation (26) thus simplifies to Equation (25). Even for flow rate ratios as diverse as those encountered in this examination, 1/9 and 9/1, Equations (25) and (26) give almost exactly the same result. Equation (25) is preferred due to its simplicty.

Applicability of the Model

The pulse-column continuous-phase backmixing model is applicable to any pulse-column operation in which only the continuous phase is recycled through the plates. Specifically, this excludes three types of operation.

(a) Regions in which finite droplets of dispersed phase are recycled through the plate holes. High frequency-low amplitude operation or high holdup could undoubtedly cause

this.

(b) Regions of mixer-settler operation in which the plate is sealed off by a dispersed-phase layer. Some of the coalesced dispersed phase under the plate would move up through the holes on the pulse upstroke, but would not break away from the plate. This would, in actuality, replace some of the continuous-phase recycle with a somewhat stagnant dispersed-phase recycle.

(c) Any dispersed phase coalescing or plate wetting tendencies that may form a layer of semi-stagnet droplets in the plate holes. As before, these would replace some of the continuous phase recycle volume.

Model Utilization

To utilize the backmixing model, one must evaluate the term Δz. The desired way to do this would be to examine mathematically one section of the pulse column and try to predict the concentration profile within that section. Undoubtedly, a second eddy diffusivity could be defined that applied specifically within the section and then experimental concentration profiles within that section would be evaluated to determine the second eddy diffusivity. This path is long and full of pitfalls. The easiest and most direct method is to evaluate Δz by Equation (26) using experimental values of E_c.

There are two primary advantages in correlating Δz instead of E_c directly. The first is that Δz becomes relatively constant at high pulse frequencies. With Δz a constant value, the effects of changes in several operating variables (G, L and $2V_p$) are predictable from Equation (25).

The second advantage is that the effects of plate geometric variables on Δz, [which are not included in Equation (26)] can be postulated more directly than can the corresponding effects on E_c. The following examples are given:

1. Plate Spacing. The model predicts that as plate spacing increases (a) the effect of the fluids entering or leaving each plate is decreased; (b) the concentration profile within a section is flattened; (c) Δz must increase, and (d) E_c increases.
2. Pulse Amplitude. An increase in pulse amplitude will (a) increase the value of $E_c/\Delta z$ due to increased $2V_p$; (b) decrease the concentration gradient within a section due to greater effective pulse distance; (c) increase Δz; and (d) increase E_c.
3. Continuous Phase Flow Rate. An increase in the continuous phase flow rate will (a) decrease the quantity of fluids recycled; (b) decrease the slope of the section concentration profile; (c) decrease Δz and (d) increases $E_c/\Delta z$. The change in E_c is in doubt.
4. Pulse Frequency at Constant $2V_p$. For an increase in pulse frequency at constant pulse volume velocity, the pulse amplitude must be decreased. Also (a) $E_c/\Delta z$ remains constant; (b) the section concentration gradient increases; (c) Δz decreases; and (d) E_c decreased.
5. Pulse Amplitude at Constant $2V_p$. For an increase in pulse amplitude at constant pulse volume velocity the pulse frequency must decrease. The model predicts (a) $E_c/\Delta z$ remains

constant; (b) the section concentration profile decreases; (c) Δz increases; and (d) E_c increases.

6. Pulse Frequency. For an increased pulse frequency, the model predicts (a) decreased concentration gradients within a section; (b) increased values of $E_c/\Delta z$; (c) increased Δz; and (d) E_c increases.
7. Plate Free Area. An increase in plate free area will (a) decrease the discontinuity at the plate; (b) decrease the section concentration gradient; (c) increase Δz; and (d) increase E_c.
8. Hole Diameter at Constant Plate Free Area. An increase in hole diameter at constant plate free area will (a) decrease any tendencies to seal off the plate by dispersed phase; (b) decrease the discontinuity at the plate; (c) decrease the section concentration gradient; (d) increase Δz; and (e) increase E_c.

Specific applications of the continuous-phase backmixing model are demonstrated in Figures 8 and 9, Chapter VI, for the pulse column, flow rates, and pulsing conditions used in this study.

Interface Mass-Transfer Model

The following mathematical model is developed to evaluate the boundary conditions at the liquid-liquid interface within a pulse column. The boundary conditions for a continuous extract phase will be presented in detail; equations for a continuous raffinate phase are also given.

The general nomenclature of Miyauchi will be used in this development

and in its future applications so as to maintain continuity between related works. Some alterations or additions will be introduced as necessary for clarity. The unusual complexity of the nomenclature is shown in Figure 1, in which subscript or superscript numbers are used. Subscript numbers indicate concentrations within the column; superscript numbers indicate concentrations of materials being fed to, or being removed from, the column. The 0, 1, n, and p sub- or super-scripts indicate the concentrated end, dilute end, and equilibrium concentrations respectively, as indicated in Figure 1.

For convenience in the derivations and in calculations, two dimensionless concentration ratios are defined as follows:

$$\phi = \frac{c_x - c_x^p}{c_x^o - c_x^p} = \frac{C_x - C_x^{1*}}{1 - C_x^{1*}}$$

$$\Upsilon = \frac{c_y - c_y^1}{c_y^n - c_y^1} = \frac{1}{K} \frac{C_y - C_y^1}{1 - C_x^{1*}}$$

where

$$C_x^{1*} = (C_y^1 - q/c_x^o)/K$$

The first of these dimensionless ratios, ϕ, represents the fraction of the total possible raffinate extraction that is yet to be accomplished. The second dimensionless ratio, Υ, expresses the fraction of the total permissible concentration increase that has occurred within the extract phase.

Corresponding dimensionless concentration ratios of Miyauchi are $\phi = X$ and $\Upsilon = Y$ if $q = 0$ (26). The corresponding expressions of Sleicher

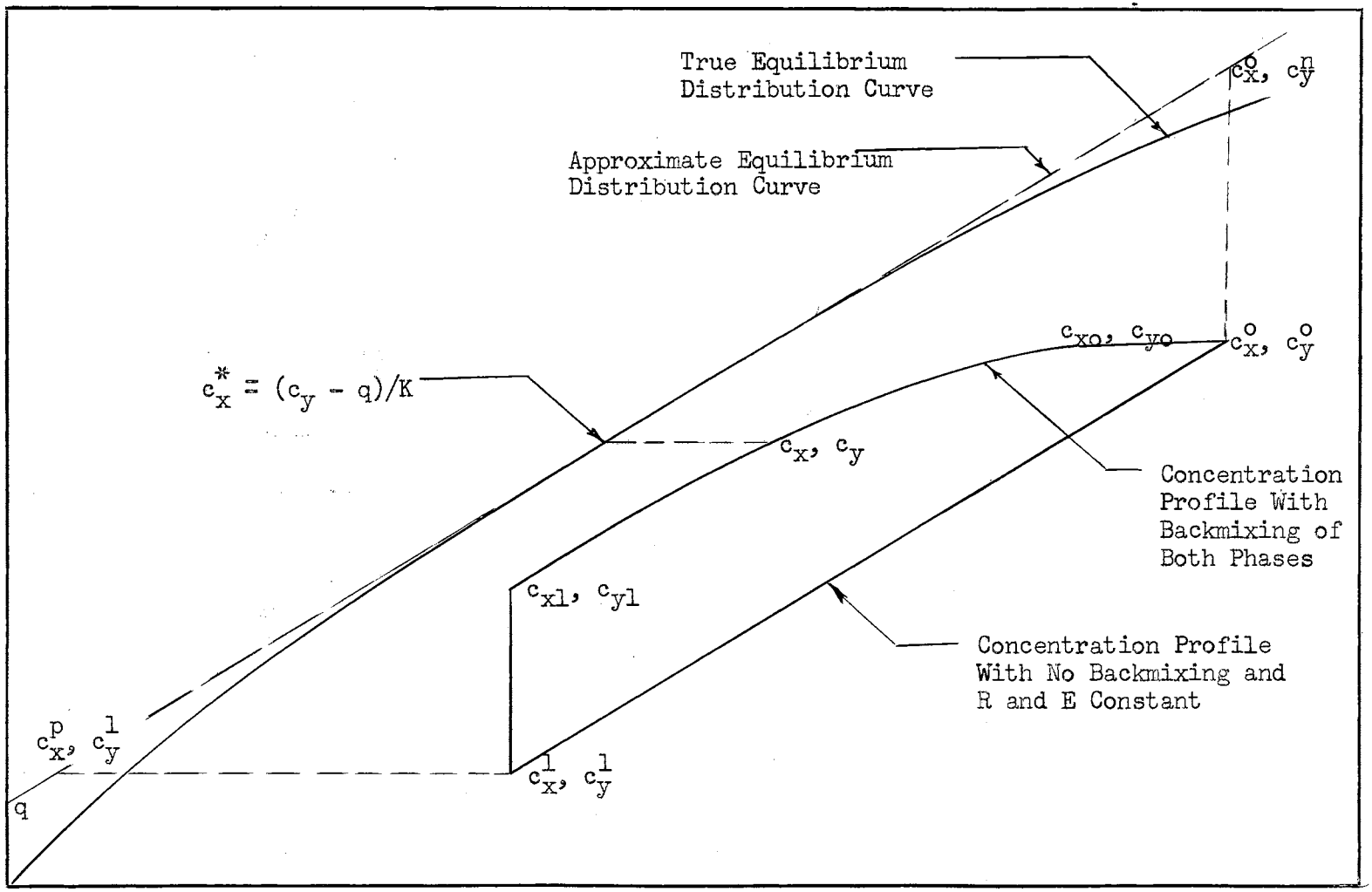

FIGURE 1. NOMENCLATURE EXAMPLE

(33) are

$$\Psi = 1 - X$$

and

$$\top = Y/\Lambda$$

Sleicher erroneously gave this last relation as $\top = 1 - Y$.

To develop the interface mass-transfer model, consider a small cross section of continuous extract phase just below the interface (see Figure 2). Solute is fed into or removed from this volume by the following four mechanisms:

1. Flow of fresh solvent into the column.

$$f_{fi} = F_y \, Ac_y^1 \tag{27}$$

2. Flow of continuous phase out of the volume.

$$f_{fo} = U_y(\epsilon_y A)c_{yl} = F_y A c_{yl} \tag{28}$$

3. Net solute transfer into the volume by the eddy mechanism.

$$f_{ei} = -E_y(\epsilon_y \, A)\left(\frac{\partial c_{yl}}{\partial z}\right) \tag{29}$$

4. Mass transfer across the interface

$$f_{ti} = (K_x a/a)A_b\left[c_{xl} - c_{xl}^*\right] \tag{30}$$

A solute material balance for steady state operation gives

$$f_{fi} + f_{ei} + f_{ti} = f_{fo} \tag{31}$$

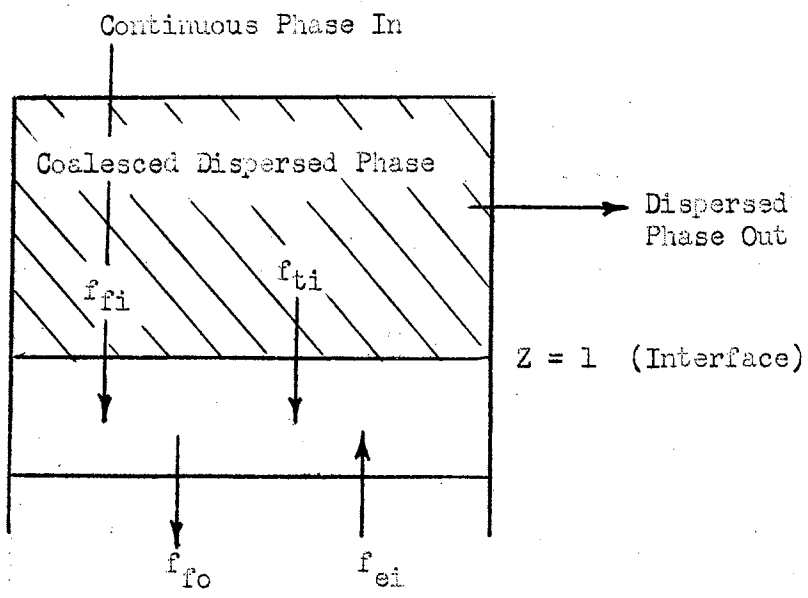

Interface Model - Continuous Extract Phase

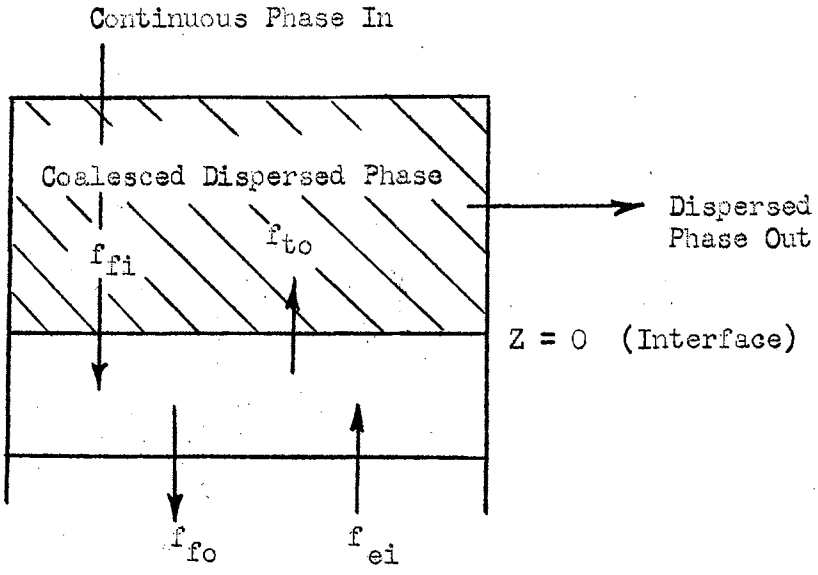

Interface Model - Continuous Raffinate Phase

FIGURE 2. INTERFACE MASS-TRANSFER MODEL

Substituting Equations (27) through (30), into Equation (31), dividing through by $c_x^{\circ} F_y A$, and letting $z = L'Z$ gives

$$C_y^1 - \frac{E_y \epsilon_y}{F_y L'} \left(\frac{\partial C_{y1}}{\partial Z}\right) + \left(\frac{K_x a}{F_y}\right) \left(\frac{A_b}{aA}\right) \left[\bar{C}_{x1} - C_{x1}^*\right] = C_{y1} \qquad (32)$$

Note that $E_y \epsilon_y / F_y L'$ equals $1/P_y B$ and $K_x a / F_y$ equals N_{oy}/L' or $N_{ox} \wedge K/L'$. Rearrangement of Equation (32) gives

$$\left(\frac{\partial C_{y1}}{\partial Z}\right) = -P_y B \left[\bar{C}_{y1} - C_y^1\right] + \left(\frac{N_{ox} \wedge K}{L'}\right) \frac{A_b}{aA} P_y B \left[\bar{C}_{x1} - C_{x1}^*\right] \qquad (33)$$

Equation (33) is the same as Equation (15), Miyauchi's extract phase boundary condition at $Z = 1$, except for the mass transfer term.

The utilization of Equation (33) requires an expression for the effective area of the interface, A_b. Because of the presence of coalescing droplets at the interface, it is not unreasonable to approximate the area in terms of droplet area. Consider an interface with effective interfacial area equal to the surface area of droplets on triangular centers, close-packed in a single layer. The number, n, of droplets of diameter D_b possible on the interface is approximated by dividing the column area by the area of hexagons that have a distance across the flats of D_b.

$$n = (\pi D^2/4)/(\sqrt{3} D_b^2/2) \qquad (34)$$

The effective interfacial area is, thus,

$$A_b = n(\pi D_b^2) = \pi^2 D^2 / 2\sqrt{3} \qquad (35)$$

In addition to A_b, it is necessary to evaluate or estimate the interfacial

area per unit column volume, a. This can be written conveniently in terms of the fractional holdup, F_h, and the average droplet diameter, D_b.

$$a = \pi D_b^2 F_h/(\pi D_b^3/6) = 6 F_h/D_b \tag{36}$$

The extraction term in Equation (33) can now be written as

$$\left(\frac{N_{ox} \Lambda K}{L'}\right)\left(\frac{D_b}{6 F_h}\right)\left(\frac{\pi^2 D^2}{2\sqrt{3}}\right)\left(\frac{4}{\pi D^2}\right) P_y B \left[\bar{C}_{xl} - C^*_{xl}\right]$$

or upon simplification

$$\left(\frac{\pi N_{ox} \Lambda K D_b}{3\sqrt{3}\ F_h L'}\right) P_y B \left[\bar{C}_{xl} - C^*_{xl}\right] \tag{37}$$

Equation (33), and thus the continuous extract-phase boundary condition at Z = 1, now becomes

$$\left(\frac{\partial C_{yl}}{\partial Z}\right) = -P_y B \left[\bar{C}_{yl} - C^l_y\right] + J' K P_y B \left[\bar{C}_{xl} - C^*_{xl}\right] \tag{38}$$

where $J' = \pi N_{ox} \Lambda D_b/3\sqrt{3}\ F_h L'$

Putting Equation (38) into dimensionless concentration ratios, we note that

$$\left(\frac{\partial C_{yl}}{\partial Z}\right) = \Upsilon'_1 K \left[\bar{1} - C'^*_x\right]$$

and

$$\phi_1 - \Upsilon_1 = \frac{C_{xl} - \frac{C^l_y}{K} - \frac{q}{c_x K} - \frac{C_{yl}}{K} + \frac{C^l_y}{K}}{1 - C^{l*}_x} = \frac{C_{xl} - C^*_{xl}}{1 - C^{l*}_x}$$

Equation (38) thus becomes

$$Y_1' = -P_y B Y_1 + J' P_y B \left[\bar{\phi}_1 - Y_1\right] \tag{39}$$

Similarly, for the continuous raffinate phase at Z = 0

$$f_{fi} = F_x A c_x^o \tag{40}$$

$$f_{fo} = F_x A c_{xo} \tag{41}$$

$$f_{ei} = E_x (\epsilon_x A) \left(\frac{\partial c_{xo}}{\partial z}\right) \tag{42}$$

$$f_{to} = (K_x a/a) A_b \left[\bar{c}_{xo} - c_{xo}^*\right] \tag{43}$$

$$f_{fi} + f_{ei} = f_{fo} + f_{to} \tag{44}$$

$$1 + \frac{E_x \epsilon_x}{F_x L'} \left(\frac{\partial C_{xo}}{\partial Z}\right) = C_{xo} + \left(\frac{K_x a}{F_x}\right) \left(\frac{A_b}{aA}\right) \left[\bar{C}_{xo} - C_{xo}^*\right] \tag{45}$$

$$\left(\frac{\partial C_{xo}}{\partial Z}\right) = -P_x B (1-C_{xo}) + \left(\frac{N_{ox}}{L'}\right) \left(\frac{A_b}{aA}\right) P_x B \left[\bar{C}_{xo} - C_{xo}^*\right] \tag{46}$$

$$\left(\frac{\partial C_{xo}}{\partial Z}\right) = -P_x B (1-C_{xo}) + J P_x B \left[\bar{C}_{xo} - C_{xo}^*\right] \tag{47}$$

where $J = N_{ox} \pi D_b / 3\sqrt{3} F_h L'$

$$\phi_o' = -P_x B \left[1-\phi_o\right] + J P_x B \left[\bar{\phi}_o - Y_o\right] \tag{48}$$

Solution for Slug Flow of the Raffinate Phase

Boundary condition (39), which includes the effect of mass transfer

at the column interface, will be utilized in the solution of the concentration-profile equations of Miyauchi, Equations (10), and (11). One special case of column operation will be considered, slug flow of the raffinate phase with a finite amount of backmixing taking place in the continuous extract phase. This situation would be approached in a pulse column operating with the dispersed phase as the raffinate phase. All equations will be expressed in terms of the dimensionless concentration ratios, ϕ and Υ.

Equations (10) and (11) become

$$\phi'' - P_x B \phi' - N_{ox} P_x B(\phi - \Upsilon) = 0 \tag{49}$$

$$\Upsilon'' + P_y B \Upsilon' + N_{ox} \Lambda P_y B(\phi - \Upsilon) = 0 \tag{50}$$

For boundary conditions, we have

$$-(\partial C_y / \partial Z) = 0 \text{ or } -\Upsilon' = 0 \text{ at } Z = 0 \tag{51}$$

$$C_x = 1 \text{ or } \phi = 1 \text{ at } Z = 0 \tag{52}$$

and

$$\Upsilon_1' = -P_y B \Upsilon_1 + J' P_y B \left[\phi_1 - \Upsilon_1\right] \text{ at } Z = 1 \tag{39}$$

The special conditions selected are

$E_x = 0$, $P_x B = \infty$

E_y and $P_y B$ finite

$\Lambda \neq 1$

For $P_xB = \infty$, Equation (49) simplifies to

$$\phi' + N_{ox}(\phi - Y) = 0 \tag{53}$$

Combining Equations (50) and (53) gives

$$[D^3 + (P_yB + N_{ox})D^2 + N_{ox}P_yB(1-\Lambda)D]\phi = 0 \tag{54}$$

Let $h = N_{ox} + P_yB$

and $k = N_{ox}P_yB(1-\Lambda)$

then the roots of Equation (54) become

$$\lambda_1 = 0$$

$$\lambda_2 = -(h/2) + \sqrt{(h/2)^2 - k}$$

$$\lambda_3 = -(h/2) - \sqrt{(h/2)^2 - k}$$

The solution of Equation (54) is

$$\phi = \sum H_i e^{\lambda_i Z} \text{ where } i = 1, 2, \text{ and } 3 \tag{55}$$

The utilization of Equation (55) in Equation (53) gives

$$Y = \sum h_i H_i e^{\lambda_i Z} \tag{56}$$

where $h_i = (1 + \lambda_i/N_{ox})$

The coefficients of Equations (55) and (56) (H_i) will be determined by application of the three boundary conditions. For boundary condition Equation (51) at $Z = 0$ we have

$$\Upsilon = -\sum h_i \lambda_i H_i = 0 \tag{57}$$

For boundary condition Equation (52) at Z = 0 we have

$$\phi = \sum H_i = 1 \tag{58}$$

For boundary condition (39) at Z = 1 we have

$$h_i H_i \lambda_i e^{\lambda i} = -P_y B \sum h_i H_i e^{\lambda i} \neq J' P_y B \quad (1-h_i) H_i e^{\lambda i}$$

Rearranging gives

$$\sum \left[(1 \neq \lambda_i / P_y B) h_i e^{\lambda i} - J'(1-h_i) e^{\lambda i} \right] H_i = 0 \tag{59}$$

The simultaneous solution of Equations (57), (58) and (59) by determinents gives values of the coefficients H_1, H_2, and H_3. The values of ϕ and Υ for any value of Z are thus found from Equations (55) and (56). The complete solution for ϕ and Υ is as follows:

$$h = N_{ox} \neq P_y B$$

$$k = N_{ox} P_y B(1-\Lambda)$$

$$\lambda_2 = -(h/2) \neq \sqrt{(h/2)^2 - k} \quad (\lambda_1 = 0)$$

$$\lambda_3 = -(h/2) - \sqrt{(h/2)^2 - k}$$

$$h_2 = 1 \neq \lambda_2 / N_{ox} \quad (h_1 = 1)$$

$$h_3 = 1 \neq \lambda_3 / N_{ox}$$

$$D_{H2} = h_3 \lambda_3$$

$$D_{H3} = -h_2\lambda_2$$

$$D_{H1} = \left[-D_{H3}\ (1 \neq \lambda_3/P_yB)e^{\lambda_3 h_3} \neq D_{H3}J'(1-h_3)e^{\lambda_3}\right] -$$

$$\left[D_{H2}\ (1 \neq \lambda_2/P_yB)e^{\lambda_2 h_2} - D_{H2}J'(1-h_2)e^{\lambda_2}\right]$$

$$D_H = D_{H1} \neq D_{H2} \neq D_{H3}$$

$$H_1 = D_{H1}/D_H$$

$$H_2 = D_{H2}/D_H$$

$$H_3 = D_{H3}/D_H$$

$$\phi = H_1 \neq H_2e^{\lambda_2 Z} \neq H_3\ e^{\lambda_3 Z}$$

$$\Upsilon = H_1 \neq h_2H_2e^{\lambda_2 Z} \neq h_3H_3e^{\lambda_3 Z}$$

Solution for Slug Flow of the Extract Phase

The concentration profile equations of Miyauchi can be solved for the case of slug flow of the extract phase with a finite amount of backmixing taking place in the raffinate phase. Equation (48) will be used to express the boundary condition at the column interface at which extraction is taking place. As in the previous equation solution, the dimensionless concentration ratios, ϕ and Υ, will be used. This eliminates the necessity that the equilibrium distribution curve must have a c_y intercept value of zero. The special conditions for the case under consideration are

E_x and P_xB are finite

$E_y = 0$, $P_yB = \infty$, and $\Lambda = 1$

Equations (49) and (50) become

$$\emptyset'' - P_x B \emptyset' - N_{ox} P_x B \, (\emptyset - \Upsilon) = 0 \tag{49}$$

and

$$\Upsilon' \neq N_{ox} \Lambda (\emptyset - \Upsilon) = 0 \tag{60}$$

The applicable boundary conditions are:

$$-(\partial C_{x1}/\partial Z) = 0 \text{ or } -\emptyset_1' = 0 \text{ at } Z = 1 \tag{61}$$

$$C_{y1} = C_y^1 \text{ or } \Upsilon_1 = 0 \text{ at } Z = 1 \tag{62}$$

$$\emptyset_o' = -P_x B(1-\emptyset_o) \neq J P_x B(\emptyset_o - \Upsilon_o) \text{ at } Z = 0 \tag{48}$$

Combining Equations (49) and (60) gives

$$\left[D^3 - (N_{ox}\Lambda \neq P_x B)D^2 - N_{ox}P_x B(1-\Lambda)\, D\right] \emptyset = 0 \tag{63}$$

Let $a = P_x B \neq N_{ox} \Lambda$

$b = N_{ox} P_x B \, (1-\Lambda)$

$\lambda_1 = 0$

$\lambda_2 = a/2 \neq \sqrt{(a/2)^2 \neq b}$

$\lambda_3 = a/2 - \sqrt{(a/2)^2 \neq b}$

The solution of Equation (63) is

$$\emptyset = \Sigma F_i e^{\lambda_i Z} \tag{64}$$

The utilization of Equation (64) in Equation (60) gives

$$\Upsilon = \sum f_i F_i e^{\lambda_i Z} \tag{65}$$

where

$$f_i = (1 \neq \lambda_i/N_{ox} - \lambda_i^2/N_{ox} P_x B)$$

As in the previous derivation, the coefficients F_1, F_2 and F_3 are determined by application of boundary conditions. For boundary condition Equation (61) we have

$$-\phi_1' = -\sum F_i \lambda_i e^{\lambda_i} = 0 \tag{66}$$

Boundary condition Equation (62) gives

$$\Upsilon_1 = \sum f_i F_i e^{\lambda_i} = 0 \tag{67}$$

Boundary condition (48) gives

$$\sum F_i \lambda_i = -P_x B \left[1 - \sum F_i\right] \neq J P_x B \left[\sum F_i (1-f_i)\right] \tag{68}$$

or upon rearrangement

$$\sum \left[(1-\lambda_i/P_y B) \neq J(1-f_i)\right] F_i = 1 \tag{69}$$

The simultaneous solution of Equations (66), (67) and (69) by determinents give the values of the coefficients F_1, F_2 and F_3. The values of ϕ and Υ for any value of Z are thus found from Equations (64) and (65).

The complete solution for ϕ and Υ is as follows:

$$a = P_x B \neq N_{ox} \Lambda$$

$$b = N_{ox} P_x B(1-\Lambda)$$

$$\lambda_1 = 0$$

$$\lambda_2 = (a/2) + \sqrt{(a/2)^2 + b}$$

$$\lambda_3 = (a/2) - \sqrt{(a/2)^2 + b}$$

$$f_1 = 1$$

$$f_2 = 1 + \lambda_2/N_{ox} - \lambda_2^2/N_{ox}\, P_x B$$

$$f_3 = 1 + \lambda_3/N_{ox} - \lambda_3^2/N_{ox}\, P_x B$$

$$D_{F2} = -\lambda_3\, e^{\lambda 3}$$

$$D_{F3} = -\lambda_2\, e^{\lambda 2}$$

$$D_{F1} = -D_{F3}\, f_3 e^{\lambda 3} - D_{F2}\, f_2\, e^{\lambda 2}$$

$$D_{F0} = [\bar{D}_{F2}(1 - \lambda_2/P_x B) + D_{F2}\, J(1-f_2)] + [\bar{D}_{F3}(1 - \lambda_2/P_x B) + D_{F3}\, J(1-f_3)]$$

$$D_F = D_{F0} + D_{F1}$$

$$F_1 = D_{F1}/D_F$$

$$F_2 = D_{F2}/D_F$$

$$F_3 = D_{F3}/D_F$$

$$\phi = F_1 + F_2\, e^{\lambda 2 Z} + F_3\, e^{\lambda 3 Z}$$

$$\Upsilon = F_1 + f_2 F_2 e^{\lambda 2 Z} + f_3 F_3 e^{\lambda 3 Z}$$

CHAPTER IV

EXPERIMENTAL APPARATUS

Pulse Column Construction

The pulse extraction unit used in this investigation is shown in Plate I. Figure 3 is a schematic diagram of the pulse column showing details of construction. In brief, the column is composed of short sections of two inch Pyrex glass pipe, perforated plates, Teflon gaskets, and Pyrex glass pipe end sections which are held together by external compression rods. This construction is similar to that reported by Burkhart and Fahien (3) and Edwards and Beyer (9). Details of the individual components are given below.

Perforated Plates

Two sets of ten perforated plates were used at different times in construction of the pulse column. Each set had identical hole geometry but differed in material of construction. A set made of aluminum was used primarily in eddy diffusivity determinations while a second set of plates, which were made from 18-8 stainless steel, was used for all extraction runs and several of the eddy diffusivity determinations. The plate thickness was 1/16 inch. Each plate contained 108 holes drilled on triangular centers with a number 44 twist drill. This method of plate construction gave holes with diameters of approximately 0.086 inches and a calculated free area of each plate of 20 per cent.

PLATE I. PULSE EXTRACTION UNIT

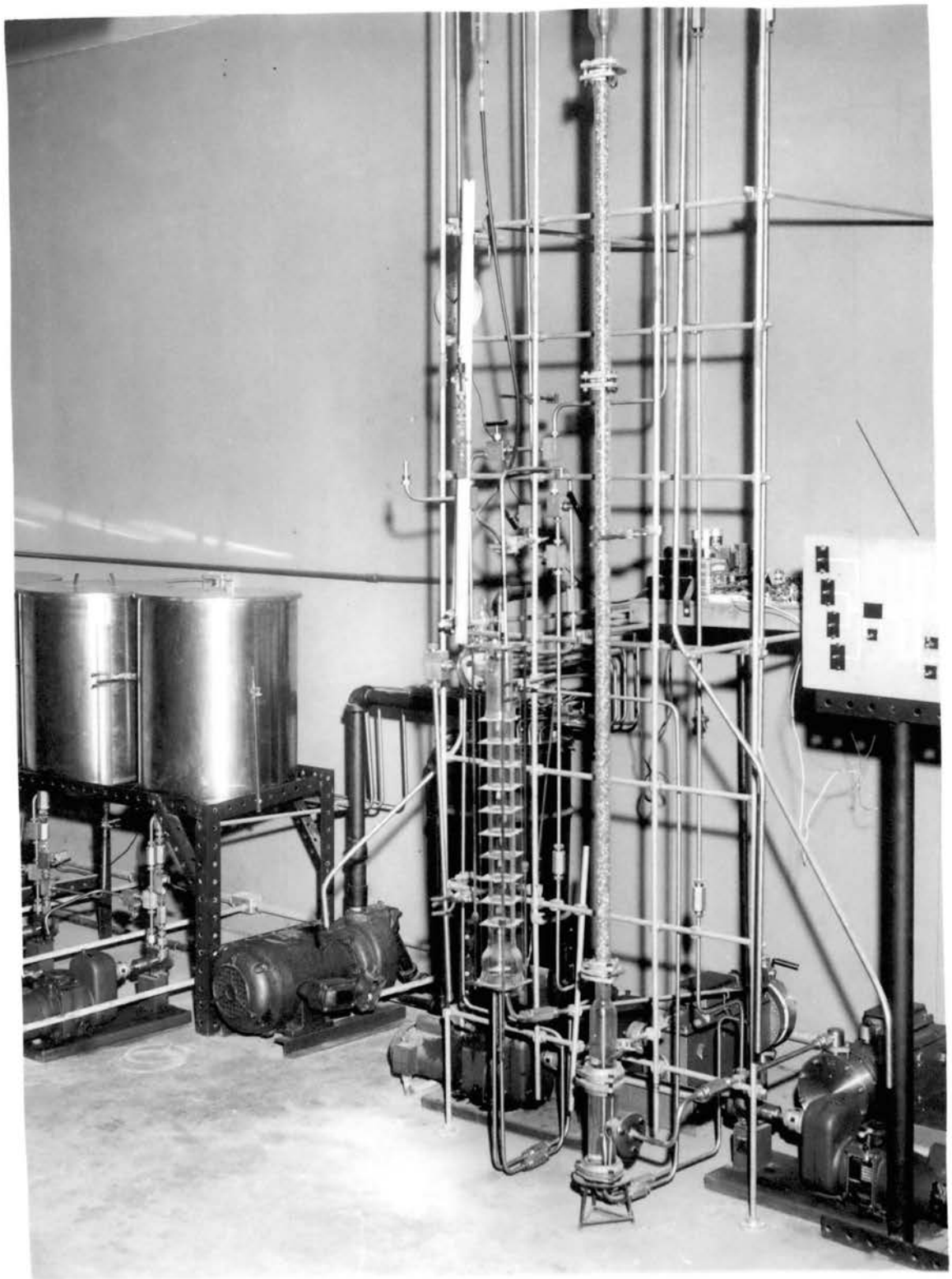

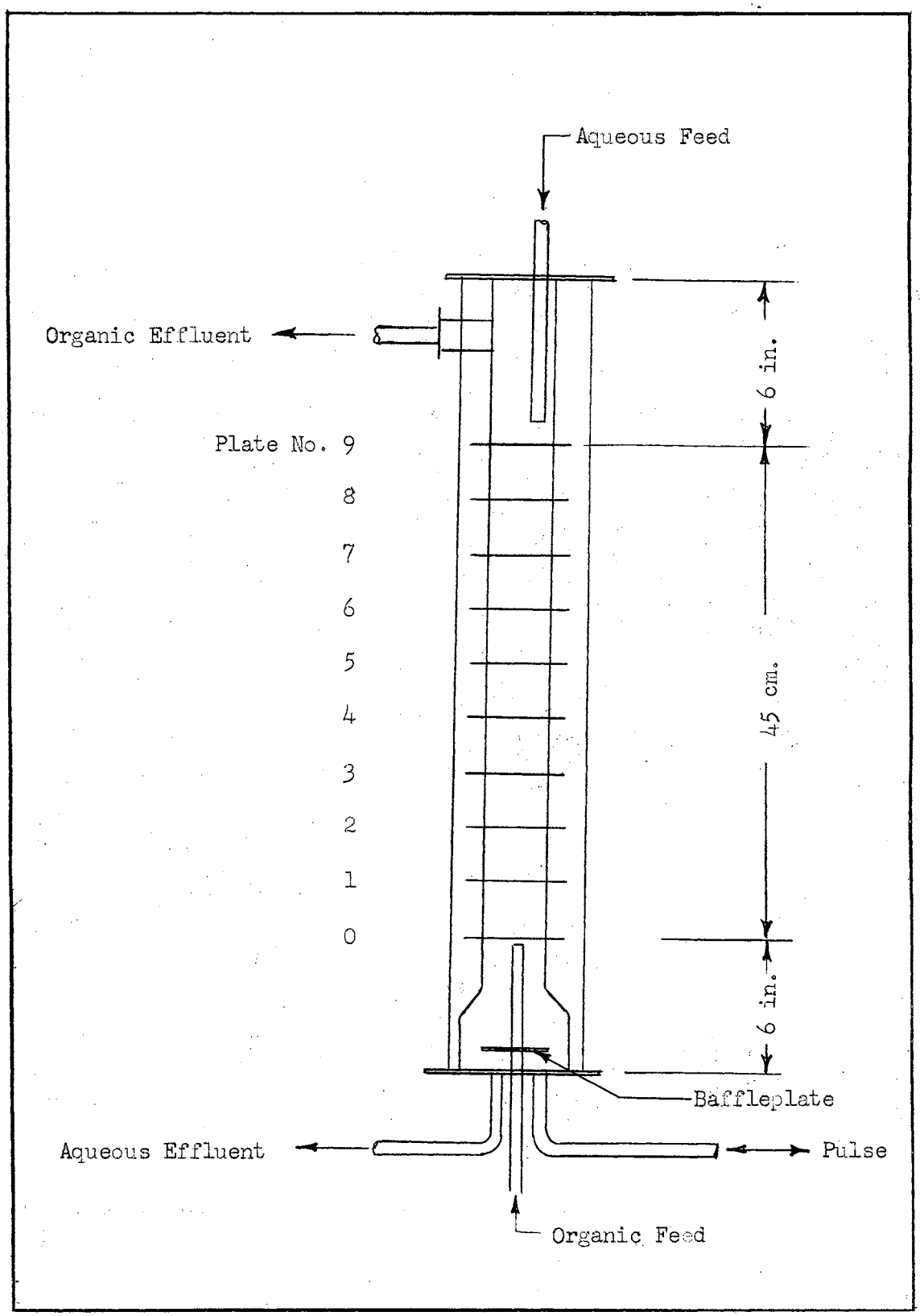

FIGURE 3. PULSE COLUMN SCHEMATIC DIAGRAM

Gaskets

Gaskets were cut from a 1/32 inch thick Teflon sheet and inserted between the perforated plates and the glass sections. The inside diameters of the gaskets were approximately equal to those of the glass sections.

Top Section

The upper disengaging section was made from a 2"x2"x1" Pyrex glass tee which was cut off at one end to give a total length of six inches. This construction allowed a maximum of four inches of disengaging space for the light phase below the 1/2-inch diameter overflow line.

The heavy phase (the continuous phase in this investigation) was introduced 3/4 inch above the top plate through a single 1/4-inch I.D. stainless-steel tube. The radial position, as indicated in Figure 4, was 120° from the front and 5/8 inch from the column center.

Bottom Section

The lower section of the column consisted of a six-inch-long Pyrex glass reducer with nominal diameters of three inches to two inches. A two-inch diameter baffleplate was made of 1/16-inch-thick Teflon and had a 5/16-inch-diameter hole in its center. The baffleplate was held in place by a force fit over the 3/8-inch O.D., 1/4-inch I.D., stainless-steel, light-phase entrance tube. The continuous phase emitted by the pulsing unit was deflected by the baffleplate such that no regular patterns of end section circulation were noted. The light phase was introduced by the single tube nozzle 1/4 inch below the bottom sieve plate.

Dispersed Phase Sampling Funnels

A small polyethylene funnel was attached to each of the stainless-

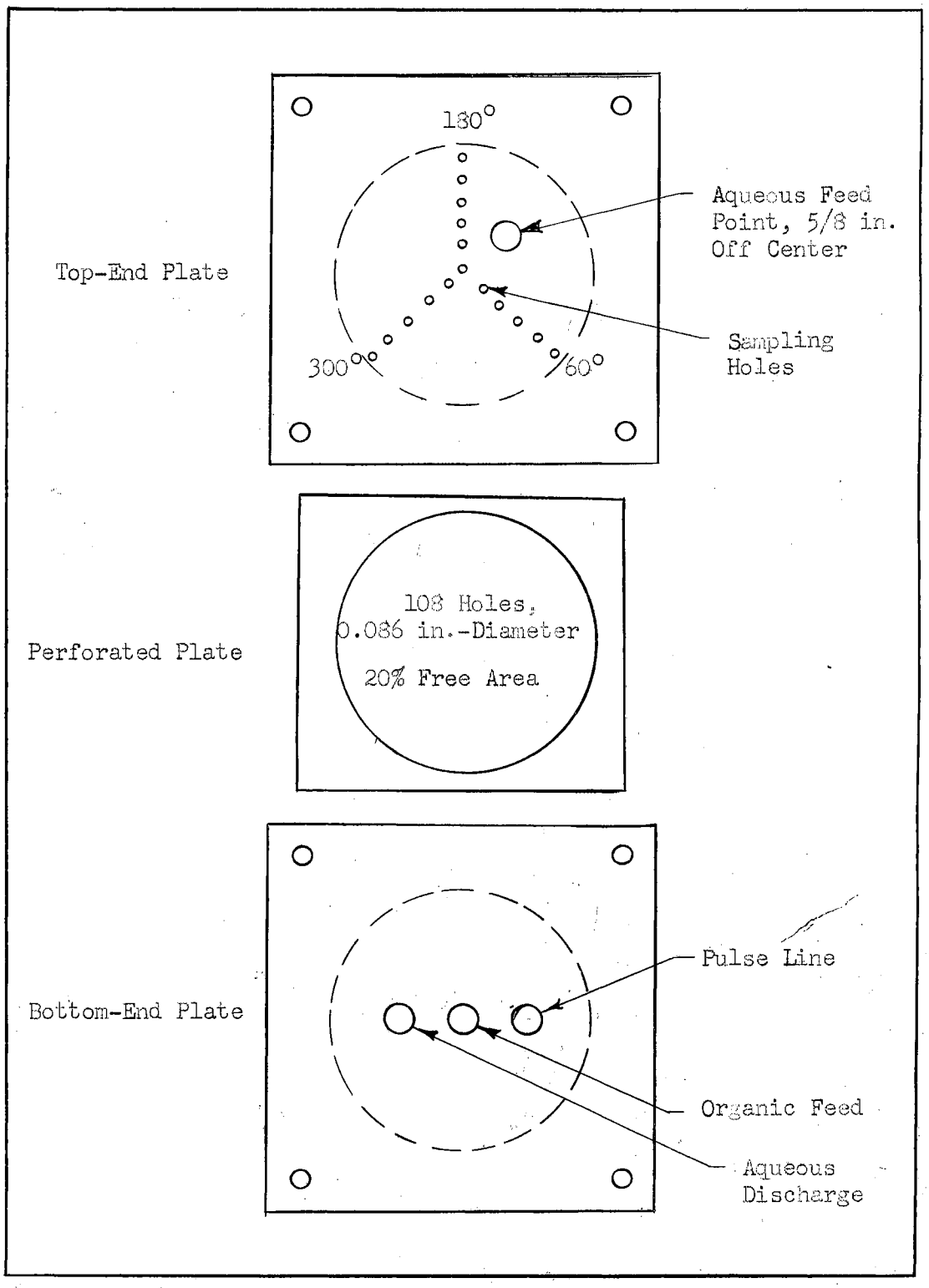

FIGURE 4. PLATE GEOMETRY DETAILS

steel perforated plates, except for the lowest plate. The funnels were formed from conventional 3/8- and 1/16-inch O.D. polyethylene tubing by heating and drawing. The funnels were mechanically attached to the plates by flaring the small funnel ends after insertion through holes in the plates. The internal hole at the top of each funnel was adjusted by heating to give a snug fit around the 1/16-inch O.D. sampling probe. The lower opening of each funnel was located midway between two plates.

The funnels were positioned in the holes adjacent to the center hole (approximately 0.167 inch center-to-center) in the radial positions of 60, 180 and 300° (see Figure 4). The funnel locations were rotated 120° on succeeding plates. Moving up the column, the positions were; plate 1 at 60°, plate 2 at 180°, plate 3 at 300°, plate 4 at 60°, etc.

Auxiliary Equipment

All equipment, except for the pulse column itself has been described previously (6). In brief, the feed and withdrawal pumps were Viking gear pumps capable of flow rates of one liter per minute or less. Pump speed and thus output was controlled by Graham transmissions.

The pulse was supplied to the column through a 3/8 inch I.D. line from a Lapp-Pulsafeeder pump, from which the check balls had been removed. The pulsing unit supplied a pulse approximating a sine wave. The maximum pulse amplitude possible in the two-inch diameter column was 0.250 inches and the maximum pulse frequency was 235 cycles per minute. Both pulse frequency and pulse amplitude were variable to any value between zero and the maximum.

Both feed streams passed through a constant-temperature bath before

entering the pulse column. The bath was cooled by tap water, and was heated by two 450 watt knife heaters which were controlled by a Fenwall thermoregulator. The temperature was controlled to within $\pm$ 2° F. of the desired value

CHAPTER V

EXPERIMENTAL PROCEDURES

Materials

Five different systems were used in the backmixing study. Four of the systems used methyl isobutyl ketone as the dispersed phase. The continuous phases were water, 38 weight per cent aqueous ethylene glycol, 62 weight per cent aqueous ethylene glycol, and 82 weight per cent ethylene glycol. The fifth system consisted of toluene and water, the organic phase being dispersed. Physical property data for the equilibrated phases are given in Table 1.

Three systems were used in the extraction study. These were (a) methyl isobutyl ketone-acetic acid-water, (b) toluene-benzoic acid-water, and (c) toluene-acetic acid-water. The methyl isobutyl ketone (purified), ethylene glycol (purified) acetic acid (glacial-reagent) and benzoic acid (U.S.P.) were all purchased from Fisher Scientific Company. The toluene (95 per cent pure) was purchased from Phillips Chemical Company. All chemicals were used as received without further purification. Distilled water was used for all work.

Eddy Diffusivity Measurements

Tracer Injection

A point source tracer injection technique, similar to that described

TABLE I

PHYSICAL PROPERTIES OF THE

EQUILIBRATED PHASES

System	MIBK-Water	MIBK-38 wt.% Ethylene Glycol	MIBK-62 wt.% Ethylene Glycol	MIBK-82 wt.% Ethylene Glycol	Toluene-Water
Aqueous Phase					
Density, gms./cm.^{3}	0.994	1.046	1.073	1.092	0.994
Viscosity, cp. at 83°F.	0.926	2.170	4.230	7.860	0.926
Organic Phase					
Density, gms./cm.^{3}	0.803	0.803	0.803	0.803	0.892
Viscosity, cp. at 83°F.	0.605	0.605	0.605	0.605	0.550
Interfacial Tension dynes/cm.	10.7	7.6	6.0	3.7	28.0

by Swift and Burger (39), was used to determine eddy diffusivities of the continuous phase. A manganous sulfate tracer solution was added at the rate of 2 ± 1 per cent of the continuous-phase flow rate. Tracer concentrations were adjusted to give continuous-phase effluent concentrations in the range of 150 to 200 parts per million of manganese for the majority of the study. The effluent concentration was increased to 250 to 300 parts per million manganese in a few runs in which only a small amount of backmixing was anticipated.

The tracer solution for each run was made by diluting a concentrate of 186,000 parts per million manganese (in distilled water) with the necessary amount of equilibrated continuous phase.

The tracer solution was injected into the column through a 0.0625-inch O.D., 0.038-inch I.D., stainless-steel tube. The flow rate of the tracer was controlled by the elevation of a 500-milliliter burette containing the tracer solution. A 1/16-inch I.D. rubber tube, five feet long, connected the burette to the upper end of the injection tube. This injection tube was inserted through the center holes of the top seven plates in the column. The discharge point was located midway between plates two and three, 12.5 centimeters above the bottom plate.

Sample Removal

Continuous phase samples were taken from the holes adjacent to the center holes at the 60° radial position (see Figure 4) for all longitudinal eddy-diffusivity measurements. Radial concentration data, in general, were also taken at the 60° position. A few runs include radial data taken at the 180° and 300° sampling positions.

Samples of approximately three milliliters were removed at various

distances above and below the tracer injection point. These samples were withdrawn through a probe similar to that used for tracer injection. A short piece of pure gum rubber tubing connected the sampling probe to a five-milliliter hypodermic syringe. The syringe served as a suction device, sample receiver, and separatory funnel. The samples from the column normally contained some dispersed-phase droplets. The droplets coalesced in the syringe almost instantaneously. Continuous-phase samples, completely free of organic droplets, were discharged from the syringe after disconnection of the rubber tubing.

Sampling normally was begun at 30 centimeters above the tracer injection point. Samples were then taken at five centimeter increments down the column, thus placing each sampling point midway between the plates. For runs in which low backmixing was anticipated, samples were taken at two or three centimeter intervals and over a shorter total distance. Appendix B lists all probe positions and the measured concentrations.

Between samplings, the probe, rubber line, and syringe were flushed with about 1.5 milliliters of fluid from the next position to be sampled. This volume was greater than three times the volumetric holdup of the probe and line. The time required for sample removal, including both the line flushing and actual sampling, was 1.5 to 5.0 minutes per sample. These rates of withdrawal approximated one per cent of the continuous phase flow rate. In some low flow rate runs, the withdrawal rates approached a maximum of 2.5 per cent of the continuous-phase flow rate.

Time Sequence

The beginning of each run involved starting the flow of the feed

streams and adjusting the flow rates to the desired values. The time was taken to be zero when the tracer solution injection was begun. After a period of 25 to 35 minutes, sampling was begun. The total time for a run was usually 55 to 65 minutes. After each run, sample stripping (see below) required about one hour and analysis for the tracer material required approximately twenty minutes.

Analysis and Sample Stripping

Analysis for the manganese tracer was performed in a Beckmann Model DU Flame Spectrophotometer. Hydrogen was used as the flame fuel. The instrument was calibrated for three different scales of operation, i.e., 0 to 200, 0 to 100, and 0 to 10 parts per million manganese in distilled water. A wave length of 403.9 millimicrons was used, with slit widths of 0.07, 0.08 and 0.10 millimeters. Calibration curves are given in Figure 37, Appendix B.

The presence of methyl isobutyl ketone in the saturated aqueous solution gave apparent manganese readings which were about 100 per cent too high. Because of this, it was necessary to remove the ketone from the column samples. The following procedure was used. The aqueous samples were weighed in tared 25- or 50-milliliter Erlenmeyer flasks soon after being removed from the pulse column. The samples were subsequently heated to 100 to 150° F. and continuously exposed to an air jet. As the samples evaporated, distilled water was added. The ketone was stripped from the samples in 30 to 45 minutes, after which they were cooled, reweighed, and then analyzed. Corrections for dilution differences resulting from the stripping procedure were applied to the manganese concentrations obtained. The relative accuracy of the concentrations obtained

was estimated to be plus or minus two per cent of the maximum scale readings, (Figure 37).

Ethylene glycol was also removed in the stripping procedure for runs T-27 through T-41 and run T-47. No stripping was necessary for samples from runs T-17 through T-26 in which toluene was the dispersed phase.

Both organic phases were tested after repeated contacts with aqueous phases containing manganese sulfate. No tracer was detectable in the toluene phase and only 0.2 parts per million was present in the methyl isobutyl ketone phase.

Flow Rate Measurements

The flow rate of each stream was measured by collecting a one to ten minute sample of the column effluent in a 1000-, 200-, or 100-milliliter graduated cylinder. The flow rates were determined to have an average variation of two per cent for all the runs and a maximum variation of ten per cent within any one run. The principal causes of the higher per centage flow rate variations were low flow rates and/or decreasing suction head pressures on the Viking feed pumps.

The graduated cylinders were checked for accuracy by weighing measured volumes of distilled water. The recorded volumetric flow rates were estimated to be accurate to within three per cent.

Pulse Amplitude and Frequency

A pulse amplitude of 0.218 ± 0.003, inches was used exclusively in this study. This value was checked repeatedly during the course of the investigation and was always within the tolerance stated. The pulse amplitude was measured on the outside of the pulse column by noting the total vertical movement of the interface at a pulse frequency of 15 cycles

per minute. Measurements were made using a five-inch vernier caliper and a one-inch micrometer caliper.

The pulse frequency was determined to be equal to 7.60 times the setting of the Graham Transmission which drove the pulsing unit. Frequencies during calibration were determined by counting the number of cycles in a one minute period or by measuring the length of time for one hundred cycles.

Temperature of Operation

The temperature of operation was controlled by the temperature of the tap water which was available for cooling the constant temperature bath. Throughout the investigation, column operating temperatures were $83 \pm 2^{\circ}$ F.

Ethylene Glycol Recovery

A five-liter pot still was used to separate the manganese sulfate tracer from the ethylene glycol-water solution. A distillation rate of one liter per hour was possible without significant entrainment.

Mass Transfer

Solute concentration profiles were measured for both phases in all three systems examined. In all but run E-6, the direction of mass transfer was from the dispersed organic phase to the continuous aqueous phase. In all cases, the entering extract phase contained no solute.

Operating Conditions

Three extraction runs were made using the toluene-acetic acid-water system. The flow rate ratio of raffinate to extract phase was about 9/1. At the concentrations involved, this flow rate ratio gave conventional

operating lines (slug flow of both phases) with slopes similar to that of the equilibrium distribution curve. The flow rate sum in all three runs was approximately 500 milliliters per minute. The pulse volume velocities, $2V_p$, of the three runs corresponded to values at which eddy diffusivities had previously been determined (in the initial portion of this study).

Three extraction runs were made using the toluene-benzoic acid-water system. All were performed at the same pulse volume velocity, 2470 cc./min., and the same flow rate ratio, R/E, of 1/9. Flow rate sums of 500, 1006, and 235 ml./min. were used for runs E-6, E-7, and E-8 respectively. As previously mentioned, the direction of benzoic acid transfer in run E-6 was from the aqueous to the organic phase.

The methyl isobutyl ketone-acetic acid-water system was used for runs E-9 through E-12. The flow rate ratio was approximately 1/1 in all four runs. Two variables were examined in these runs, namely the flow rate sum and the pulse frequency. The acid concentration in the feed stream was also varied more in this set of runs than in the others. Specific feed concentrations for all runs are included in Appendix C.

Sampling

Both continuous and dispersed phases were sampled throughout the plated section of the pulse column. Normally nine samples were taken of each phase within the column and two or more samples taken of the column effluents.

Dispersed-phase samples were collected utilizing the polyethylene sampling funnels for nine of the ten runs. The stainless-steel probe was inserted into a funnel approximately 1/8 inch. Dispersed phase

was removed from the funnel as rapidly as it entered, thus maintaining the level in the funnel about 1/8- to 1/4- inch from the lower end of the funnel. The samples obtained were completely free of contamination from the continuous phase. Run E-4 was in the mixer-settler region of pulse column operation so that sampling directly under a plate was practical.

The rate of dispersed-phase sample withdrawal was a function of the organic phase flow rate. Normally 1.5 to 4.0 minutes were required per three-milliliter sample. The samples constituted less than two per cent of the flow rate, except for run E-8 in which the samples were approximately 3.5 per cent of the flow rate.

The continuous phase was sampled with the probe inserted in the middle hole of each plate and with its lower end midway between the plates. Approximately one to two minutes were required to remove a three-milliliter sample. This rate of sample removal was approximately 0.3 to 3.0 per cent of the aqueous flow rate. At these sampling rates, the dispersed phase contamination of the continuous phase was minimized.

In runs E-10, E-11, and E-12, effluent samples of both phases were taken at seven to ten minute intervals. The approach to equilibrium and column stability was thus observable. In the remaining seven runs, effluent samples were taken after 30 minutes of operation and after the run was complete. The last 30 to 45 minutes constituted the internal sampling period.

Analysis

The raffinate and extract phase samples were weighed in tared 50-milliliter Erlenmeyer flasks, then titrated with sodium hydroxide solutions.

For the toluene-acetic acid-water system, sodium hydroxide normalities of 0.975, 0.488, 0.0965 and 0.0483 were used for titration. For the toluene-benzoic acid-water system, 0.0107 and 0.00535 normal caustic solutions were used. For the third system, methyl isobutyl ketone-acetic acid-water, a 0.0965 normal caustic solution was used. Phenolphthalein indicator was used for all samples.

The normalities of the 0.975 and the 0.0965 caustic solutions were determined by titration with 1/10-normal hydrochloric acid solution purchased from Fisher Scientific Company. Other concentrations were obtained by dilution.

Equilibrium Distribution Data

A few points on the equilibrium distribution curves were checked for the extraction systems used. The two immiscible phases were agitated at 83 $\pm$ 2° F. with the distributing solute in 500-milliliter separatory funnels and then settled. Samples of 6- to 20-milliliters volume were taken from each phase, weighed, and titrated. Comparisons of experimental data and literature values are given in Figures 30, 31 and 32.

Droplet Diameters

During the 30-minute stabilization period before sampling, photographs were taken of sections of the pulse column. From these photographs, an average droplet diameter was estimated. Normally, three photographs were taken at each of three different spaces along the column length and the best single photograph from the nine was used for the estimation. A photograph from run E-12 and the corresponding calculations are given in Appendix D.

Flooding Measurements

Insufficient Pulsation Flooding

Methods for the determination of insufficient pulsation flooding have been described in detail elsewhere (6). For convenience, the method used here will be summarized. Flow rates were established at the desired values and the pulse volume velocity was set above that anticipated for flooding. At approximately seven-minute intervals, the pulse frequency was decreased until flooding occurred. During the seven minutes, flow rates were checked as described previously. Flooding, as evidenced by a build-up of dispersed phase under the bottom plate, became evident within two or three minutes after a frequency change.

Emulsion Flooding

Two different degrees of emulsion flooding were observed in this study. Each has been described previously, but both have not been measured by the same investigator (21), (29), (40). The first of these degrees of emulsion flooding was a simple carry-over of small droplets of dispersed phase. This carry-over of dispersed phase usually amounted to about 0.01 per cent of the continuous phase and was detected by collection of continuous phase effluent samples in 100-, 200-, or 500-milliliter volumetric flasks. Samples were collected at repeatedly higher frequencies until flooding was evident. A ten-minute stabilization period was allowed after each frequency increase before sampling was begun. After one hour of settling, dispersed phase was evident in the narrow necks of all flasks containing samples which were taken at frequencies greater than the emulsion flooding frequency. Aside from the presence of the small droplets in the continuous phase, the column operation appeared satisfactory.

The second degree of emulsion flooding occurred at still higher pulse frequencies. This flooding was initially characterized by a greater amount of entrainment in the dispersed phase. The conclusive evidence of flooding was a sharp increase in dispersed-phase holdup and a rapid, uncontrollable column interface rise.

CHAPTER VI

RESULTS AND DISCUSSION

Backmixing

Gross axial turbulence of the continuous phase in a pulse column has been characterized by axial eddy diffusivities. Five different two-phase systems were utilized. The five primary variables examined in the study were the flow rate sum, flow rate ratio, continuous-phase fluid, dispersed-phase fluid, and the pulse frequency. In addition, plate material and column height were examined superficially. The major effect or significance of each variable was evaluated.

A mathematical model was developed in Chapter III which describes backmixing of the continuous phase in a pulse column. This mathematical model was used in the interpretation of the experimental backmixing data obtained in this investigation. An effective concentration distance, Δz, which was defined in the development of the mathematical model, was also evaluated. This parameter formed a basis for interpretation and correlation of backmixing data.

Eddy Diffusivity Measurement

The numerical value of the eddy diffusivity for each backmixing run was calculated from the slope of the $\ln(c/c_o)$ versus z curve as indicated by Equation (3). Some typical curves are given in Figures 5, 6, and 7, and additional numerical data are given in Appendix B. The

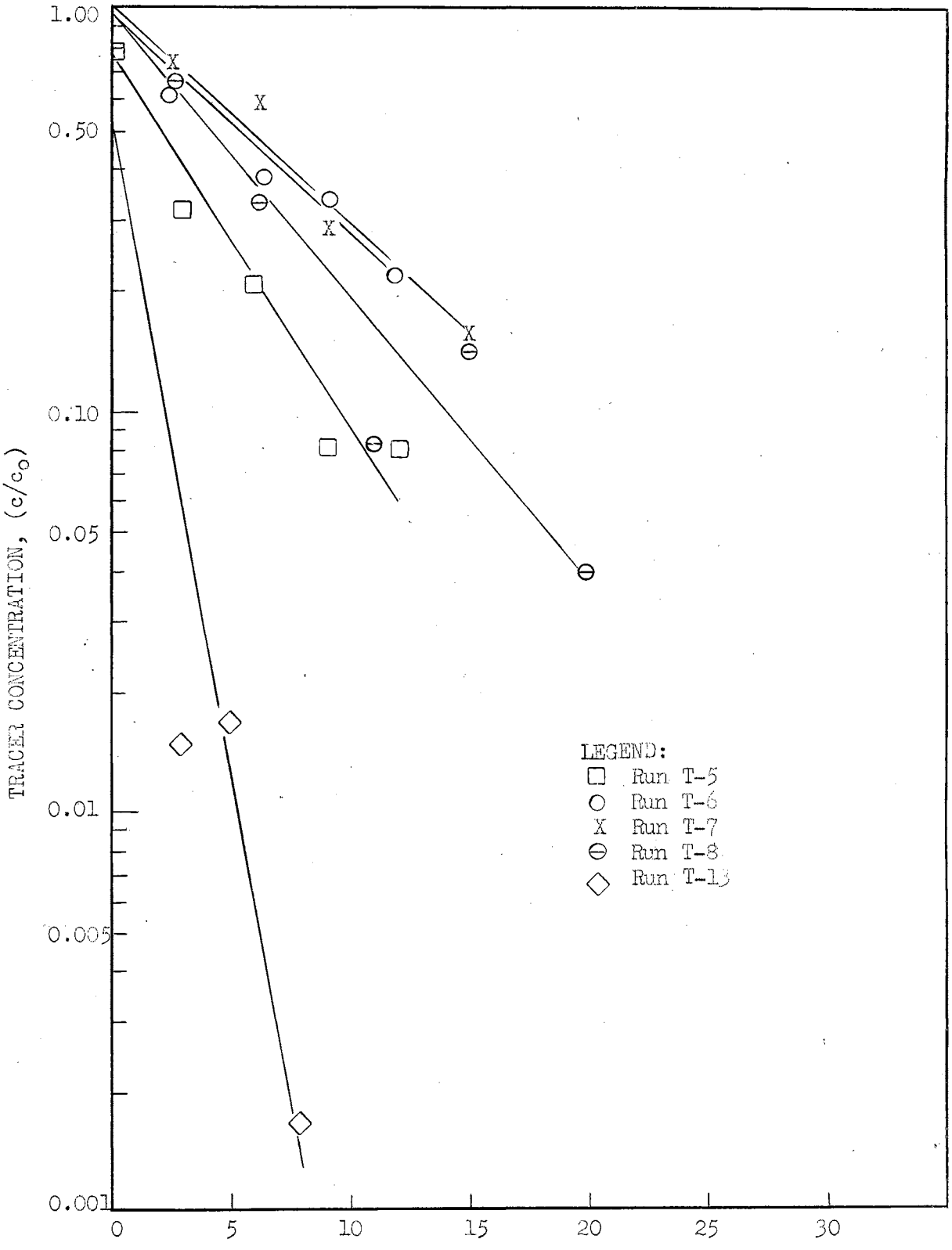

FIGURE 5. TYPICAL TRACER CONCENTRATION CURVES, MIBK-WATER SYSTEM

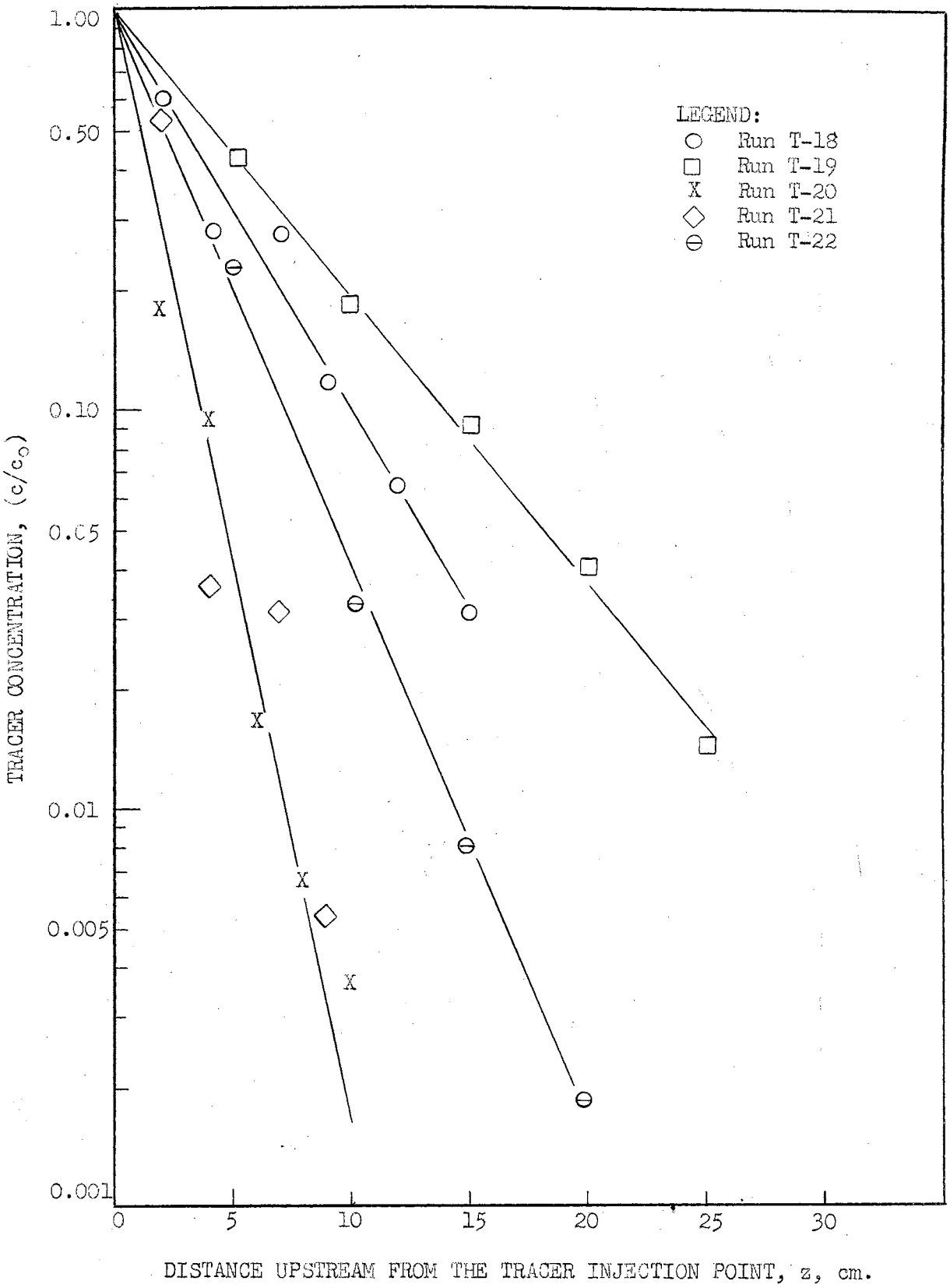

FIGURE 6. TYPICAL TRACER CONCENTRATION CURVES, TOLUENE-WATER SYSTEM

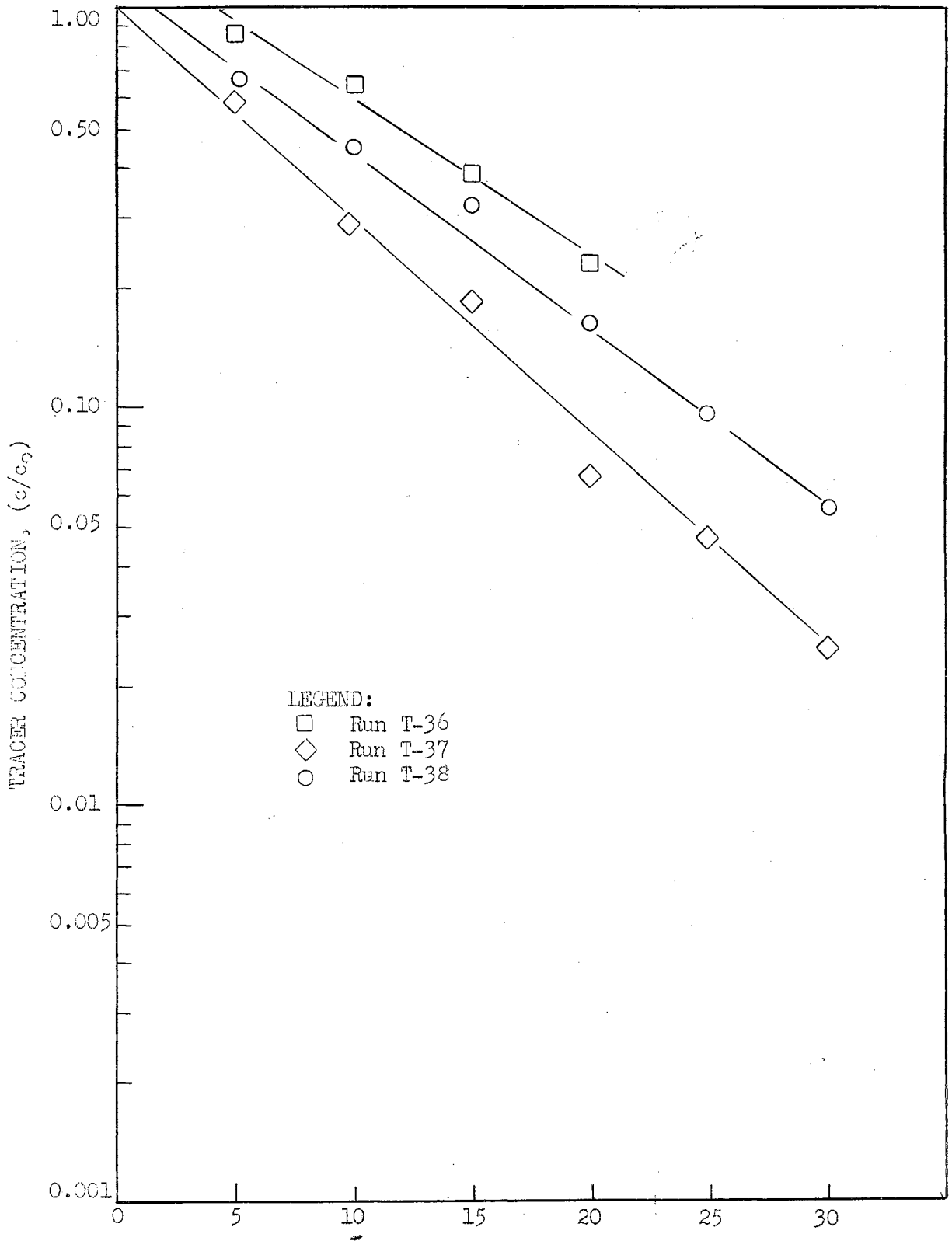

FIGURE 7. TYPICAL TRACER CONCENTRATION CURVES, MIBK-AQUEOUS ETHYLENE GLYCOL SYSTEMS

"method of least squares" calculation technique was used in all cases to determine the slope of the curve, b, which by definition is equal to $-F_c/E_c$. The superficial continuous-phase velocity, F_c, was calculated from the experimentally-evaluated flow rates and the column diameter.

As is indicated in Figures 5 and 7, the value of the intercept, B, was not always zero. Of the 41 runs reported, nine of the $\ln(c/c_o)$ versus z curves had intercepts that were clearly different than zero. The other 32 runs were calculated with $\ln(c/c_o) = 0$ at $z = 0$ as one point on the curve.

Specific Application of the Backmixing Model

Before examining the experimental backmixing results obtained in this investigation, it is of interest to state some specific interpretations of the continuous-phase backmixing model that apply to this work. First, the model would predict that for a given column geometry, and without obstructed continuous-phase recycle, all systems would behave identically. Figure 8 indicates the calculated response of $E_c/\Delta z$ to increases in pulse volume velocity, $2V_p$, for the conditions of a flow rate ratio of 1/1 and a two-inch internal diameter column. If the value of Δz is assumed to remain relatively constant over the pulse volume velocity range being examined, then one could expect a near linear response of eddy diffusivity to pulse frequency, independent of the system being utilized.

The mathematical model in its present form is restricted to operations in which continuous-phase recycle across the perforated plates is unlimited by the presence of the dispersed phase. It is, however, sufficient at this time to recognize that even if operation in the mixer-settler zone or excessive plate wetting by the dispersed phase are excluded,

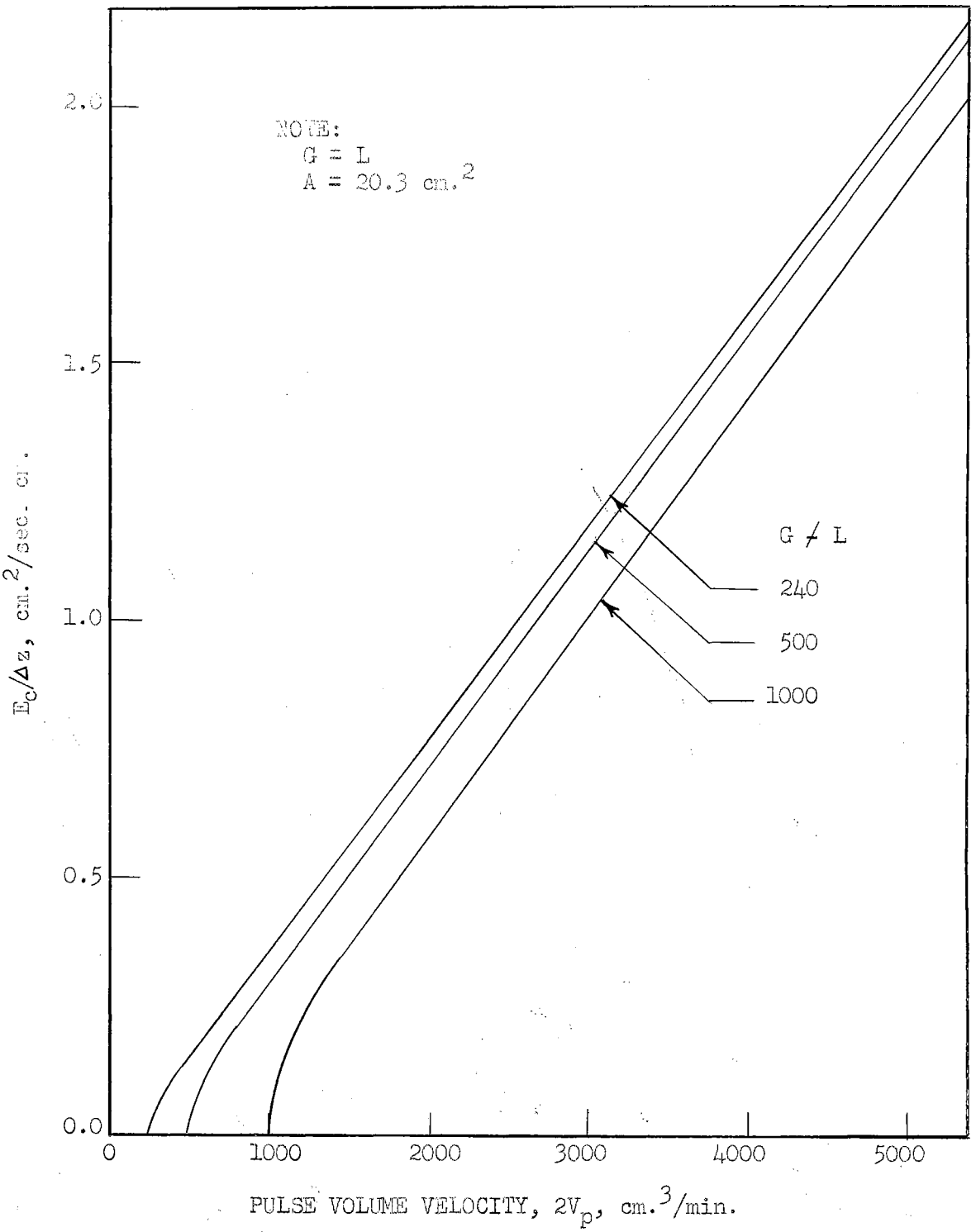

FIGURE 8. EFFECT OF THE PULSE VOLUME VELOCITY ON $E_c/\Delta z$

the model predicts that decreased backmixing at high pulse frequencies can be obtained. Specifically, this can mean a decreasing rate of change of the eddy diffusivity with pulse frequency, as the pulse frequency is increased. At these high pulse frequencies a lesser portion of the fluids which are recycled through the perforated plates are continuous phase, hence continuous-phase backmixing is decreased. The term "plate sealing" will be used to express this phenomena.

A third point of interest that is evident in Figure 8 is the result of two basic assumptions in the proposed backmixing model. The first of these is that no backmixing is possible without continuous-phase recycle across the perforated plates. The second is that no recycle exists when the pulse volume velocity, $2V_p$, is equal to the flow rate sum, $G \neq L$. The result of these two assumptions is that the eddy diffusivity equals zero when the pulse volume velocity equals the flow rate sum.

Figure 9 presents the predicted response of $E_c/\Delta z$ to the flow rate sum, $G \neq L$, at constant values of the pulse-volume velocity, $2V_p$. These curves were calculated from Equation (25) for a flow rate ratio, G/L, of 1/1 and pulse volume velocities, $2V_p$, of 1500, 2500, and 3800 $cm.^3/min.$

An examination of these curves shows the response of $E_c/\Delta z$ to be relatively linear with respect to the flow rate sum, $G \neq L$, except at high flow rate sums. These high flow rate sums are in the region immediately preceeding insufficient pulsation flooding and, hence, are only of minor interest. The primary value of these curves is to show that if Δz were to remain relatively constant for a given pulse frequency, then one could predict that E_c would decrease almost linearly with an increase in $G \neq L$.

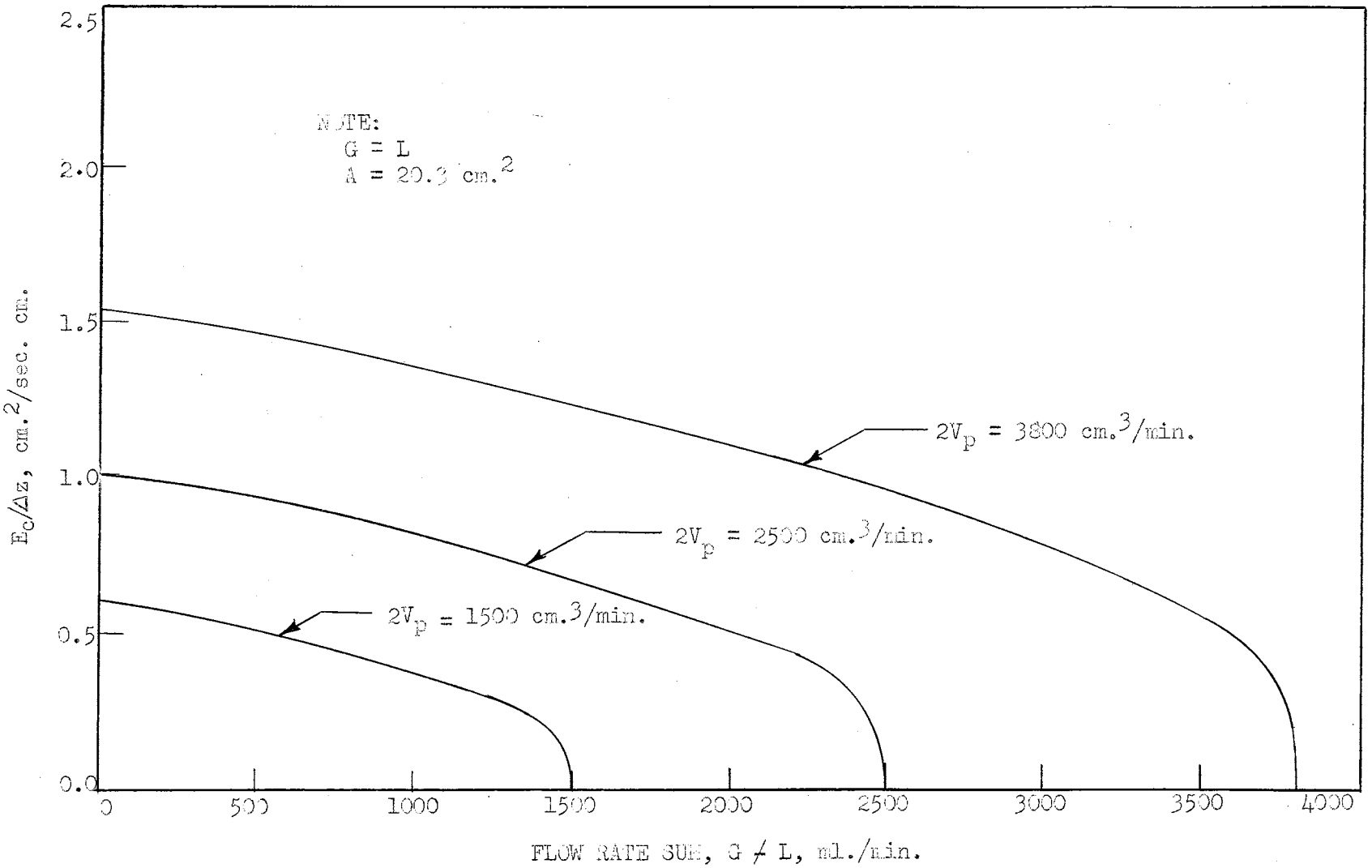

FIGURE 9. EFFECT OF THE FLOW RATE SUM ON $E_c/\Delta z$

Pulse Frequency

Of all the variables studied, pulse frequency had the greatest effect on backmixing. The experimental backmixing study was conducted in such a way that all but three of the 41 eddy diffusivity values reported, could be used directly in interpretation of the effects of pulse frequency on pulse-column backmixing. The results obtained on each of the five two-phase systems which were studied in this investigation, are given in Figures 10 through 14.

Each system exhibited a response to pulse frequency which was, to some extent, predictable from the backmixing model of Chapter III. Initially, the values of the eddy diffusivities increased relatively linearly with increases in pulse frequency, f, or with increases in pulse amplitude. As the pulse frequencies were increased to higher values, the effects of plate sealing became evident, resulting in decreased responses to pulse frequency. At still higher pulse frequencies, the eddy diffusivities passed through maximums and then decreased, also as a result of plate sealing.

An increase in dispersed-phase holdup must also be considered as contributing to the decrease in the eddy diffusivity at these higher pulse frequencies. This increase in dispersed-phase holdup decreases the recycle of continuous phase through the perforated plates and thus decreases the continuous-phase backmixing.

The curves through the experimental data points in Figures 10 through 14 are all drawn to conform to the backmixing model requirement that $E_c = 0$ when $2V_p = G \neq L$. There is certainly experimental and theoretical evidence to indicate that this is true. There does exist, however, one additional possibility that cannot be discounted, which is that E_c

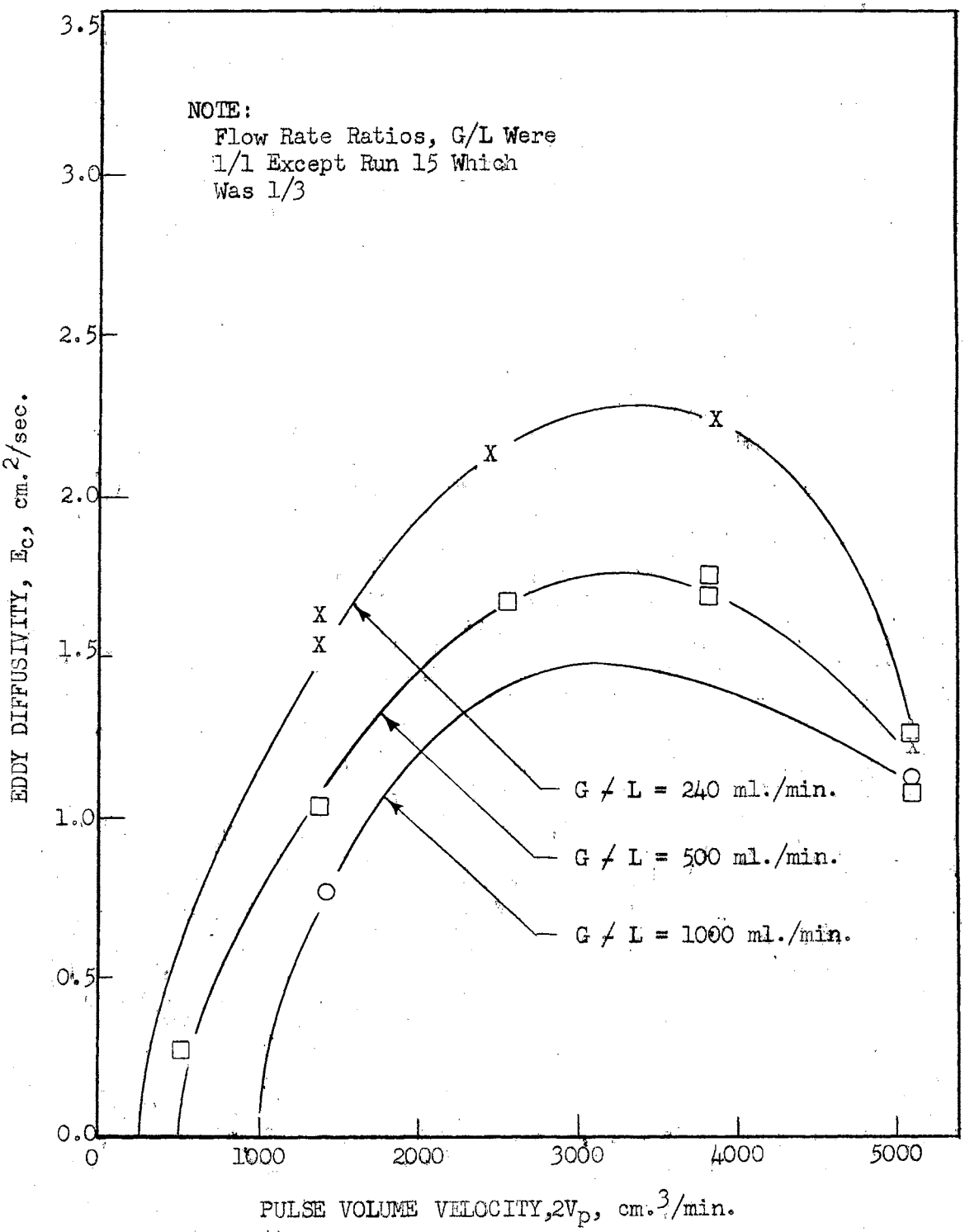

FIGURE 10. EDDY DIFFUSIVITY CORRELATION, MIBK - WATER SYSTEM

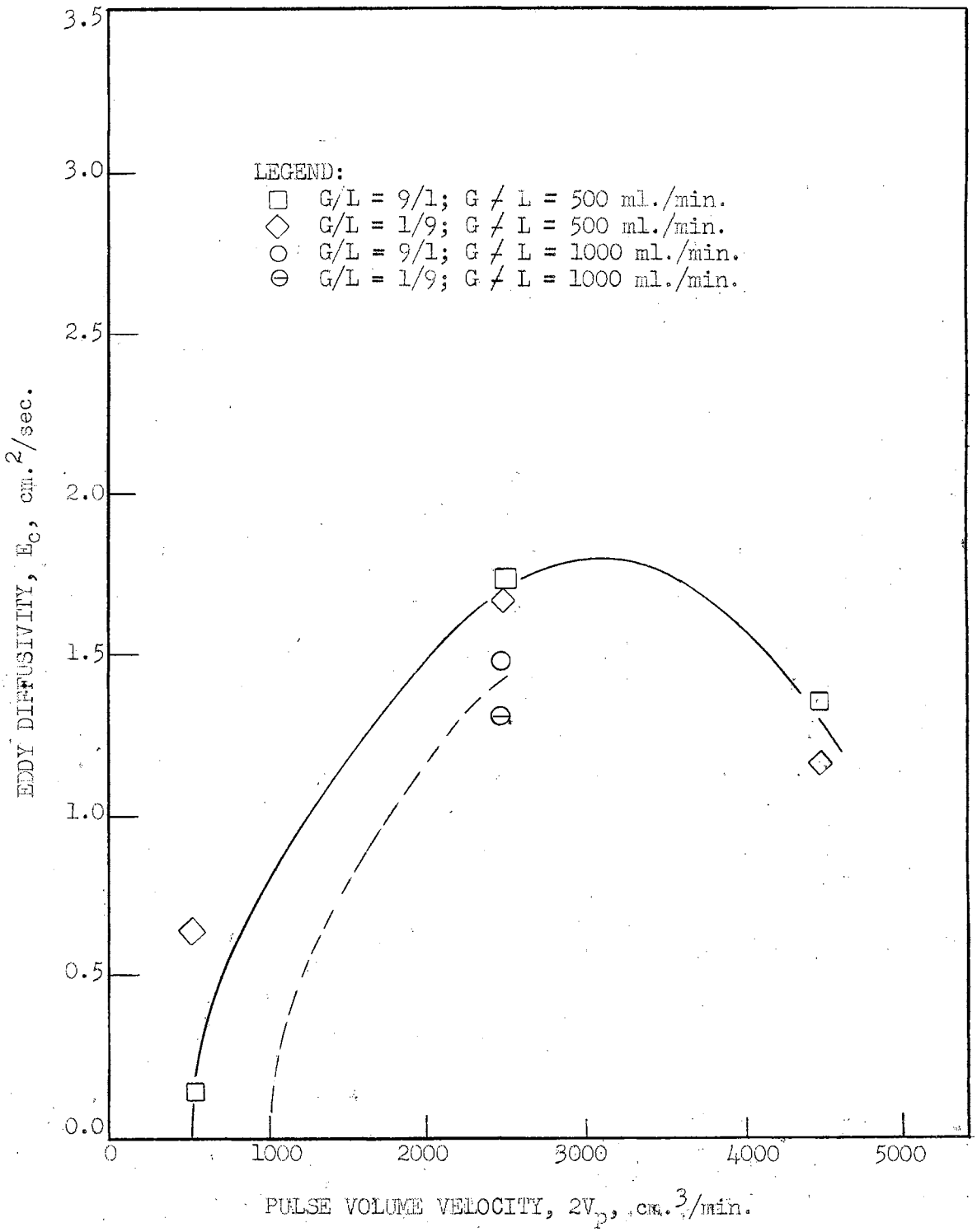

FIGURE 11. EDDY DIFFUSIVITY CORRELATION, TOLUENE-WATER SYSTEM

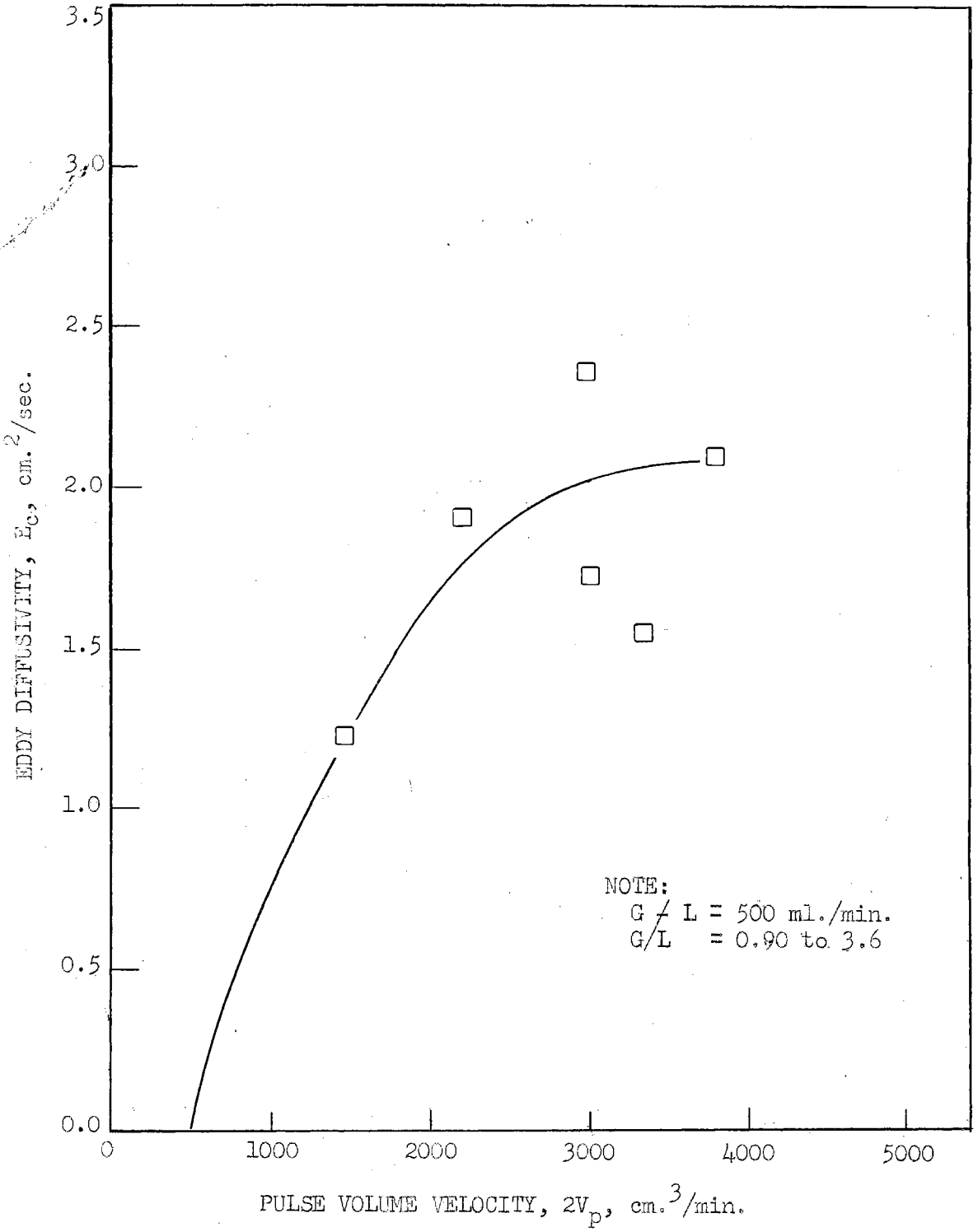

FIGURE 12. EDDY DIFFUSIVITY CORRELATION, MIBK-38% ETHYLENE GLYCOL SYSTEM

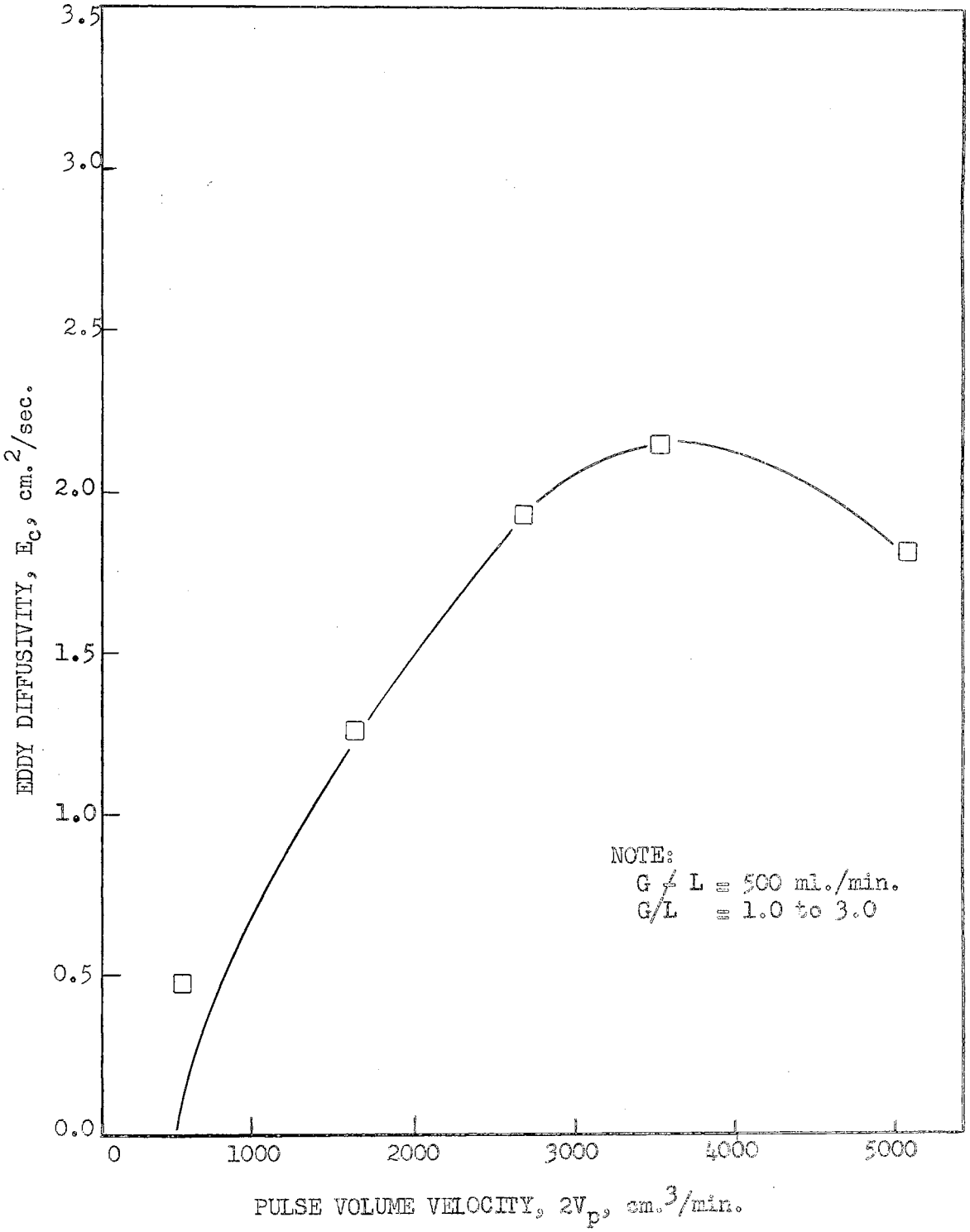

FIGURE 13. EDDY DIFFUSIVITY CORRELATION, MIBK-62% ETHYLENE GLYCOL SYSTEM

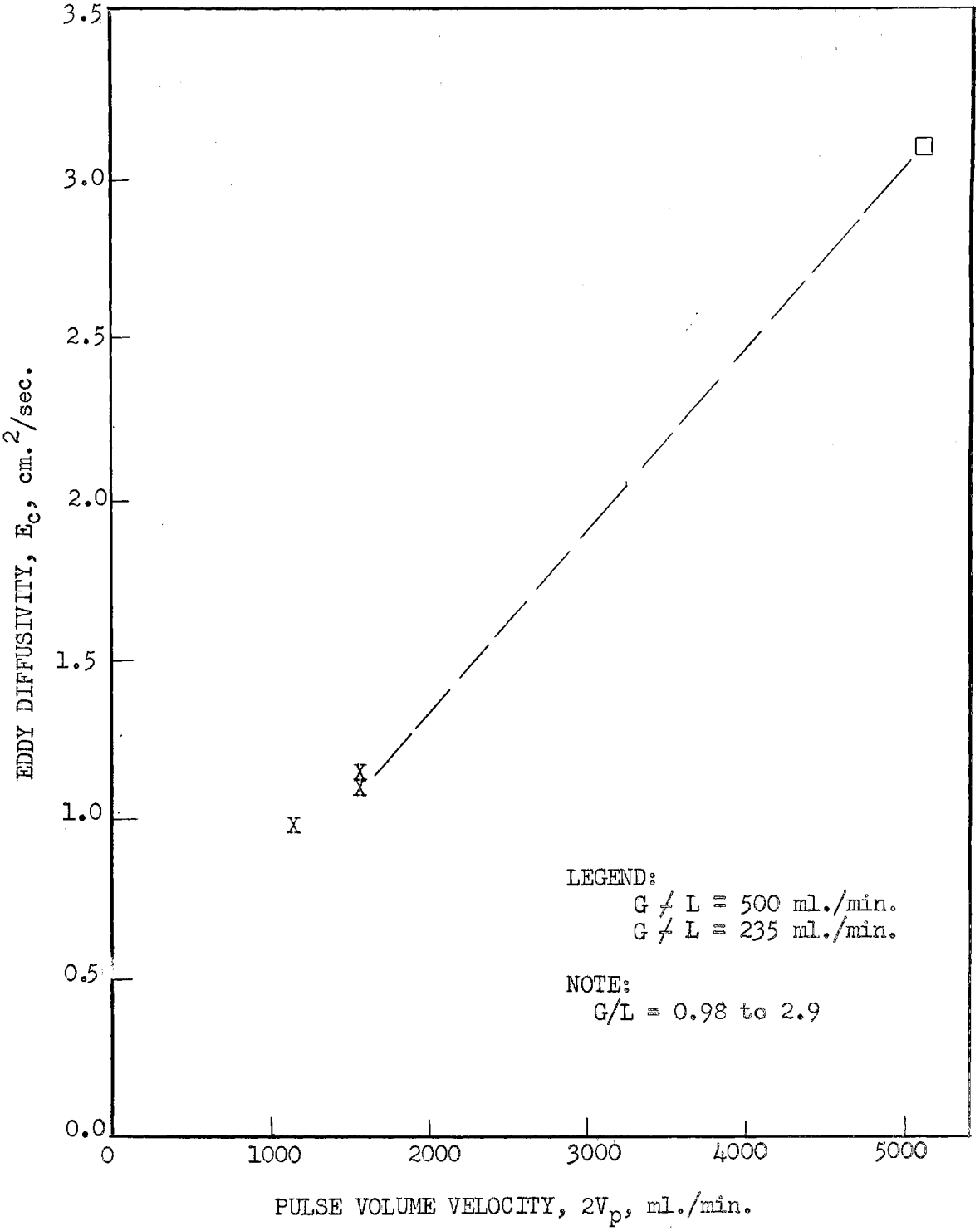

FIGURE 14. EDDY DIFFUSIVITY CORRELATION, MIBK-82% ETHYLENE GLYCOL SYSTEM

approaches zero as $2V_p$ approaches zero. When the pulse volume velocity, $2V_p$, equals the flow rate sum, $G \neq L$, the column enters the region of insufficient pulsation flooding and becomes inoperative. The eddy diffusivity curve would thus terminate with some positive value of the eddy diffusivity, the point where the pulse volume velocity equals the flow rate sum.

Fluid Systems

Figures 15 and 16 test one idealization of the backmixing model. This idealization is that the continuous-phase backmixing is independent of the liquid system. This relation is of course limited by the qualifications that operation is not in the mixer-settler region, that no plate sealing occurs, and that no differences in plate wetting characteristics are present. Of these three limitations, only plate sealing need by considered here because the other effects were non-existent, or were minimized in this study.

The frequency at which the maximums in the eddy diffusivity curves occur provides an arbitrary but convenient demarcation between regions of plate sealing and those of no plate sealing. All of the experimental data from Figures 10 through 14 which were in the region of no plate sealing are shown in Figures 15 and 16. These data can be interpreted as yielding a single curve at a given flow rate sum that is common to all of the five two-phase systems investigated. These five systems had a continuous-phase density range of 0.994 to 1.092, a continuous-phase viscosity range of 0.926 to 7.86 cp., and an interfacial tension range of 3.7 to 28 dynes/cm. These data indicate that some validity exists in the assumption that continuous-phase backmixing is independent of the fluid system.

Because backmixing is postulated to be independent of the fluid

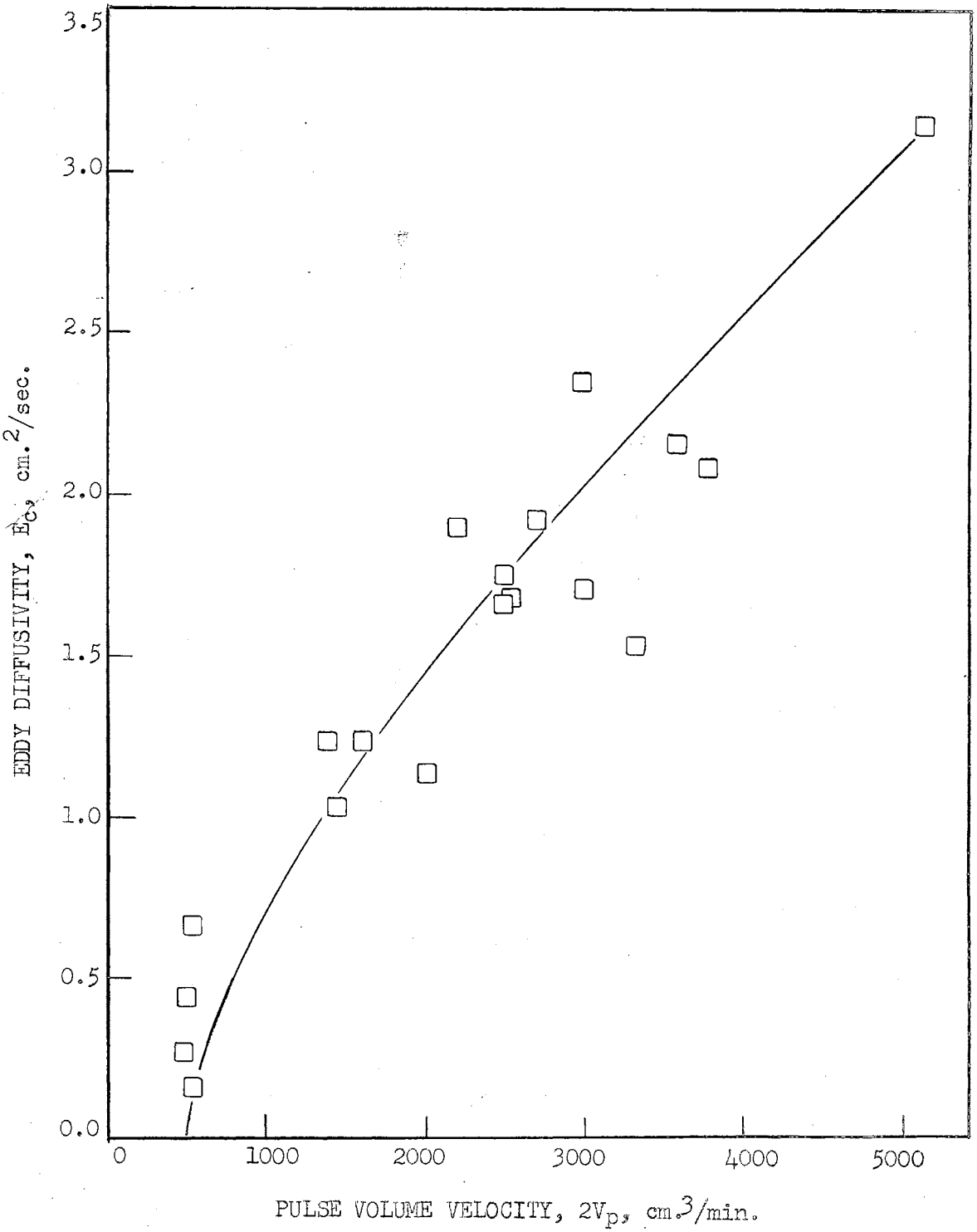

FIGURE 15. EDDY DIFFUSIVITY CORRELATION FOR NO PLATE SEALING, G / L = 500 ml./min.

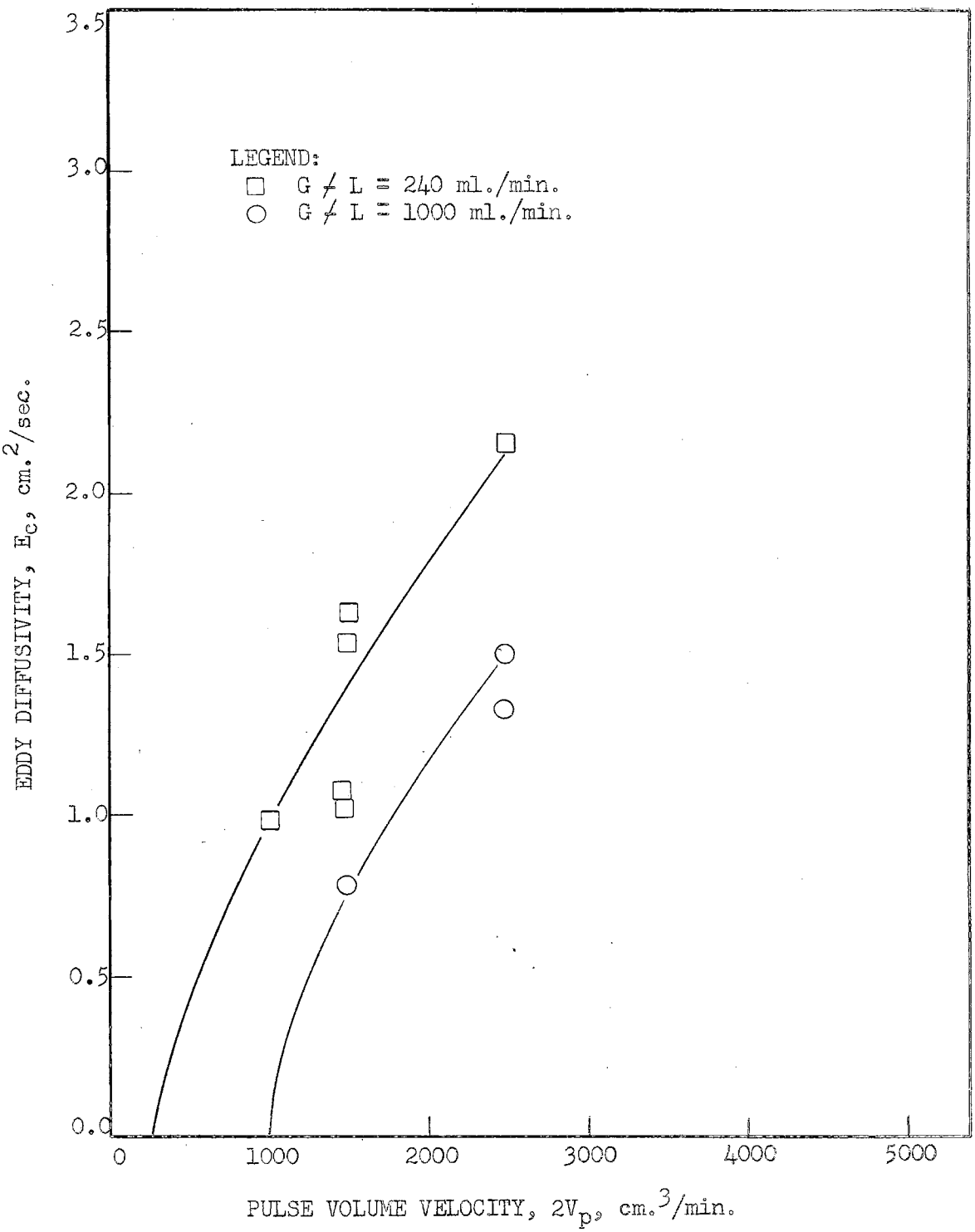

FIGURE 16. EDDY DIFFUSIVITY CORRELATION FOR NO PLATE SEALING, G ≠ L = 240 AND 1000 ml./min.

system when no plate sealing is present, it becomes increasingly important to predict the conditions at which plate sealing occurs. The maximums in the eddy diffusivity curves, Figures 10 through 14, again serve as a convenient index of plate sealing. For the MIBK-water system and the toluene-water system at a flow rate sum, $G + L$, of 500 ml./min. the value of the maximum eddy diffusivities, E_c max., are almost equal, 1.75 and 1.80. These systems differed considerably in interfacial tension (10.7 and 28.0 dynes/cm.) but only slightly in density difference (0.191 and 0.102) and continuous-phase viscosity, (0.605 and 0.550 cp.).

The three systems utilizing ethylene glycol in the continuous phase varied considerably in viscosity (2.17, 4.23 and 7.86 cp.) and slightly in interfacial tension (7.6, 6.0, and 3.7 dynes/cm.) and in density difference (0.243, 0.270, and 0.289). The values of E_c max. for the three systems at $G + L = 500$ ml./min. were 2.06, 2.14 and 3.13 for the 38-, 62- and 82-weight per cent ethylene glycol solutions, respectively. The most satisfactory correlation available for E_c max. is shown in Figure 17 in which E_c max. is shown to be a linear function of the continuous-phase viscosity for these five systems.

Flow Rate Sum

The effect of the flow rate sum on eddy diffusivity is evaluated graphically in Figure 18 for three different pulse volume velocities. The data for $2V_p = 1450$ include the MIBK-water system, the MIBK-38 per cent aqueous ethylene glycol system, and the MIBK-82 per cent aqueous ethylene glycol system. All flow rate ratios, G/L, were 1/1 except for run 33, in which $G/L = 3$. The data at $2V_p = 2450$ were for the toluene-water and the MIBK-water systems with flow rate ratios approximating 9/1,

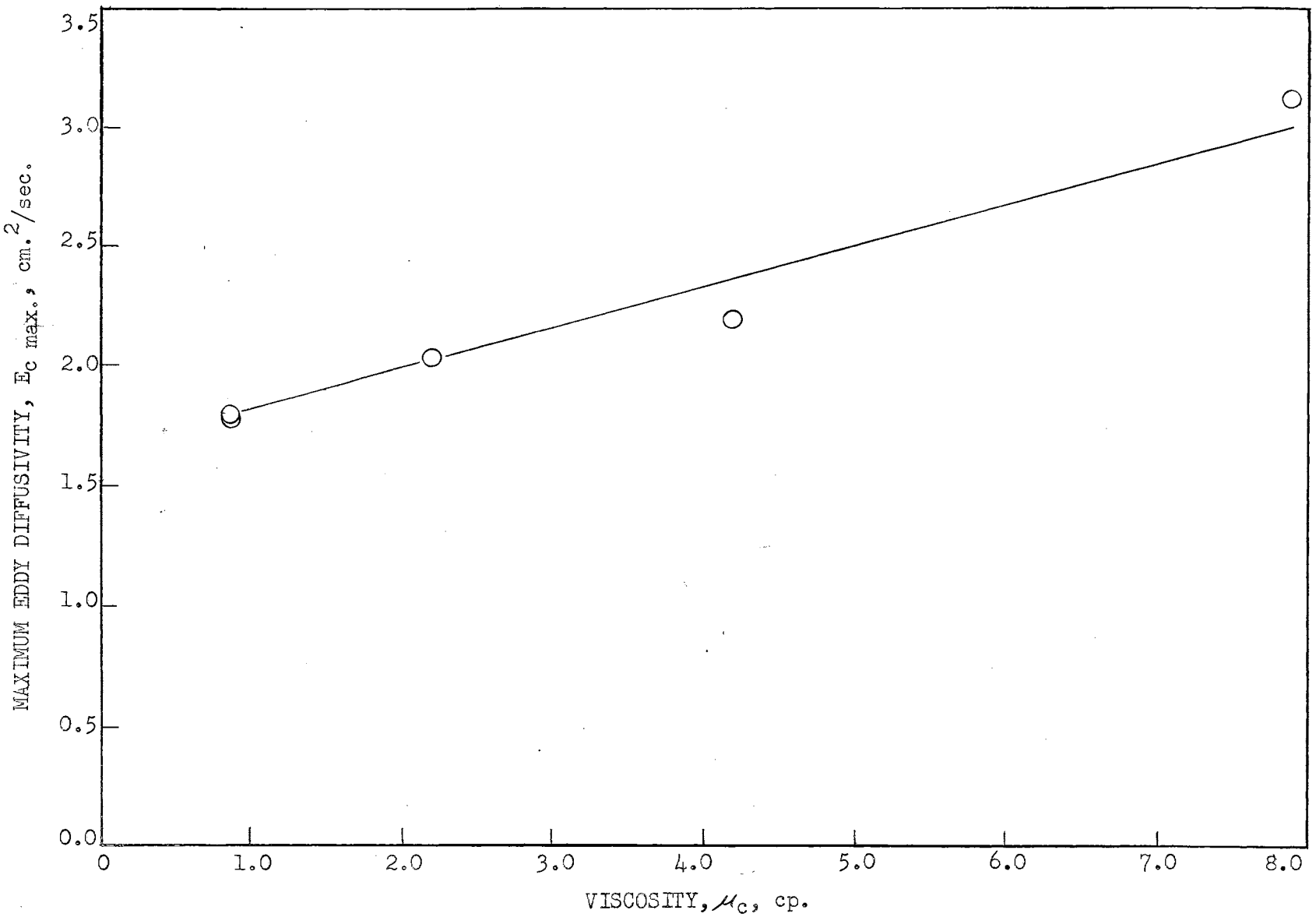

FIGURE 17. EFFECT OF VISCOSITY OF PLATE SEALING

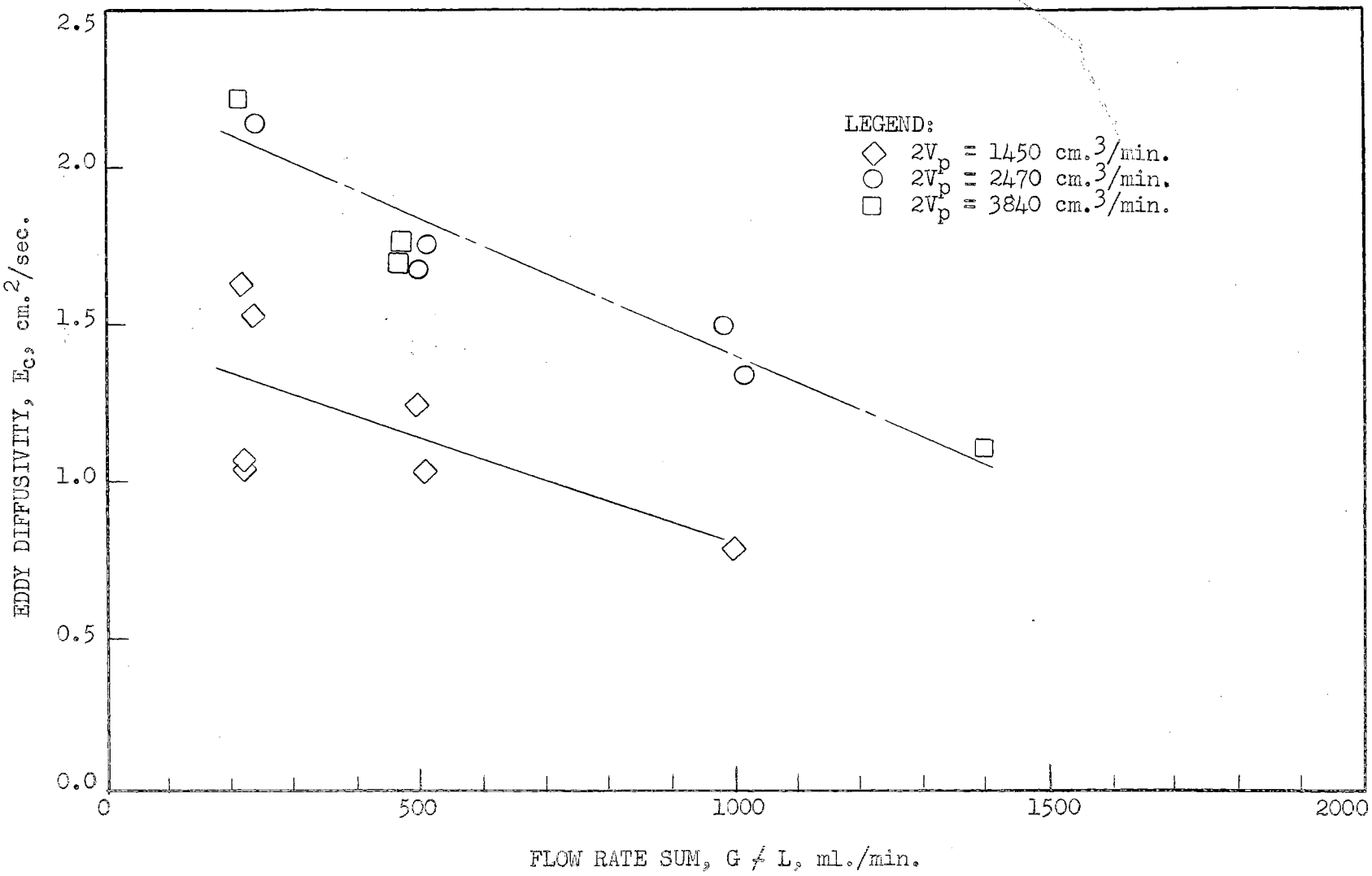

FIGURE 18. EFFECT OF THE FLOW RATE SUM ON EDDY DIFFUSIVITY

1/1, and 1/9. The third set of data, for a pulse volume velocity of 3840, involved only the MIBK-water system and flow rate ratios of 1/1 and 1/3. Each of the three sets of data were correlated with some degree of acceptability with a straight line. A better fit of the data undoubtedly could be obtained by a more complex relation between the variables, but this does not appear justified at present.

A comparison of the experimental results of Figure 18 with the predicted response of $E_c/\Delta z$ in Figure 9 indicates one important relation; namely, that the value of Δz remains relatively constant at a single value of $2V_p$, independent of the flow rate sum, system properties, and the flow rate ratio. This relation is later utilized in correlating values of Δz.

Flow Rate Ratio

The effect of the flow rate ratio, G/L, was best demonstrated by the toluene-water system, as is shown in Figure 11. Eight runs are shown in the graph, corresponding to two sets of four runs each. The flow rate ratios for these two sets were approximately 1/9 and 9/1 but yet the eddy diffusivities at corresponding pulse volume velocities were nearly the same. The continuous-phase backmixing model of Chapter III [Equation (26)] predicts $E_c/\Delta z$ for G/L = 1/9 and $2V_p$ = 2470, divided by $E_c/\Delta z$ for G/L = 9/1 and $2V_p$ = 2470, is equal to 1.17. The ratio of the experimentally-determined values of E_c at the same flow rate ratios and pulse volume velocity, was 0.96. Although these two numbers are not directly comparable because of the uncertainties in the effective concentration distances, Δz, they do lend added confidence to the utility of the mathematical backmixing model.

In the region approaching insufficient pulsation flooding, as in

runs 21 and 25, the flow rate ratio appears to have a more pronounced effect on E_c. For these two runs, G/L was approximately 1/9 and 9/1, respectively, while $G \neq L = 500$ and $2V_p = 545$. The ratios of $E_c/\Delta z$ and the ratios of E_c were 3.42 and 4.56, respectively, the 1/9 flow rate ratio data again being the larger value.

At a higher flow rate sum ($G \neq L = 1000$) as in runs 20 and 23, the calculated value of the ratio of $E_c/\Delta z$ is 1.42. The experimental value of the ratio of E_c for these runs is 0.89. This must be considered poor agreement, due either to experimental inaccuracy or to wide divergence in the values of Δz for the two conditions. A fifth pair of runs, T-6 and T-15, were made using the MIBK-water system at flow rate ratios of 1/1 and 1/3 respectively. These data are shown in Figure 10 for $G \neq L = 500$ and $2V_p = 3840$. The ratio of the calculated $E_c/\Delta z$ and the ratio of the experimental E_c values for the two runs are 0.93 and 1.04, respectively.

Column Height

The effect of column height and an indication of the reproducibility of backmixing data were evaluated in runs T-11 and T-46: Run T-11 was a conventional run using all ten plates in the pulse column, the total distance from the dispersed phase entrance to the liquid interface being 19.8 inches. In run T-46 the interface was positioned midway between plates 4 and 5 (see Figure 3) giving an effective column height of 9.5 inches. Both runs were made at a pulse volume velocity of 1450 cm.^{3}/min. and at a flow rate ratio of 1/1. The flow rate sums were 237 and 222 ml./min. for runs T-11 and T-46 respectively. The eddy diffusivities obtained were 1.53 and 1.64, a deviation of 6.7 per cent. A comparison of these data with other paired data, such as runs T-36 and T-38, and T-8 and T-44, in

which the average per cent deviation was 6.8, indicates that column height had no effect on backmixing for the two-fold range examined.

Plate Material

Aluminum plates were used in the column during the early phases of the over-all study, which includes most of the backmixing data. Runs T-27, 28, 29, 30, 42, 43, 44, 45, 46, and 47, as well as all extraction runs, utilized the stainless steel plates. Runs T-11 and T-46, and runs T-8 and T-44, were pairs of duplicate determinations in which different plate materials were employed. Eddy diffusivities of 1.53 - 1.64 and 1.20 - 1.10 were obtained. Again, within the reproducibility of the experiment, these data indicate that changing plate materials from aluminum to stainless steel had little or no effect on backmixing.

Backmixing Data Rejection

Some comment must be made concerning runs T-1, 2, 3, 4, 9, and 12. These runs were omitted from the study because of insufficient or inadequate tracer concentration-profile data. The primary difficulty was that backmixing was often less than anticipated, hence the concentration of the manganese tracer in many of the continuous-phase samples was below that required in the analysis. Only in run T-1 was the situation reversed, all concentrations being greater than desired for analysis (200 ppm of Mn.).

Effective Concentration Distance, Δz

Calculated values of the effective concentration distance, Δz, are given in Table II. These data include all runs on the five two-phase systems at flow rate sums of 240, 500, and 1000 ml./min. in which plate sealing effects were judged to be absent. As has been described previously,

TABLE II

CALCULATED VALUES OF THE EFFECTIVE

CONCENTRATION DISTANCE

Run Number	System	G ≠ L ml./min.	$2V_p$ ml./min.	$E_c/\Delta z$ Calculated cm./sec.	E_c Experimental $cm.^2/sec.$	Δz cm.
T-5	MIBK-H_2O	510	1450	0.484	1.035	2.14
7	"	500	2560	0.955	1.670	1.75
13	"	485	512	0.287	0.265	3.86
17	Tol.-H_2O	482	2470	0.798	1.741	2.18
18	"	491	2470	0.995	1.671	1.68
21	"	500	545	0.122	0.657	5.37
25	"	502	545	0.0367	0.141	3.85
31	MIBK-EG	488	2980	1.068	2.350	2.20
32	(38%)	492	2220	0.699	1.886	2.70
33	"	495	1438	0.401	1.236	3.08
34	"	501	3750	1.415	2.061	1.46
35	"	545	3330	1.295	1.541	1.19
41	"	465	2980	1.135	1.715	1.51
28	MIBK-EG	475	512	0.0525	0.448	8.52
29	"	496	3590	0.955	2.176	2.28
30	(62%)	483	2050	0.693	1.121	1.62
39	"	485	2720	0.970	1.920	1.98
40	"	505	1615	0.516	1.232	2.39
47	MIBK-EG (82%)	525	5100	1.99	3.120	1.57
T-11	MIBK-H_2O	237	1450	0.541	1.525	2.82
43	"	233	2470	0.969	2.150	2.22
46	"	222	1450	0.548	1.638	2.99
36	MIBK-EG	237	1450	0.550	1.029	1.87
37	(82%)	250	1023	0.364	0.974	2.60
38	"	227	1450	0.547	1.043	1.91
T-14	MIBK-H_2O	1010	1450	0.286	0.780	2.73
20	Tol.-H_2O	1012	2470	0.934	1.324	1.42
23	"	985	2470	0.658	1.491	2.27
EM-1*	Kerosene-	935	8120	3.13	10.41	3.34
2	H_2O	940	8120	3.01	11.20	3.72
3	"	904	8120	3.11	10.57	3.40
4	"	948	9041	3.49	10.17	2.92
5	"	937	8120	3.16	10.65	3.37
6	"	1175	8120	3.01	11.20	3.72
7	"	935	5800	2.16	8.11	3.76

* From the experimental data of Swift and Burger (39), Table IX

the maximum in the correlation of E_c as a function of $2V_p$, Figures 10 through 14, formed the criteria for judging when plate sealing effects were present. The data are correlated in Figure 19 in the form of Δz as a function of the pulse volume velocity, $2V_p$. These data indicate that over the ranges examined, Δz is not strongly dependent on the flow rate sum, flow rate ratio, or fluid system.

A question that arises is whether the column geometry affects the effective concentration distance. Some experimental backmixing data of Swift and Burger which are available in the literature, are given in Table IX, Appendix B. These data are for a pulse column of the same internal diameter as that used in this study but of a different plate geometry and for different pulsing conditions. The calculated values of Δz are included in Table II and are correlated as a function of the pulse volume velocity in Figure 19. The significant deviation between the two sets of data indicate that Δz must be primarily a function of column geometry and/or pulse amplitude.

Concentration Profiles

Concentration profiles for the plated section of the pulse column were determined experimentally for both the extract and the raffinate phases for operations in both the mixer-settler and the emulsion regions. A total of ten runs are reported, involving three three-component systems. The concentration profiles for these ten runs were predicted from the simplified mathematical model of Miyauchi (26) using the eddy diffusivity values (both with and without plate sealing) from the first phase of this study.

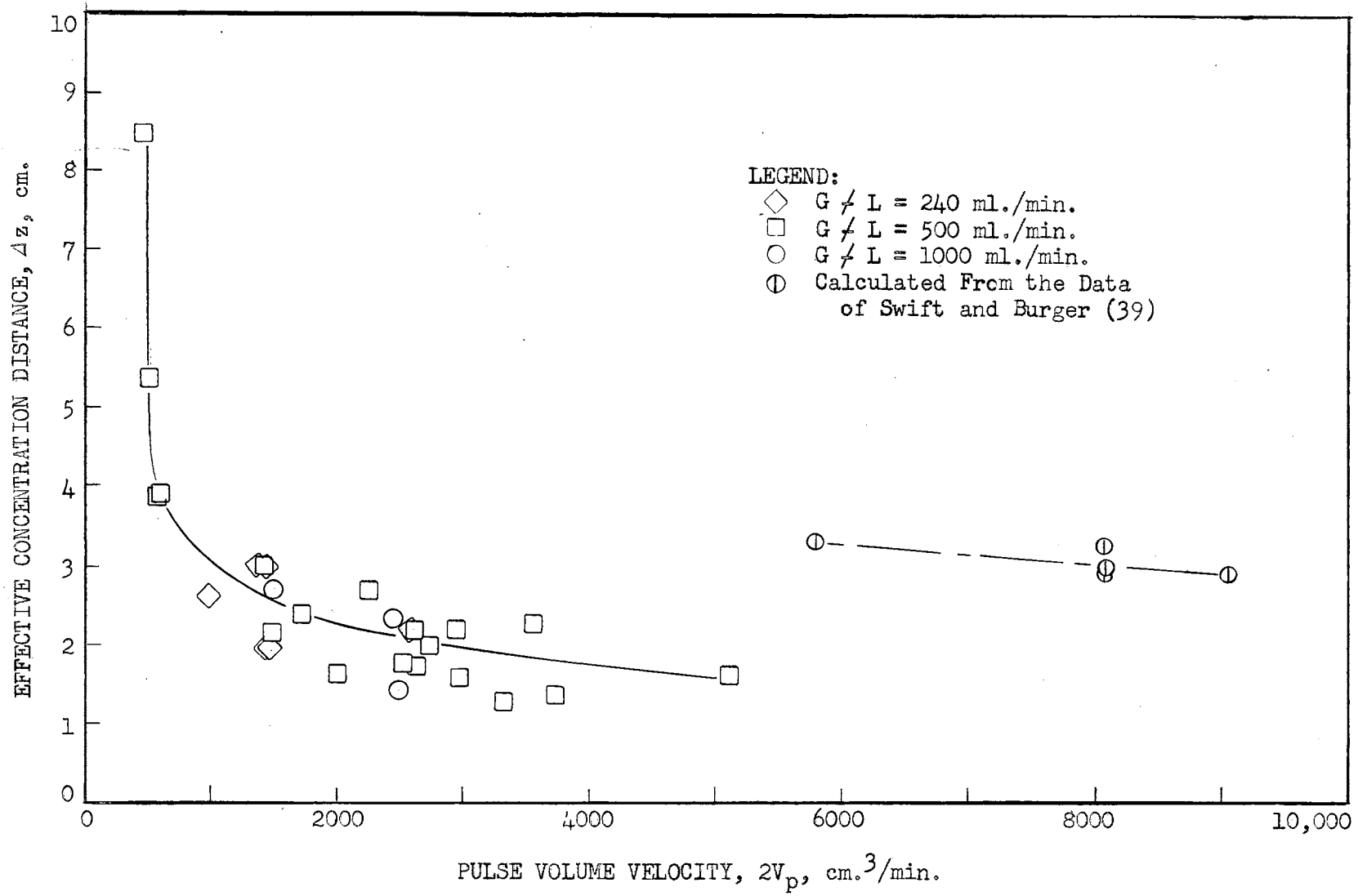

FIGURE 19. EFFECT OF THE PULSE VOLUME VELOCITY ON THE EFFECTIVE CONCENTRATION DISTANCE

Boundary conditions for mass transfer at the column interface were derived in Chapter III and applied to the mathematical backmixing model of Miyauchi. The two cases considered were for plug flow of the raffinate phase and for plug flow of the extract phase; the other phase in each case was considered to undergo a finite amount of backmixing. The resulting backmixing model (with extraction occurring at the column interface) was also used to predict the concentration profiles of both phases for the ten extractions runs.

An additional modification to the backmixing model of Miyauchi was the redefinition of the dimensionless concentration ratios X and Y. The terms $\emptyset$ and Υ, which were defined in Chapter III and applied to the backmixing model, allowed for straight equilibrium distribution curves with non-zero intercepts. This modification increased the utility of the model considerably, especially at higher concentrations.

Before discussing the results obtained for each extraction system, one clarification must be made. Both the experimental data and calculations using the interface mass-transfer model indicate that the concentration of the continuous extract phase in the column at $z = o$, C_{yo}, is greater than the stream leaving the column, C_y^o. This result appears erroneous unless one considers the fact that the point $z = o$ is not the true bottom of the pulse column, but rather the point of the dispersed-phase entrance. Below this point, there is a large disengaging section from which backmixing occurs. The backmixing from this lower section transfers solute up the column with no net transfer of continuous phase volume. To maintain steady state conditions, the concentration of solute in the continuous phase which is flowing into the disengaging section, C_{yo}, must be greater

than the concentration of solute in the continuous phase flowing out, C_y^o.

MIBK-Acetic Acid-Water System

The MIBK-acetic acid-water system concentration profiles, both experimental and theoretical, for extraction runs E-9, E-10, E-11, and E-12, are shown in Figures 20 through 23. A tabulation of these data and their respective operating conditions are given in Tables X through XV, Appendix C. The range of operating variables for these four runs includes feed concentrations of 0.0396 to 0.0490 lb.moles/ft.^{3}, flow rate sums of 235 and 500 ml./min., and pulse volume velocities of 1450 to 5120 ml./min.

The theoretical concentration profiles were calculated for runs E-9, E-10, and E-12, using two sources of values for eddy diffusivities; data from Figures 15 and 16 for no plate sealing, or from Figure 10 for cases in which the plate sealing phenomena was observed. These runs were at pulse volume velocities of 3840, 3840, and 5120 cm.^{3}/min. respectively. Run E-11 was made using a pulse volume velocity of 1450 cm.^{3}/min.; hence, it was not effected by plate sealing. Figures 20 through 23 indicate that the theoretical concentration profiles which are based on eddy diffusivities with no sealing agreed best with the experimental data. The addition of the interface mass-transfer boundary condition to the model of Miyauchi also significantly improved the agreement for the extract phase (finite backmixing) without altering that of the raffinate phase (in slug flow).

The existance of plate sealing during a pulse column operation causes a decrease in backmixing of the continuous phase and therefore a lowering of the eddy diffusivity value. It is evident that if the values of E_c that were determined when plate sealing occurred in the two component system were used to calculate a concentration profile during extraction

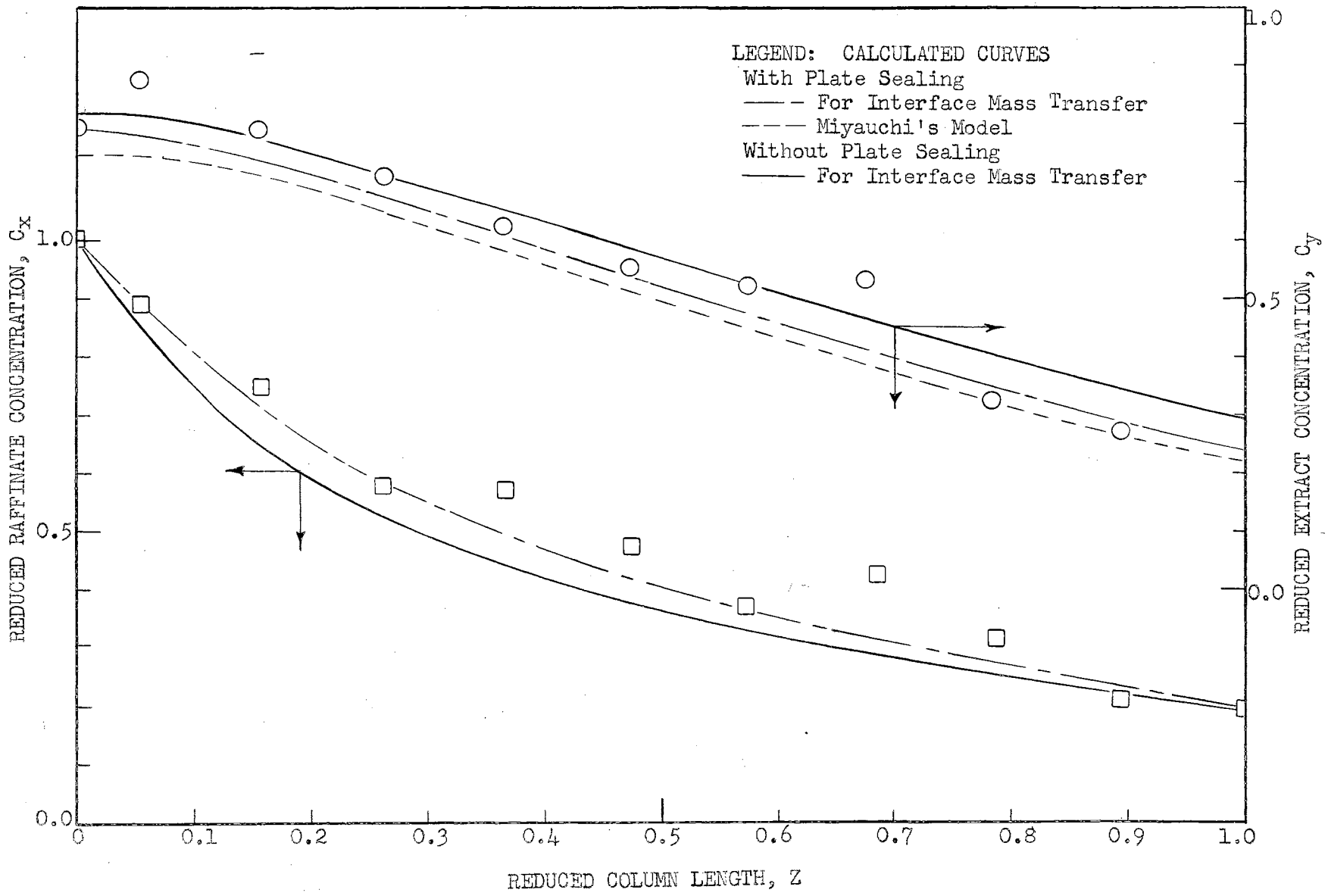

FIGURE 20. EXPERIMENTAL AND CALCULATED CONCENTRATION PROFILES, RUN E-9

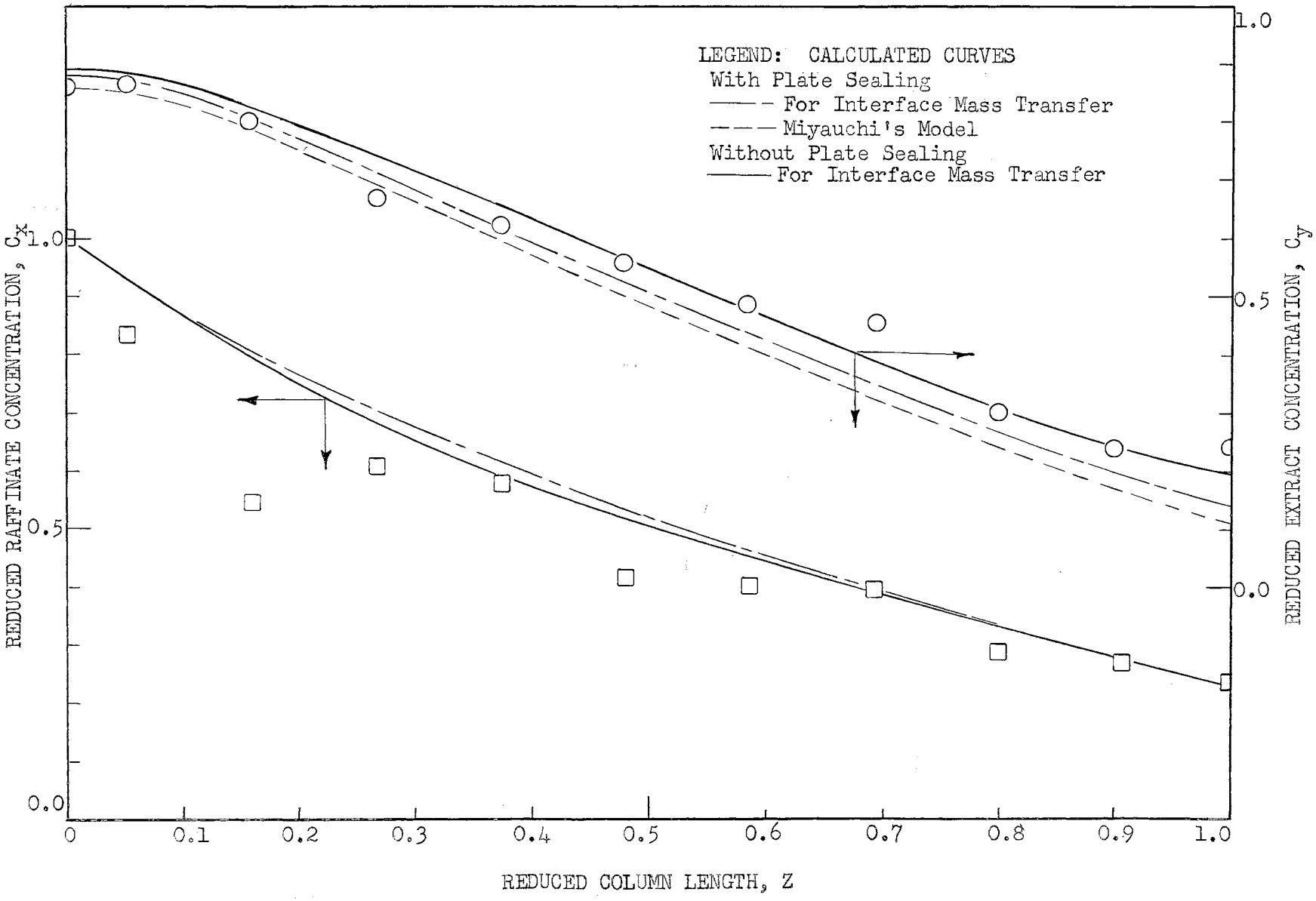

FIGURE 21. EXPERIMENTAL AND CALCULATED CONCENTRATION PROFILES, RUN E-10

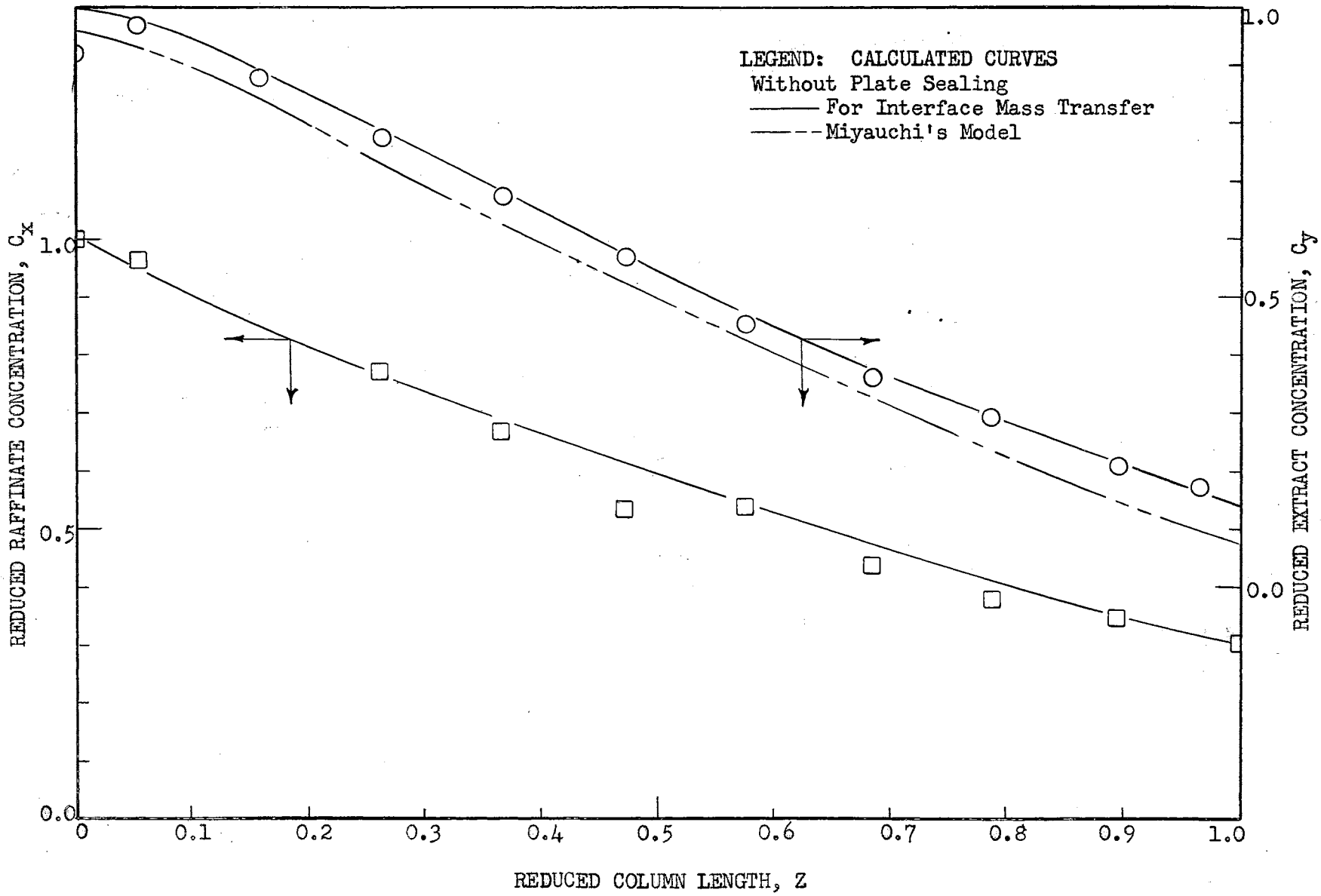

FIGURE 22. EXPERIMENTAL AND CALCULATED CONCENTRATION PROFILES, RUN E-11

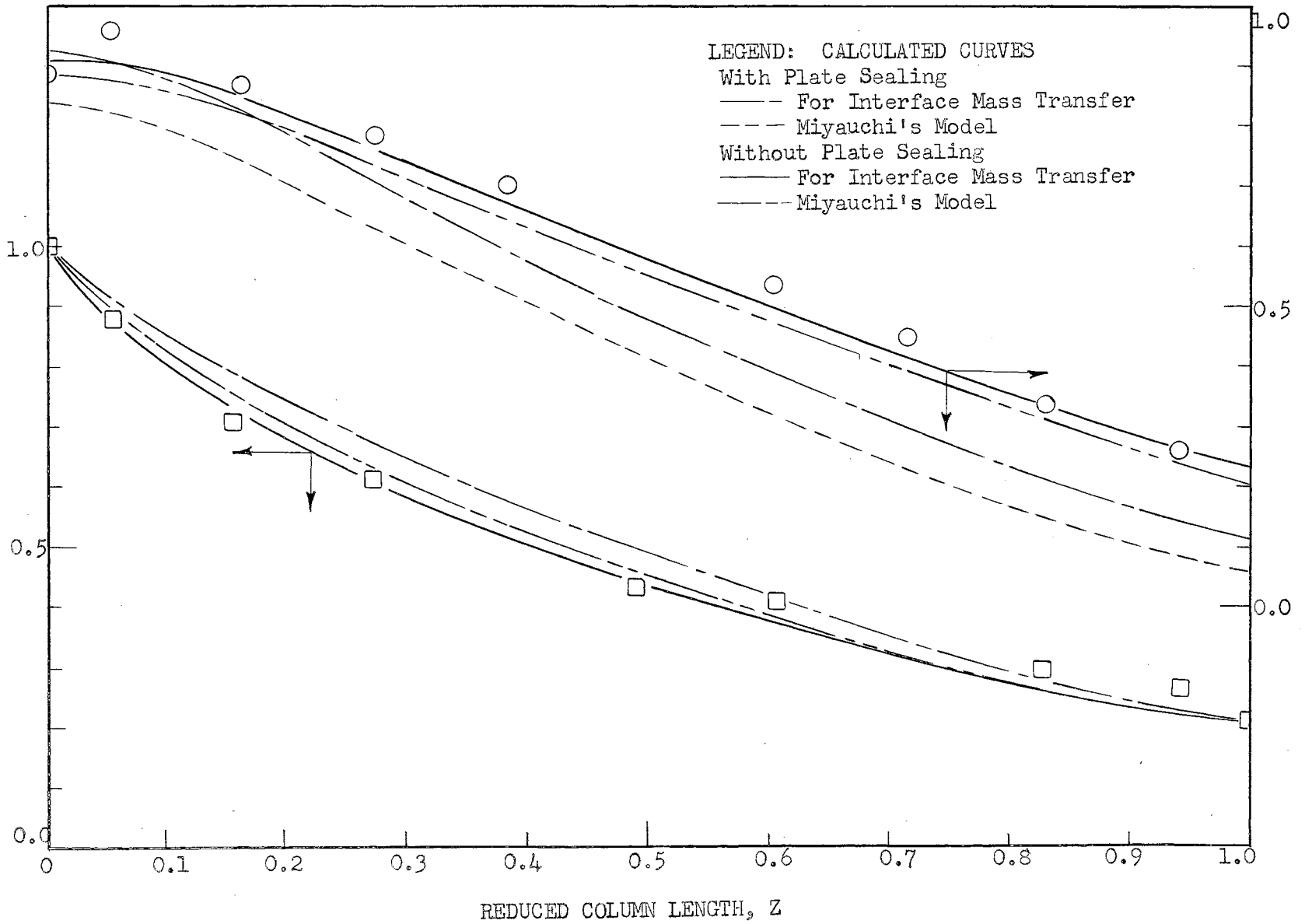

FIGURE 23. EXPERIMENTAL AND CALCULATED CONCENTRATION PROFILES, RUN E-12

when no plate sealing was evident, then the calculated concentrations would be too low. This conclusion is confirmed in Figures 20 through 23.

Toluene-Benzoic Acid-Water System

In runs, E-6, E-7, and E-8, the primary variables were the flow rate sum and direction of mass transfer. A pulse volume velocity of 2470 ml./min. was used for each run, this value being in the region below that in which plate sealing occurs. For runs E-7 and E-8 the flow rate sums were 1006 and 235 ml./min. and the flow rate ratios were 0.111 and 0.1185, respectively. Benzoic acid was transferred from the dispersed toluene phase to the aqueous continuous phase in both of these runs. As shown in Figures 24 and 25 and Tables XVI to XX, Appendix C, the agreement between experimental and calculated concentration profiles was good for run E-8 and only fairly good for run E-7. The interface mass-transfer boundary condition improved the agreement between theoretical and experimental profiles for run E-8 but had no effect on the profile for run E-7.

Run E-6 was the one run of the study in which mass transfer was from the continuous aqueous phase to the dispersed organic phase. A flow rate sum of 500 ml./min. and flow rate ratio of 0.111 was used. Again, the calculated concentration profiles were in fair agreement with experimental data, see Figure 26. It is difficult to judge if the interface mass-transfer boundary condition materially improved Miyauchi's equation; but for the aqueous raffinate phase, the discontinuity at the entrance is predicted, just as one would expect for backmixing within this phase. The latter is the same phenomena encountered by Geankoplis, et.al. (15), (16).

Toluene-Acetic Acid-Water System

Concentration profile data for the three runs of this system are

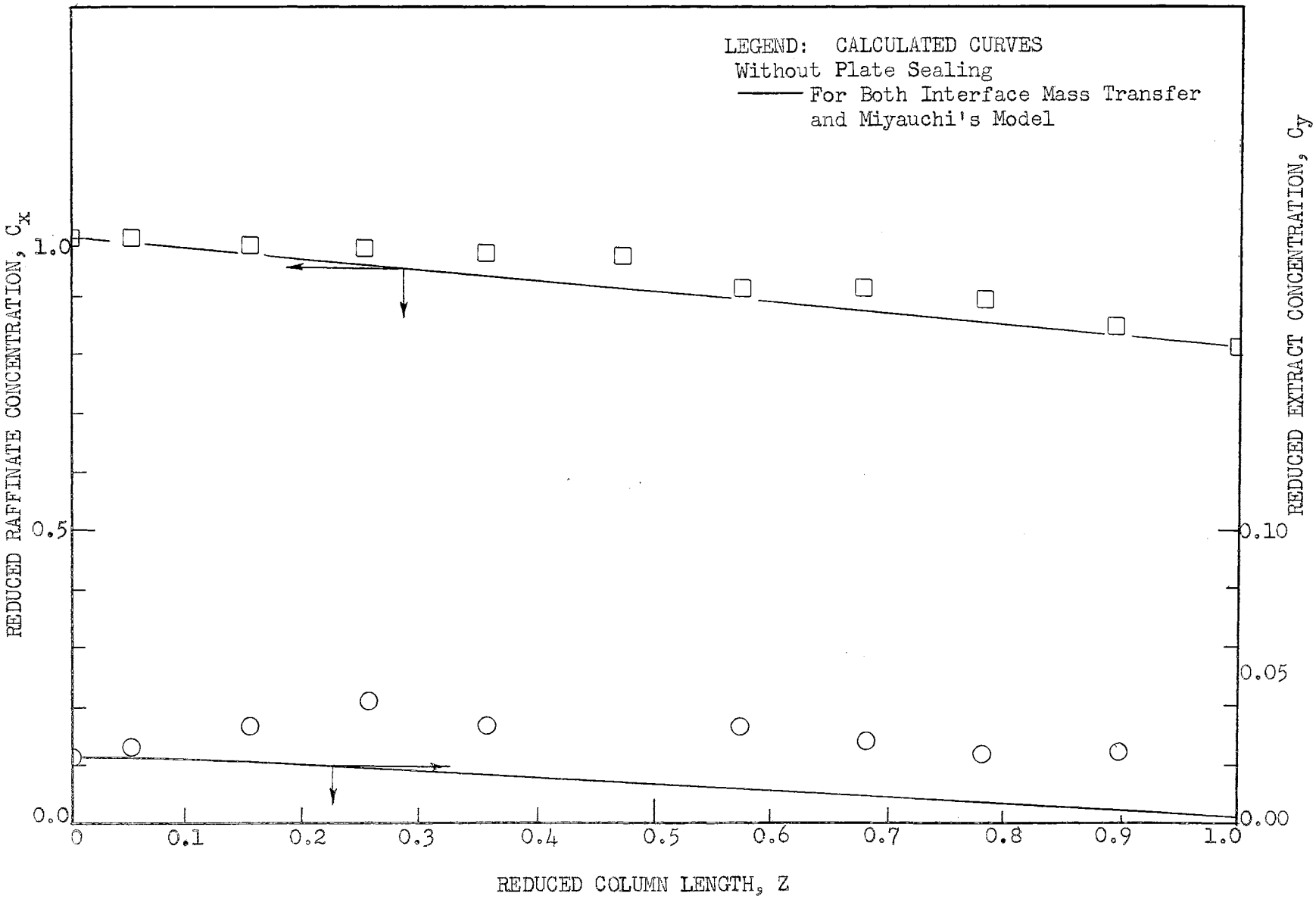

FIGURE 24. EXPERIMENTAL AND CALCULATED CONCENTRATION PROFILES, RUN E-7

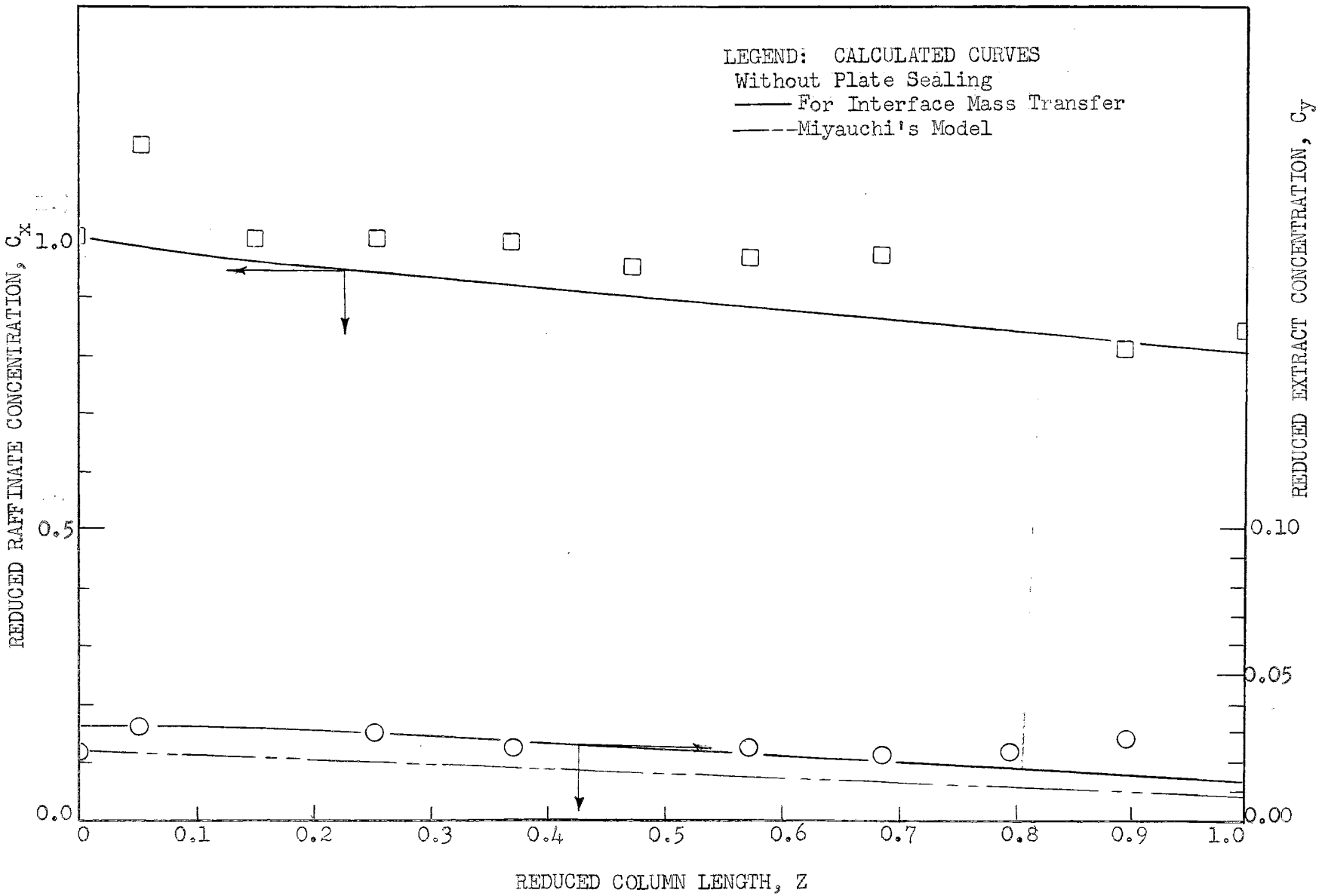

FIGURE 25. EXPERIMENTAL AND CALCULATED CONCENTRATED PROFILES, RUN E-8

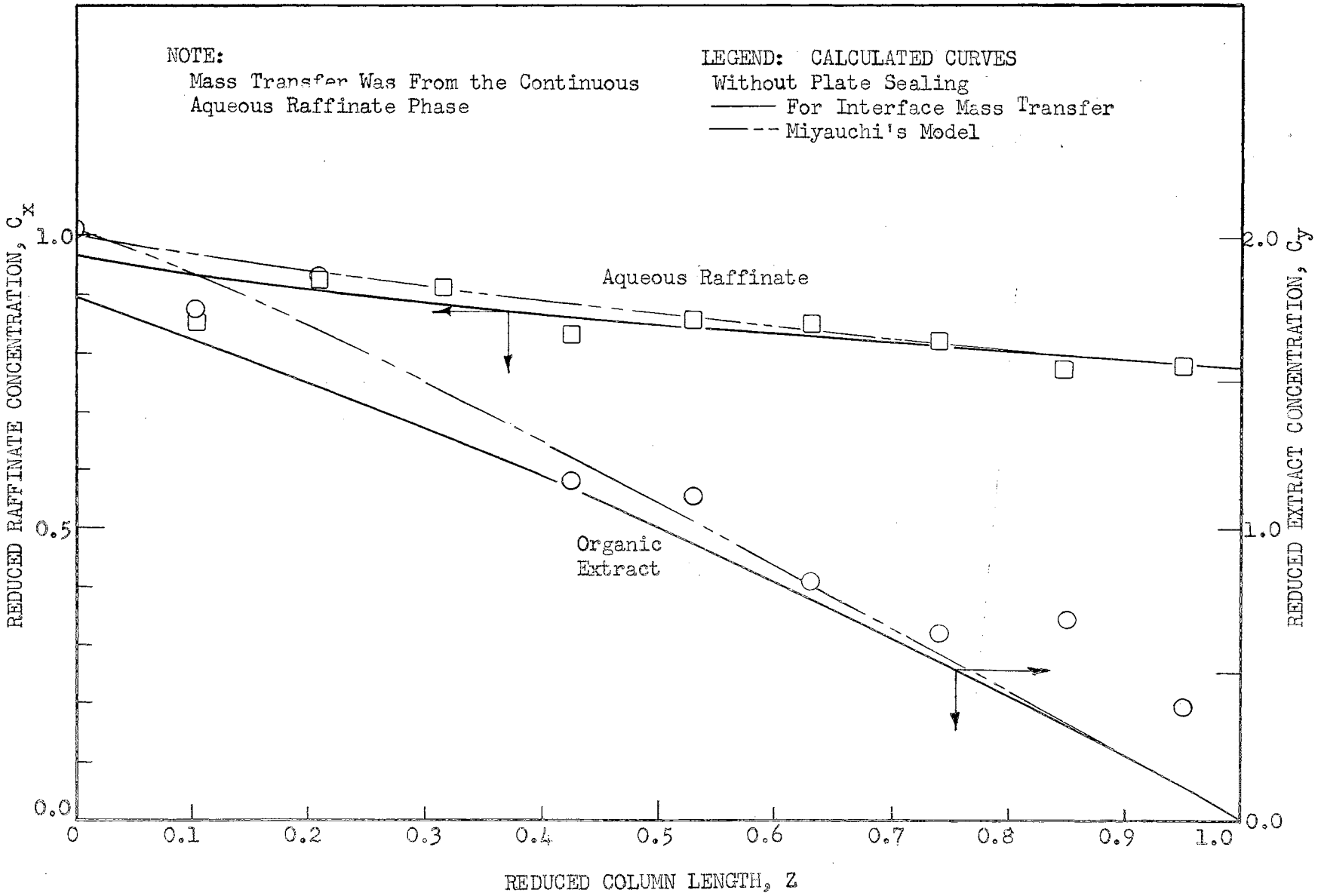

FIGURE 26. EXPERIMENTAL AND CALCULATED CONCENTRATION PROFILES, RUN E-6

shown in Figures 27, 28 and 29. These runs were all at a flow rate sum of 500 ml./min., but at pulse volume velocities of 2470, 545 and 4460 ml./min. for runs E-3, E-4, and E-5, respectively. The general agreement between experimental and calculated concentration profiles is fair, but not as good as for the other two systems. The principal difficulty encountered with this system was in proper representation of the equilibrium distribution. For runs E-3 and E-5, the representation was by a straight equilibrium distribution curve with a non-zero intercept. A McCabe-Thiele type diagram is given in Figure 32 in which the linear approximation is shown. In run E-4 backmixing was very low and the concentration of the continuous extract phase at the dilute end of the column approached zero. These low concentrations required the representation of the non-linear equilibrium distribution curve with a straight line of zero intercept.

Run E-4 was the one run of the examination which was in the mixer-settler region of operation. Samples of the dispersed phase were taken with the stainless-steel sampling probe from the coalesced phase under each plate, instead of from the polyethylene funnels attached to the perforated plates. A comparison of the experimental and theoretical concentration profiles (Figure 32, and Tables XXII and XXIV, Appendix C) indicate that poor agreement was attained. The poor agreement can probably be attributed to the experimental technique used, the eddy diffusivity value being too low, and/or the representation of the equilibrium distribution data being inadequate.

Mass-Transfer Correlations

The number of over-all transfer units, N_{ox}, the over-all mass-transfer

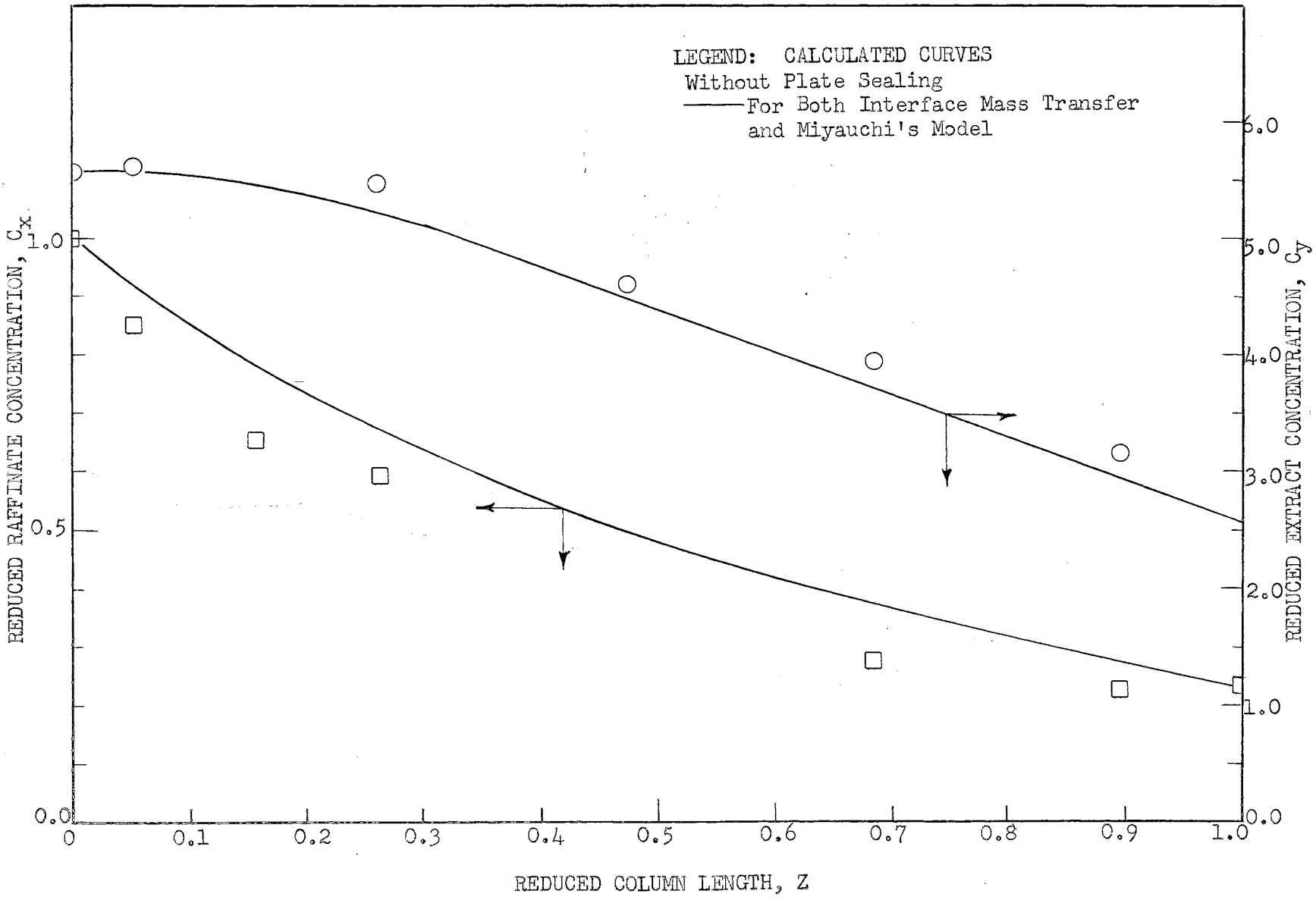

FIGURE 27. EXPERIMENTAL AND CALCULATED CONCENTRATION PROFILES, RUN E-3

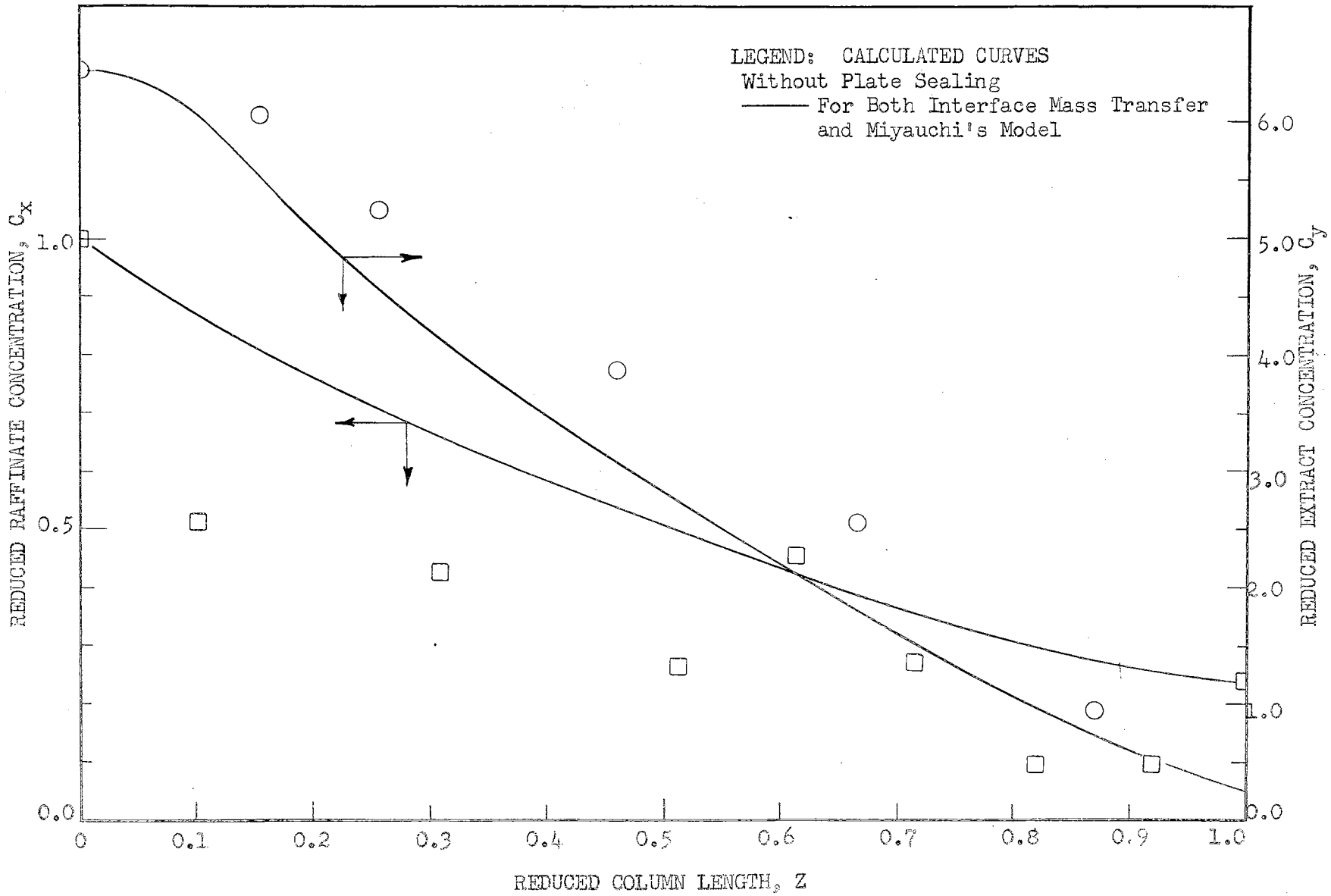

FIGURE 28. EXPERIMENTAL AND CALCULATED CONCENTRATION PROFILES, RUN E-4

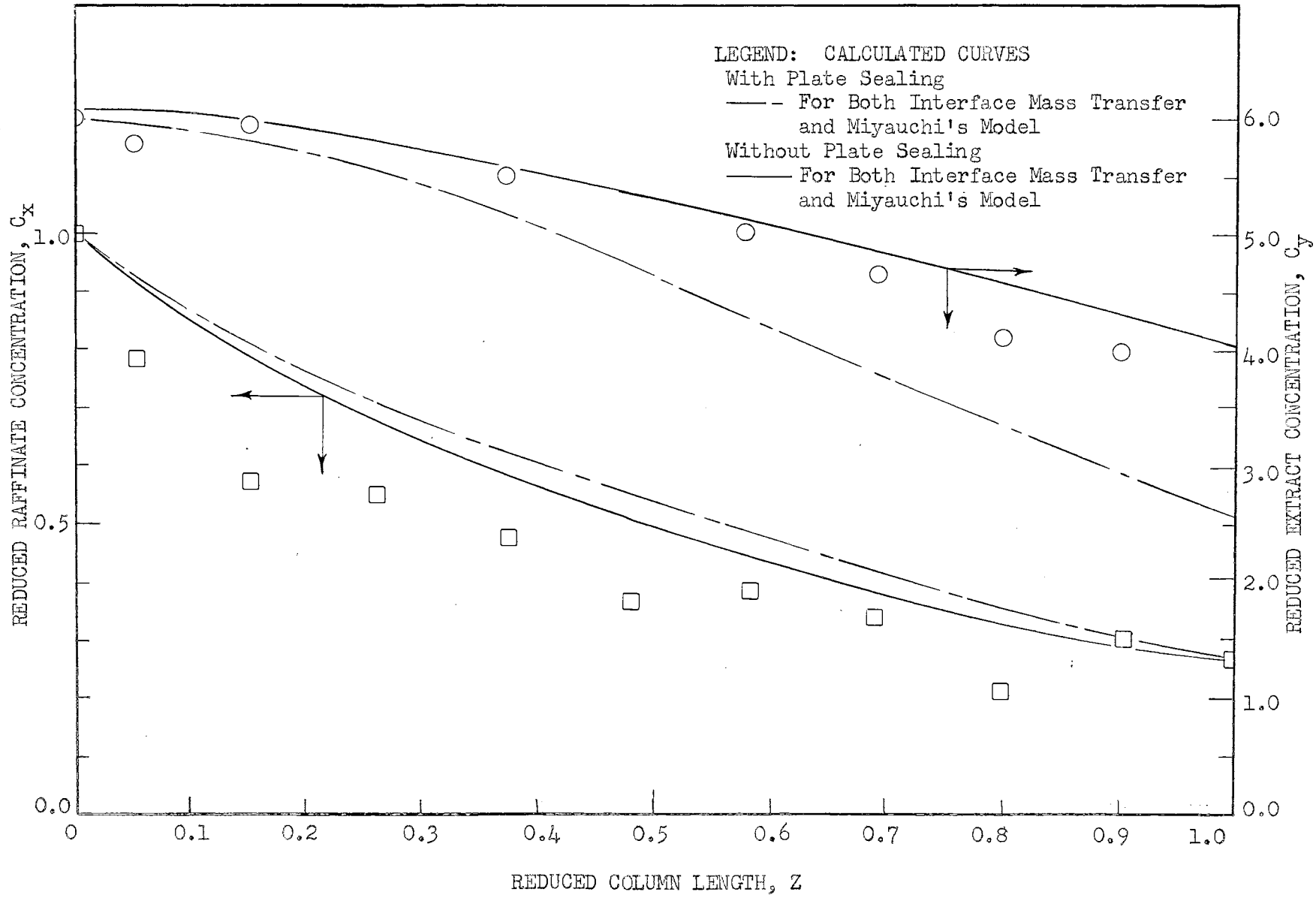

FIGURE 29. EXPERIMENTAL AND CALCULATED CONCENTRATION PROFILES, RUN E-5

coefficients, $K_x a$, and the heights of transfer units HTU, are tabulated in Table III. Too few runs were made on any one of the systems to draw valid conclusions as to the various results.

Calculation Methods

Some comments must be made on the calculation methods used. In any extraction study, a certain amount of inaccuracy is involved in over-all material balances. For the runs in this study, all material balance errors were below seven per cent, except for runs E-3 and E-8 in which these values were 18.8 and 13.5 per cent, respectively. Although appearing excessive, these errors were really equivalent to only small variations in the absolute magnitude of the continuous or the dispersed phase flow rates, 11.6 and 4.2 ml./min. respectively. To circumvent any inconsistancies in the calculations, all values of F_x/F_y for calculation of A were taken as equal to R/E, i.e., to $\Delta c_y/\Delta c_x$.

For calculation of the Peclet numbers, $P_y B$ or $P_x B$, superficial eddy diffusivities, E_c, were used. The superficial eddy diffusivity of the continuous phase is equal to $E_x \epsilon_x$ or $E_y \epsilon_y$, depending on the direction of mass transfer. For example, the extract-phase Peclet numbers can be written as

$$P_y B = (F_y L'/E_y \epsilon_{ye}) = (F_y L'/E_c)(\epsilon_{yt}/\epsilon_{ye})$$

where ϵ_{ye} = void fraction of the extract phase during an extraction run.

ϵ_{yt} = void fraction of the continuous phase during an E_c determination.

The fraction $(\epsilon_{yt}/\epsilon_{ye})$ is nearly one (0.99, for example, in run E-9) and

TABLE III

NUMBER OF TRANSFER UNITS AND OVER-ALL

MASS-TRANSFER COEFFICIENTS

Run Number	Plate Sealing	With Interface Mass Transfer			Miyauchi's Model		
		N_{ox}	$K_x a$ l/hr.	H_{ox} ft.	N_{ox}	$K_y a$ l/hr.	H_{ox} ft.
E-3	No	2.13	58.7	0.75	2.13	58.7	0.75
E-4	No	1.86	50.0	0.87	1.86	50.0	0.87
E-5	No	2.36	66.0	0.66	2.36	66.0	0.66
	Yes	1.90	53.2	0.82	1.90	53.2	0.82
E-6	No	0.27	7.8	5.74	0.30	8.7	5.20
E-7	No	0.23	14.2	6.89	0.23	14.2	6.89
E-8	No	0.29	5.6	5.47	0.26	5.2	5.92
E-9	No	6.12	42.8	0.26			
	Yes	4.23	29.6	0.37	3.85	26.9	0.41
E-10	No	3.00	48.6	0.52			
	Yes	2.67	43.2	0.59	2.50	40.4	0.63
E-11	No	2.24	41.4	0.71	2.00	36.9	0.79
E-12	No	4.30	87.1	0.35	3.94	80.0	0.39
	Yes	3.07	62.3	0.50	2.80	56.9	0.54

was taken as equal to 1.0 for all runs.

The solution of the equations of Miyauchi or those in Chapter III for concentration profiles during extraction require a trial and error procedure. For Miyauchi's equations, there are two quantities, ϕ_1 and Υ_o whose values are known from material balance relations. Convergence on a known value of ϕ_1 for assumed values of N_{ox} was found to be the most satisfactory for all extraction runs except run E-8, in which the experimental value of ϕ_1 was questionable. For the equations involving mass transfer at the column interface, the value of Υ_o is unknown, hence ϕ_1 was used in the solution.

Equilibrium Distribution Data

Equilibrium distribution data for the three systems were taken from the literature (1), (13), (28), (30), (32). These data were at 25 and 27° C. while extraction temperatures for this study were approximately 28 $\pm$ 1° C. These data are plotted in Figures 30, 31, and 32, along with four experimental check values obtained in this study for 83° F. (28.3° C.). No significant variations between literature and experimental data were noted.

Column Stability

Column stability during extraction was observed during runs E-10, E-11, and E-12. Samples of the effluent raffinate, c_{x1}, and the effluent extract, c_{yo}, were taken at convenient intervals throughout the runs. These data are included in Appendix C and are shown in Figure 33 for run E-11. In general, good column stability was noted for all three runs. The stream concentrations appeared to reach steady state within 20 to 25 minutes except for the extract phase in run E-12, which steadily decreased

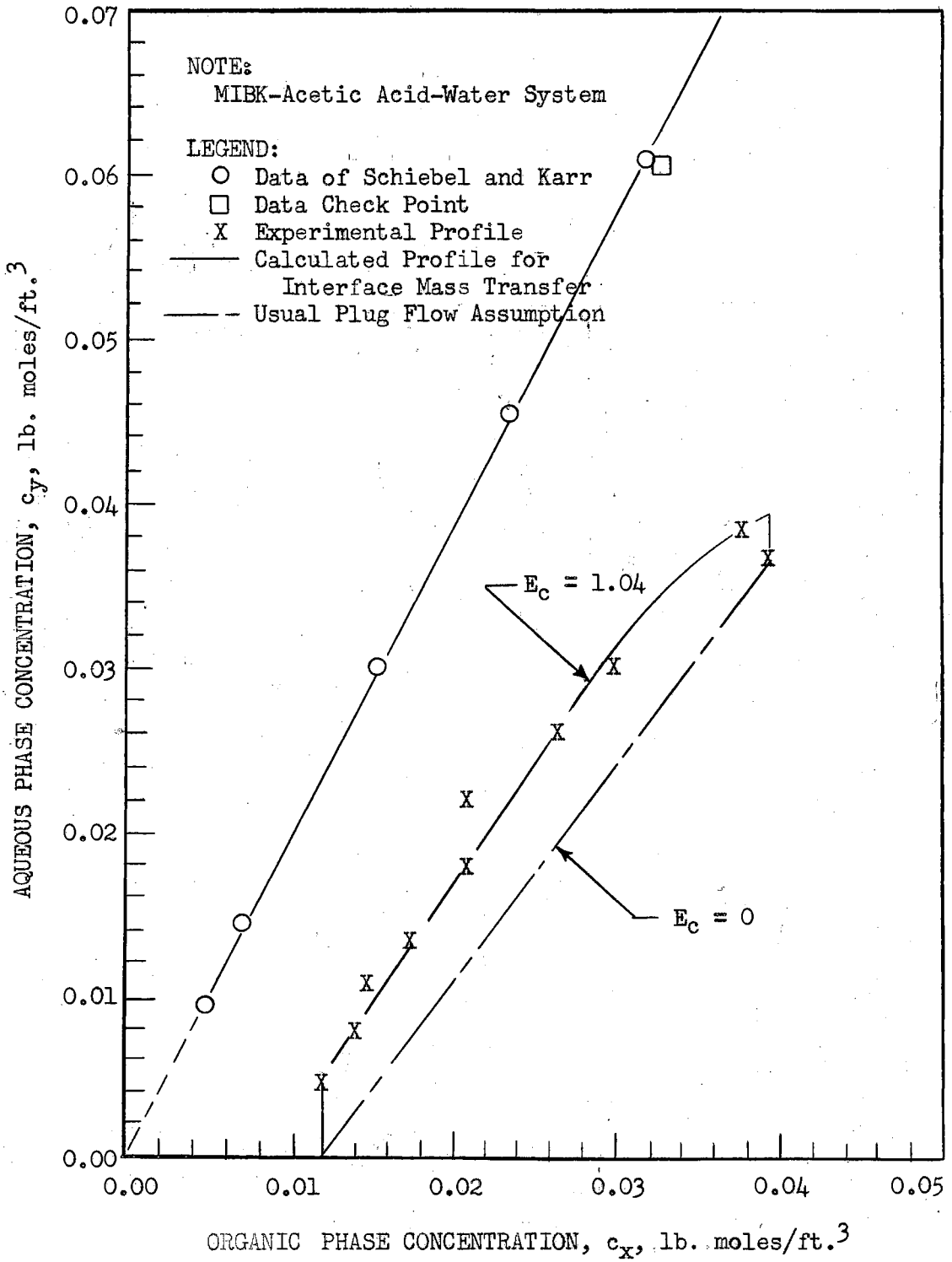

FIGURE 30. EQUILIBRIUM DISTRIBUTION AND OPERATING CURVES, RUN E-11

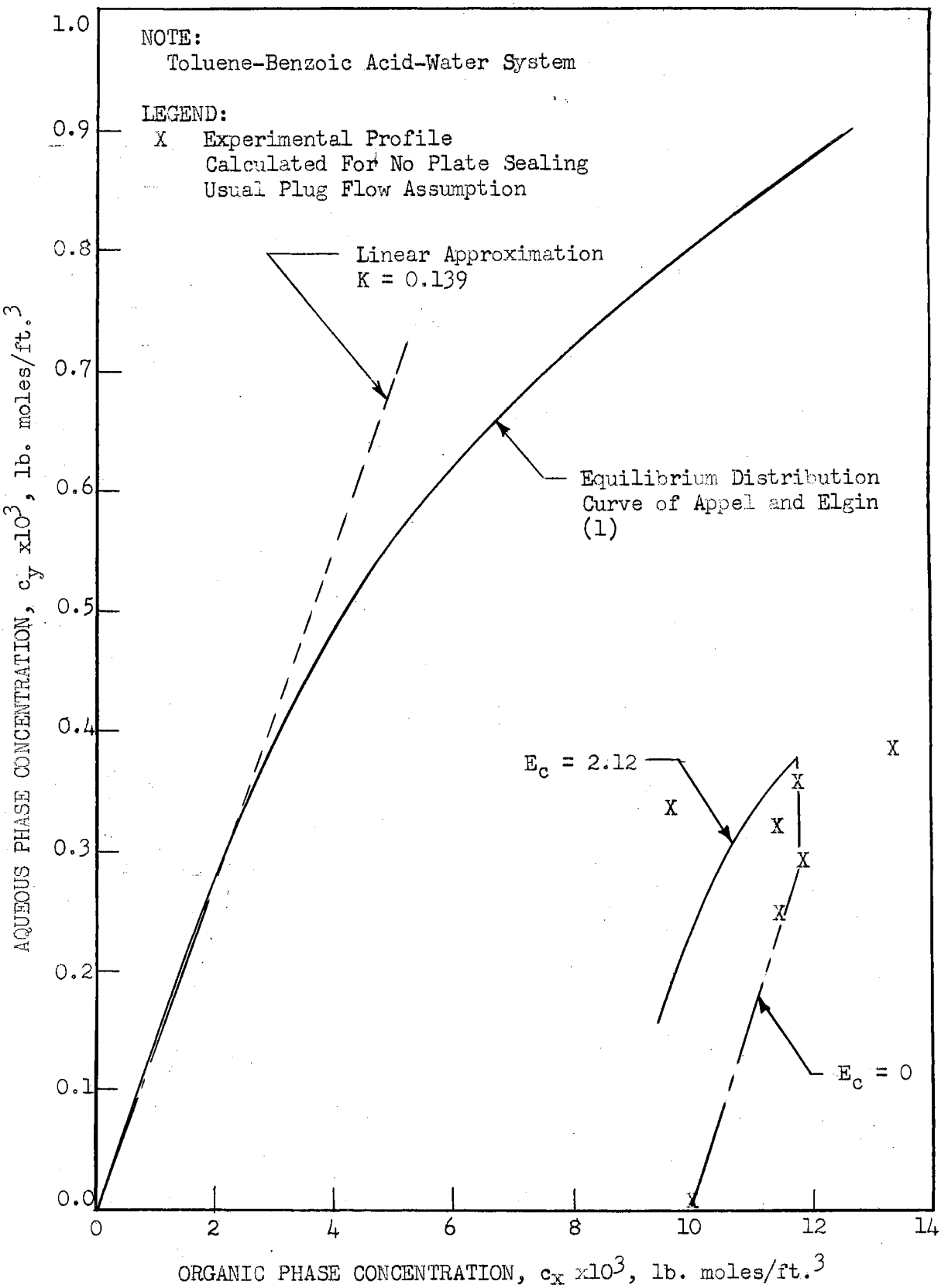

FIGURE 31. EQUILIBRIUM DISTRIBUTION AND OPERATING CURVES, RUN E-8

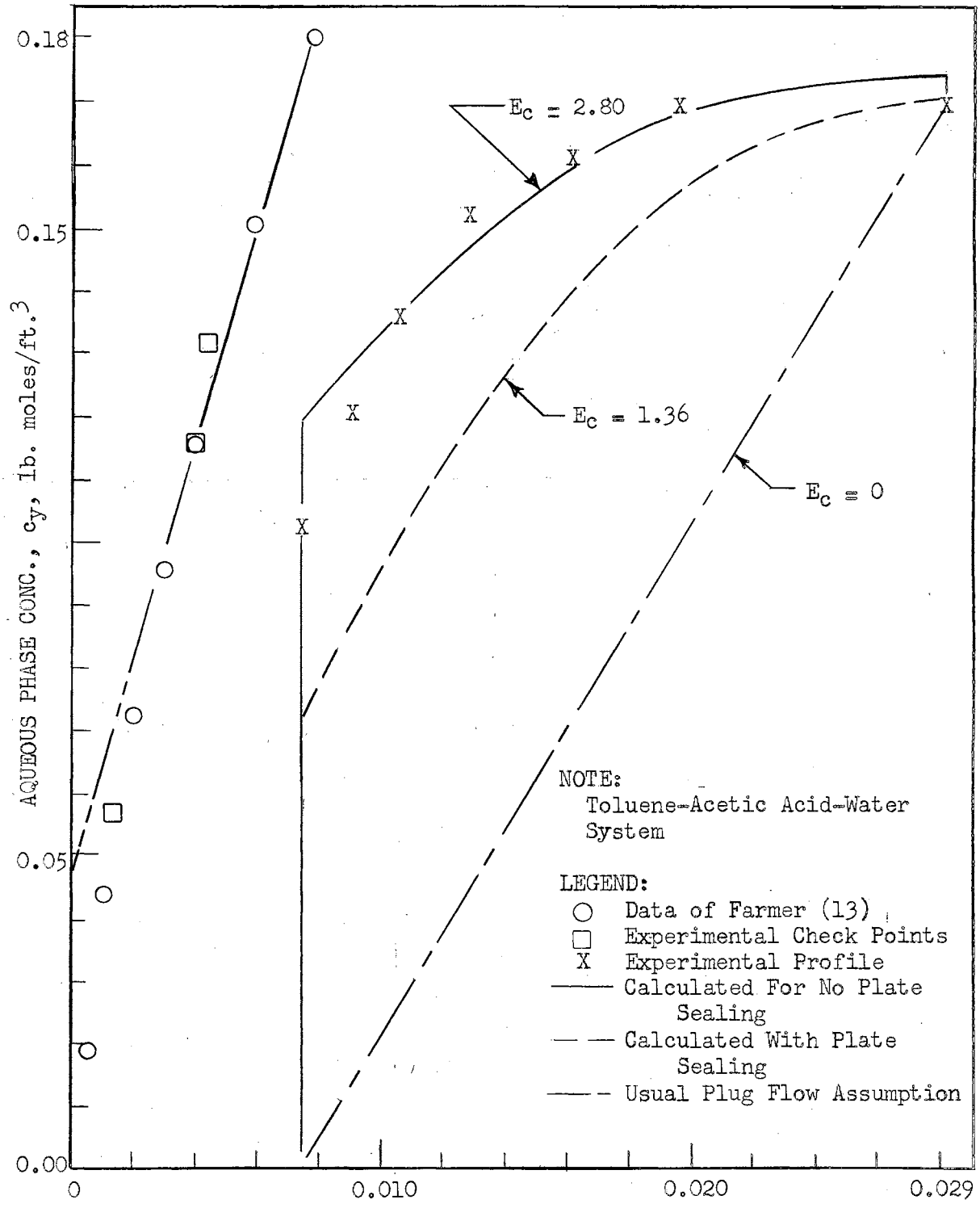

FIGURE 32. EQUILIBRIUM DISTRIBUTION AND OPERATING CURVES, RUN E-5

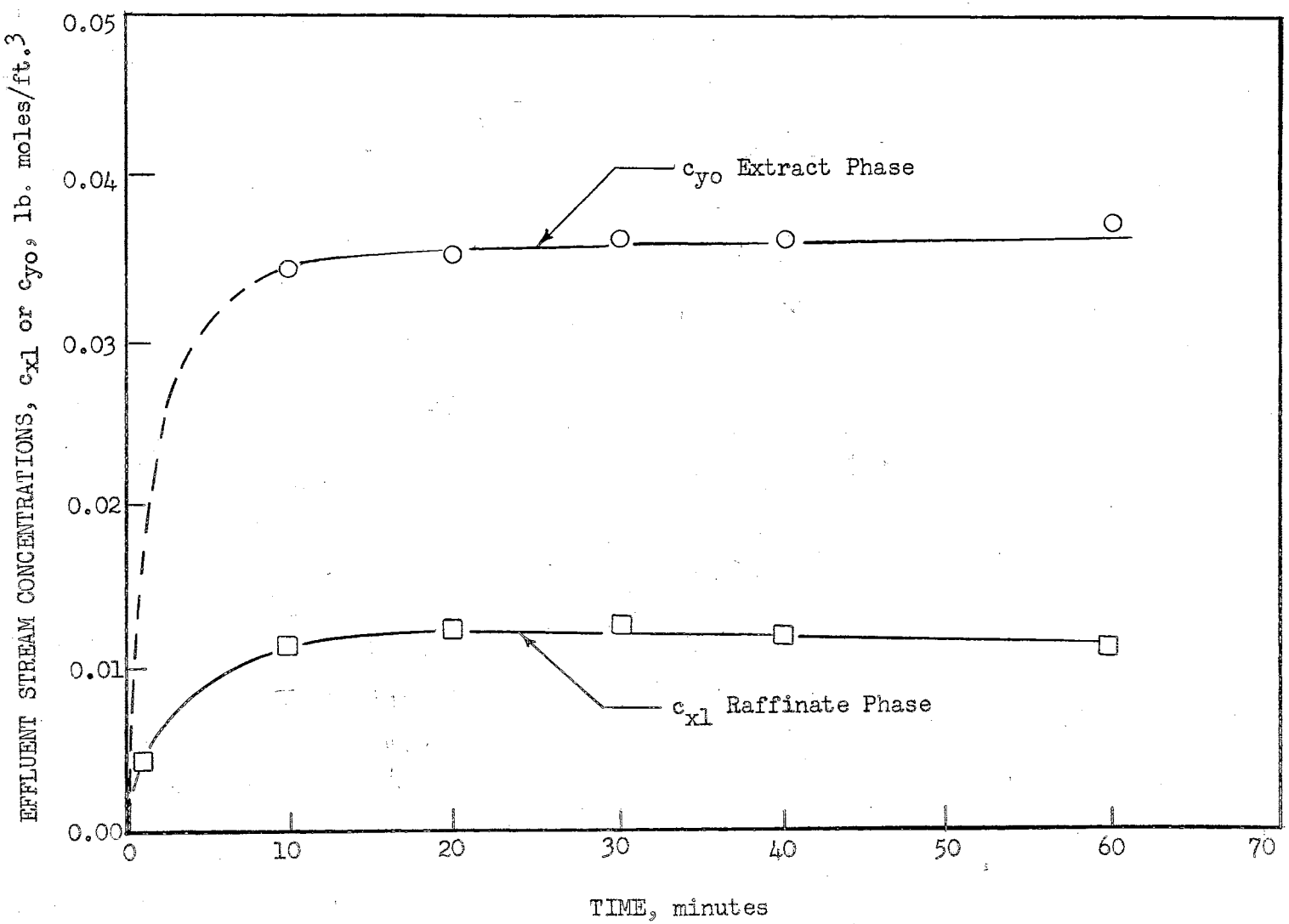

FIGURE 33. EFFLUENT STREAM CONCENTRATIONS AS A FUNCTION OF TIME, RUN E-11

during the run due to a slowly increasing flow rate of the raffinate phase.

Rejection of Data

Runs E-1 and E-2 were not reported in this study, both being for the MIBK-acetic acid-water system. These runs were primarily used to develop sampling techniques and to test the polyethylene sampling funnels. In run E-1, samples were removed from the funnels too rapidly, thus entraining continuous phase. In run E-2, the feed tank ran dry before the run was complete. Aside from these two runs, all extraction data were reported.

Flooding and Holdup

Two different types of emulsion flooding were observed in the operation of this column. The first was characterized by the carry-over of a small, but finite, quantity of organic droplets dispersed in the continuous aqueous phase, and the second by severe emulsion flooding occurring within the pulse column. Flooding curves for the four MIBK-aqueous ethylene glycol systems are given in Figure 34. These data show that the semi-logarithmic relation of Equation (17) holds true and that the intercept constant decreased as the ethylene glycol concentration increased in the continuous phase.

In Figure 35, the more severe type of emulsion flooding is shown for the Toluene-water and the MIBK-water systems. The Toluene-water system also includes two runs made during mass transfer of acetic acid from the organic to the aqueous phase. These data were also correlated with Equation (17). The slopes of the curves in Figures 34 and 35 are approximately equal, even with wide changes in interfacial tension (28.0 to 3.74

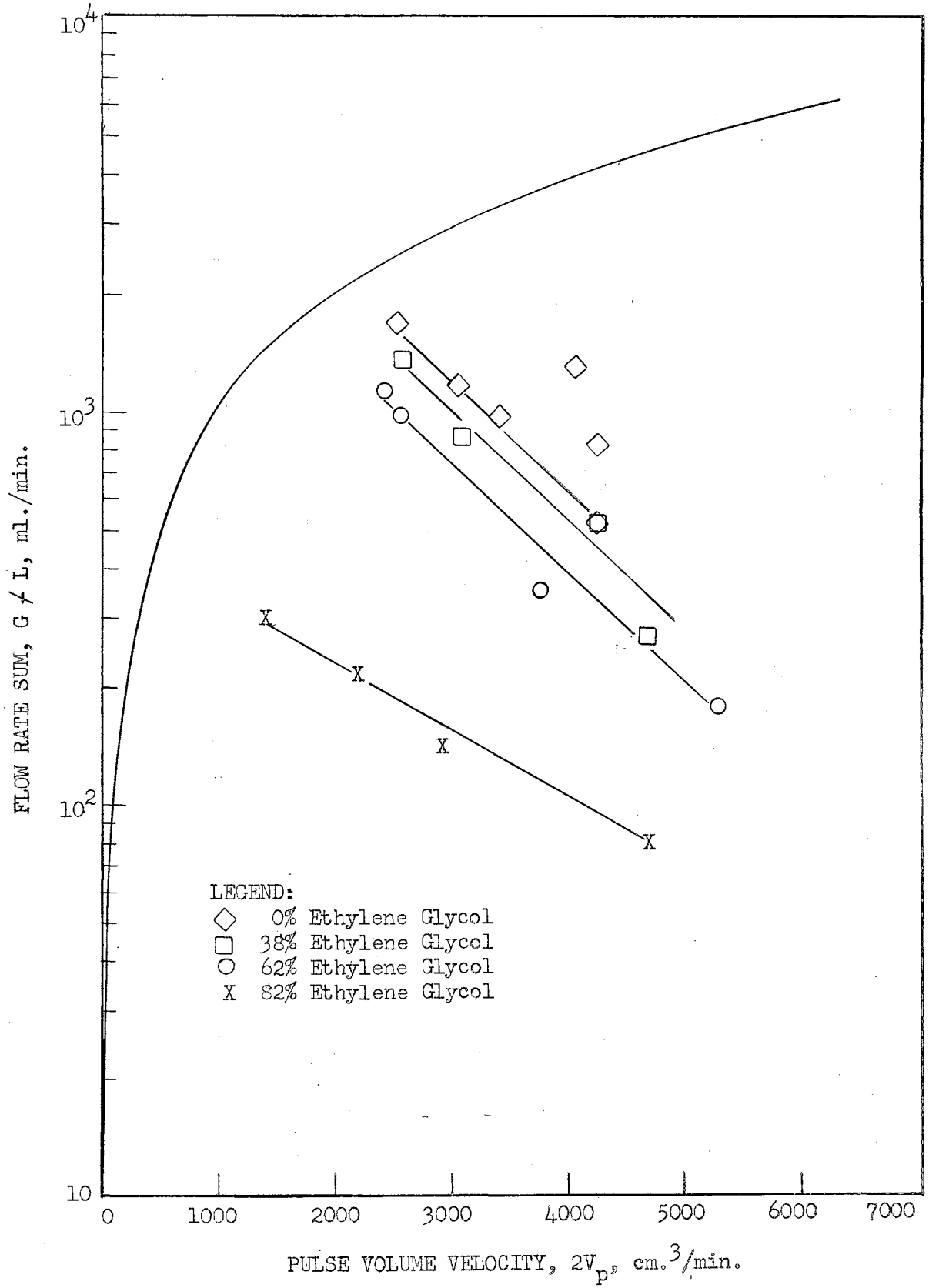

FIGURE 34. EMULSION FLOODING FOR MIBK-AQUEOUS ETHYLENE GLYCOL SYSTEMS

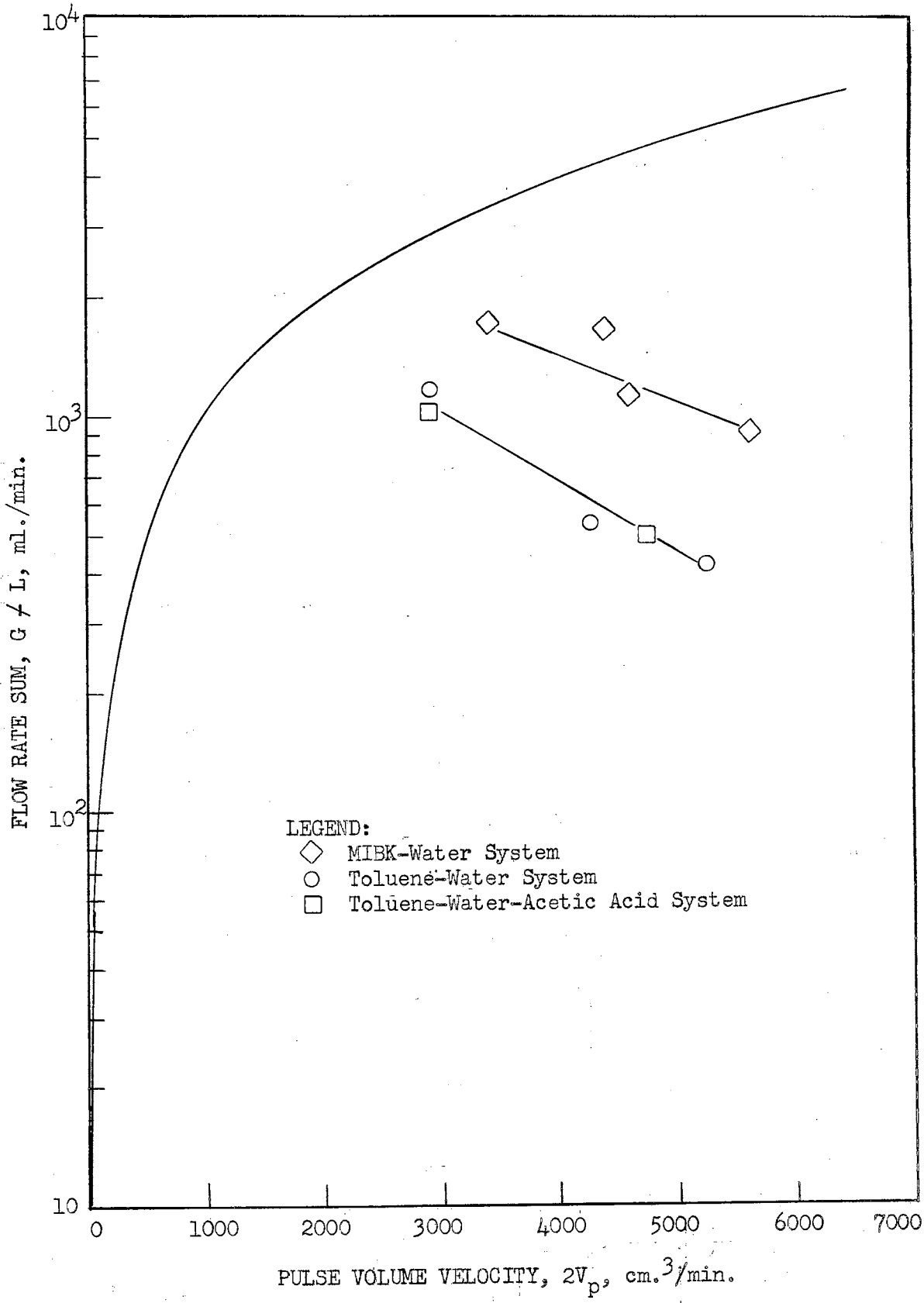

FIGURE 35. EMULSION FLOODING FOR THE MIBK-WATER AND THE TOLUENE-WATER SYSTEMS

dynes/cm.) and viscosity (7.86 to 0.83 cp.). This indicates that for this column geometry, the physical property factor, C_1, in Equation (17) is constant. For the column geometry of this study, S_1 is equal 0.030, S_2 equals 20.2, and C_1 equals 0.0005. No acceptable correlation was found for the intercept values, C_2.

Holdup of dispersed phase in the column was determined for most of the eddy diffusivity runs and all of the extraction runs. These data are given graphically in Figure 36 for the non-extraction runs and in tabular form in Appendices B and C. For operation in the emulsion region and at flow rate sums of both 500 and 240 ml./min., the per cent dispersed-phase holdup decreased with decreasing pulse volume velocity. As operation entered the mixer-settler region the fractional holdup of dispersed phase increased sharply.

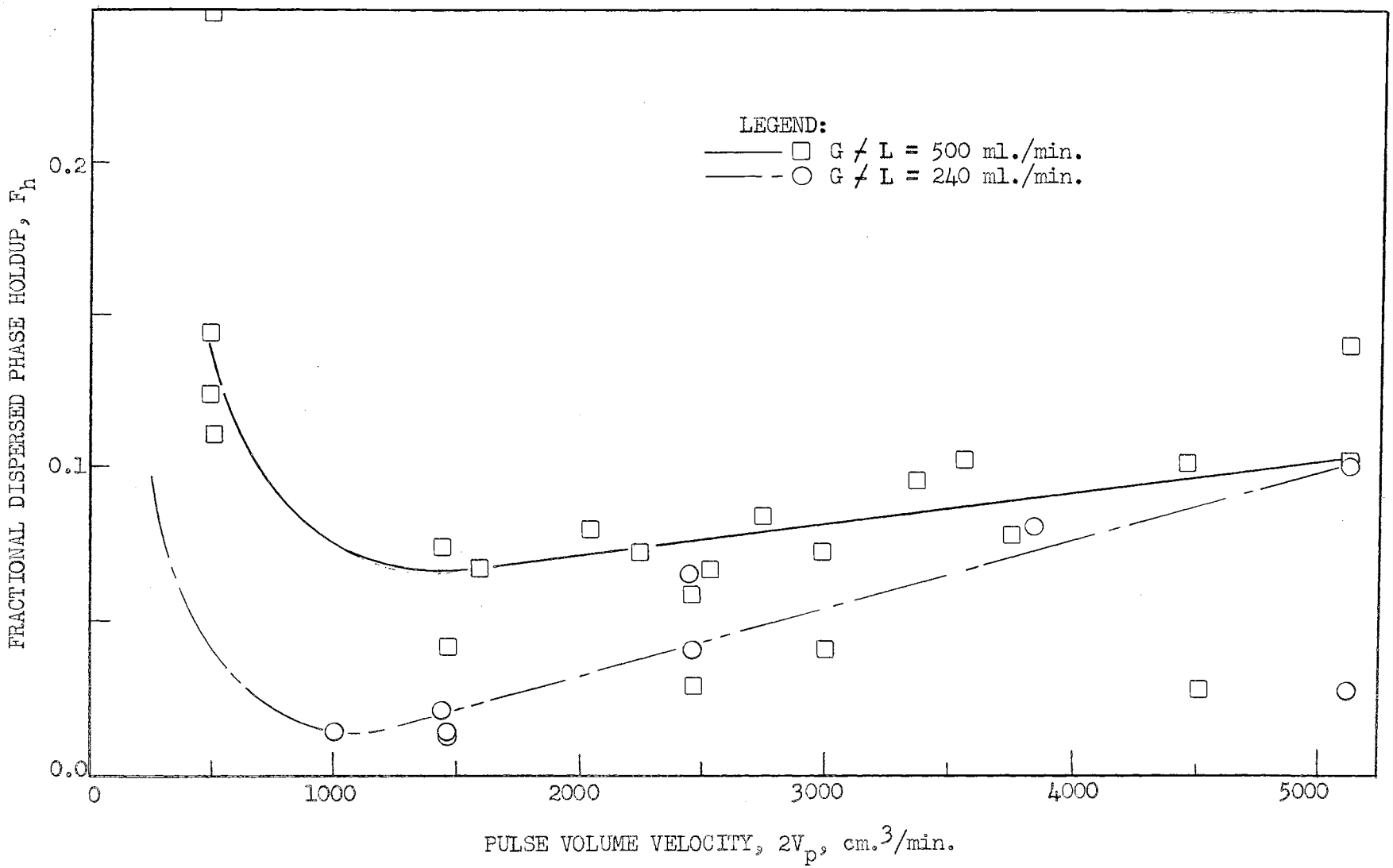

FIGURE 36. FRACTIONAL HOLDUP OF DISPERSED PHASE

CHAPTER VII

CONCLUSIONS AND RECOMMENDATIONS

Restatement of the Study

This study was primarily designed to examine backmixing in a pulse column and the effect of backmixing on concentration profiles during extraction. A reasonable theoretical backmixing model was developed to aid in interpretation of these experiments and to predict response to other operating variables. The theoretical model of Miyauchi was examined for applicability to pulse column extraction.

Conclusions

Backmixing

Backmixing in the pulse column was characterized by the superficial eddy diffusivity for five two-component liquid-liquid systems. These data indicated that backmixing was strongly dependent on pulse frequency and on the flow rate sum. Little or no effect was noted for changes in the flow rate ratio, column height, or plate material.

A plate sealing effect was noted for four of the five systems studied. The high viscosity, low interfacial-tension systems were least effected. The plate sealing effect was evident at high frequencies and holdup, just as was predicted by the theoretical backmixing model which was developed. For the region in which no plate sealing occurred, all the systems that were examined had identical eddy diffusivities.

A mathematical model was proposed which describes the gross longitudinal turbulence effects (backmixing) in terms of two types of mixing, i.e., mixing between plates and recycle across plates. The concentration of the continuous phase that is recycled across the plates, was characterized by an effective concentration distance. This effective concentration distance was determined (experimentally) to approach a constant value at high pulse frequencies for the one column geometry that was examined.

The effects of several geometric and operating variables on the eddy diffusivity, were predicted from the proposed backmixing model. Eddy diffusivities (backmixing) were postulated to increase with increases in the (a) plate spacing; (b) perforated-plate free area; (c) perforated-plate hole diameter; (d) pulse amplitude; and (e) pulse frequency at a constant pulse amplitude.

Concentration Profiles

An experimental method was developed to sample effectively the dispersed phase within the pulse column under conditions of high dispersion. Experimental concentration profiles within the column were determined for both phases in ten runs involving three different extraction systems and both directions of mass transfer. High backmixing was noted in the continuous phase for all runs obtained while operating in the emulsion region. The dispersed phase was assumed to pass through the column in slug flow.

Concentration profiles of both phases were calculated for each extraction run and compared with the experimentally measured profiles. The eddy diffusivity values used in the calculations were those determined in the backmixing phase of this study. Without exception, eddy diffusivity

values that were based on the absence of the plate sealing phenomena, gave the most satisfactory agreement between the theoretical and experimental concentration profiles.

A simplified mathematical model describing mass transfer at the column interface was developed and the resulting boundary condition was applied to the backmixing model of Miyauchi (26). In each system examined, this new boundary condition improved the agreement between the experimental and theoretical profile for the continuous phase without adversely effecting the dispersed phase profile agreement.

Dimensionless concentration ratios were also defined and used in the solution of the Miyauchi model. These extend the equations of Miyauchi to systems where equilibrium distribution curves must be represented as straight lines with non-zero intercepts.

Emulsion flooding and dispersed phase holdup data were obtained on five systems with widely different physical properties. The slopes of these curves were approximately equal when plotted as ln $(G \neq L)$ as a function of $2V_p$. The physical property term, C_1, in Swift's empirical flooding equation was concluded to be constant for this column geometry (37).

Recommendations

It has been demonstrated that concentration profiles within a pulse column can be calculated when continuous phase backmixing can be characterized by eddy diffusivities. The values of the over-all mass-transfer coefficients obtained in this manner are free from errors due to improper representation of the concentration driving forces. This evaluation of

backmixing in pulse columns must be systematically extended to include column geometric details. In particular, hole size, plate free area, and plate spacing must be thoroughly examined. The backmixing model proposed in this study should aid in interpretation of these data.

The plate sealing phenomena which was observed in this study should be examined further. In particular, it is recommended that this effect should be evaluated both with and without mass transfer present. The effects of dispersed-phase holdup, plate wetting, droplet coalescence, and drop formation on the plate sealing phenomena should be observed in addition to the perforated-plate geometric variables.

A SELECTED BIBLIOGRAPHY

1. Appel, F. J., and J. C. Elgin, "Countercurrent Extraction of Benzoic Acid Between Toluene and Water," Ind. Eng. Chem., 29, 451 (1937).

2. Bernard, R. A. and R. H. Wilhelm, "Turbulent Diffusion in Fixed Beds of Packed Solids," Chem. Eng. Progr., 46, 233 (1950).

3. Burkhart, L. E., and R. W. Fahien, "Extraction Efficiency of a Pulse Column of Varied Geometry," United States Atomic Energy Commission Report ISC-860 (1956).

4. Carins, E. J. and J. M. Prausnitz, "Longitudinal Mixing in Packed Beds," Chem. Engr. Science, XII, 20 (1960).

5. Carberry, J. J., and R. H. Bretton, "Axial Dispersion of Mass in Flow Through Fixed Beds" A. I. Ch. E. Journal, 4, 367 (1958).

6. Claybaugh, B. E., "Limiting Flow Capacities in a Pulse Extraction Column," M. S. Thesis, Oklahoma State University, (1959).

7. Cohen, R. M., and G. H. Beyer, "Performance of a Pulse Extraction Column," Chem. Eng. Progr., 49, 279 (1953).

8. Ebach, E. A., and R. R. White, "Mixing of Fluids Through Beds of Packed Solids," A. I. Ch. E. Journal, 4, 161 (1958).

9. Edwards, R. B., and G. H. Beyer, "Flooding Characteristics of a Pulse Extraction Column," A. I. Ch. E. Journal, 2, 148 (1956).

10. Eguchi, W., and S. Nagata, "Studies on the Pulsed Plate Column," Chemical Engineering, Japan, 23, (March, 1959).

11. Eugenio, Manuel R., "The Effect of Pulsation on Liquid-Liquid Mass-Transfer Resistances," United States Atomic Energy Commission Report ANL-5874 (1958).

12. Fahien, R. W., and J. M. Smith, "Mass Transfer in Packed Beds," A. I. Ch. E. Journal, 1, 29 (1955).

13. Farmer, W. S., "Controlling Variables in Liquid-Liquid Extraction from Single Drops," United States Atomic Energy Commission Report ORNL-635 (1951).

14. Geankoplis, C. J., "Spray Tower Extraction-Correspondence," Ind. Eng. Chem., 44, 2457 (1952).

15. Geankoplis, C. J. and A. N. Hixson, "Mass Transfer Coefficients in an Extraction Spray Tower," Ind. Eng. Chem., 42, 1141 (1950).

16. Geankoplis, C. J., P. L. Wells, and E. L. Hawk, "Extraction in a Pilot-Unit Spray Tower," Ind. Eng. Chem., 43, 1848 (1951).

17. Gilliland, E. R., and E. A. Mason, "Gas and Solid Mixing in Fluidized Beds," Ind. Eng. Chem., 40, 1191 (1949).

18. Gilliland, E. R., and E. A. Mason, "Gas Mixing in Beds of Fluidized Solids," Ind. Eng. Chem., 44, 218 (1952).

19. Jacques, G. L., and T. Vermeulen, "Longitudinal Dispersion in Solvent-Extraction Columns: Peclet Numbers for Ordered and Random Packing," United States Atomic Energy Commission Report UCRL-8029, (1957).

20. Karr, A. E., "Performance of a Reciprocating-Plate Extraction Column," A. I. Ch. E. Journal, 5, 446 (1959).

21. Li, W. H., and W. M. Newton, "Liquid-Liquid Extraction in a Pulsed Perforated Plate Column," A. I. Ch. E. Journal, 3, 56 (1957).

22. Lynn, S., W. H. Corcoran, and B. H. Sage, "Material Transport in Turbulent Gas Streams: Radial Diffusion in a Circular Conduit," A. I. Ch. E. Journal, 3, 11 (1957).

23. Marr, B. W., and A. L. Babb, "Longitudinal Mixing in a Pulsed Sieve-Plate Extraction Column," Ind. Eng. Chem., 51, 1011 (1959).

24. McHenry, K. W., Jr., and R. H. Wilhelm, "Axial Mixing of Binary Gas Mixtures Flowing in a Random Bed of Spheres," A. I. Ch. E. Journal, 83, (1957).

25. McMullen, A. K., T. Miyauchi, and T. Vermeulen, "Longitudinal Dispersion in Solvent-Extraction Columns: Numerican Tables," United States Atomic Energy Commission Report UCRL-3911 Supplement, (1958).

26. Miyauchi, T., "Longitudinal Dispersion in Solvent-Extraction Columns: Mathematical Study," United States Atomic Energy Commission Report UCRL-3911, (1957)

27. Newman, M. J., "Spray Tower Extraction," Ind. Eng. Chem., 44, 2457 (1952).

28. Scheibel, E. G., and A. E. Karr, "Semicommercial Multistage Extraction Column Performance Characteristics," Ind. Eng. Chem., 42, 1048, (1950).

29. Sege, G., and F. W. Woodfield, "Pulse Column Variables," Chem. Eng. Progr., 50, 396 (1954).

30. Seidell, A., Solubilities of Organic and Inorganic Compounds, Supplement to 2nd Ed., D. Van Nostrand Co., Inc., New York (1928) II, 1008.

31. Sherwood, T. K., "Mass, Heat and Momentum Transfer Between Phases," Chem. Eng. Progr. Symposium Series, 55, 71 (1959).

32. Sherwood, T. K., J. E. Evans, and J. V. Longcor, "Extraction in Spray and Packed Columns," Ind. Eng. Chem., 31, 1144 (1939).

33. Sleicher, C. A., Jr., "Axial Mixing and Extraction Efficiency," A. I. Ch. E. Journal, 5, 145 (1959)

34. Smoot, L. D., B. W. Marr and A. L. Babb, "Flooding Characteristics and Separation Efficiencies of Pulsed Sieve-Plate Extraction columns," Ind. Eng. Chem., 51, 1005 (1959).

35. Snedecor, G. W., Statistical Methods, The Iowa State College Press, Ames, Iowa (1959).

36. Strang, David A., and C. J. Geankoplis, "Longitudinal Diffusivity of Liquids in Packed Beds," Ind. Eng. Chem., 50 (1958).

37. Swift, W. H., "Limiting Flow Capacity in Solvent Extraction Pulse Columns, Part I, The Effect of Pulse and Cartridge Geometry Variables," United States Atomic Energy Commission Report HW-33953, (1954).

38. Swift, W. H. and L. L. Burger, "Backmixing in Pulse Columns with Particular Reference to Scale-up," United States Atomic Energy Commission Report HW-28867, (1953).

39. Swift, W. H. and L. L. Burger, "Backmixing in Pulse Columns II Experimental Values and Effects of Several Variables," United States Atomic Energy Commission Report HW-29010, (1953).

40. Thornton, J. D., "Recent Developments in Pulse-Column Techniques," Chem. Eng. Progr. Symposium Series No. 13, Part III, 50, 39 (1954).

APPENDIX A

DEFINITION OF TERMS

a - Pulse Amplitude, cm.

a - Contact area per unit volume, $ft.^2/ft.^3$

a - Column radius, ft., for Equation (8)

A - Column cross sectional area, $cm.^2$

A_b - Effective area of coalescing droplets at the interface, $ft.^2$

b - Intercept value in Equation (17), ml./min.

b - Slope of the $\ln c/c_o$ vs z curve and equal to $-F_y/E_c$, $cm.^{-1}$

c_x - Concentration of the raffinate phase, lb. moles/$ft.^3$

c_x^* - Concentration of the raffinate phase in equilibrium with c_y, lb. moles/$ft.^3$

c_y - Concentration of the extract phase, lb. moles/$ft.^3$

C_x - Reduced concentration of the raffinate phase, c_x/c_x^o

D - Pulse column diameter, cm.

D - Molecular diffusivity, $cm.^2/sec.$

D - Differential operator, $\partial / \partial Z$

D_b - Average droplet diameter, cm.

E - Superficial axial eddy diffusivity, $cm.^2/sec.$

E_x - Axial eddy diffusivity of the raffinate phase based on the void fraction ϵ_x and equal to E/ϵ_x, $cm.^2/sec.$

f - Pulse frequency, cycles/minute

f - Rate of mass transfer, moles/hr.

F - Superficial flow velocity, ft./hr. or cm./sec.

F_h - Fractional holdup of dispersed phase

G - Dispersed phase flow rate, ml./min.

HTU - Height of a transfer unit based on pulg flow of both phases, ft.

I - Plate spacing

J - Defined by Equation (38)

J' - Defined by Equation (47)

K_x - Over-all mass-transfer coefficient based on raffinate phase concentrations, lb. moles/hr. (ft.^{2} area)(lb. moles/ft.^{3}).

L - Continuous phase flow rate, ml./min.

L' - Column height, measured from the dispersed phase nozzle to the column interface, cm. or ft.

N_{ox} - Number of over-all transfer units, equal to $K_x a\ L'/F_x$.

N_{oy} - Number of over-all transfer units, equal to $K_x a\ L'/F_y$ and $N_{ox}\ K\Lambda$.

P_xB - Peclet number of the raffinate phase based on column length, equal to $F_x L'/\epsilon_x E_x$.

P_yB - Peclet number of the extract phase based on column length, equal to $F_y L'/\epsilon_y E_y$.

r - Radial distance from the center of the column, cm.

R/E - Slope of the operating line for plug flow and constant F_x and F_y, equal to $(c_y^o - c_y^1)/(c_x^o - c_x^1)$.

$2V_p$ - Pulse volume velocity, the rate of pulsing fluids up and down the column and equal to $2aAf$, ml./min.

z - Distance measured up the column, ft.

z' - Distance measured down the column, equal to $-z$.

Δz - Effective concentration distance. Twice the distance above or below a plate which, when referred to the apparent concentration profile, gives the average concentration of the continuous phase crossing the plate.

Z - Reduced distance up the column, equal to z/L'.

ϵ - Void fraction, the fraction of the column available for the flow

of a phase.

Λ - Absorption factor, F_x/F_yK

ϕ - A dimensionless ratio expressing the concentration of the raffinate phase at some point in the column by comparing the concentration change yet to be accomplished with the maximum concentration change possible. Equal to $(C_x - C_x^{1*})/(1 - C_x^{1*})$

Υ - A dimensionless ratio expressing the concentration of the extract phase at some point in the column by comparing the concentration change already accomplished with the maximum concentration change possible. Equal to $(C_y - C_y^1)/(1 - C_x^{1*})K$

Superscripts

o - As in c_x^o, refers to the material in the feed or product lines entering or leaving the column at the dilute end.

1 - As in c_x^1, refers to the material in the feed or product lines entering or leaving the column at the dilute end.

' - $\partial/\partial Z$

" - $\partial^2/\partial Z^2$

* - As in C_x^{1*}, refers to that raffinate concentration which is in equilibrium with the corresponding extract concentration, C_y^1. Note that even though $C_{x1} = C_x^1$, this does not mean $C_{x1}^* = C_x^{1*}$.

Subscripts

c - Continuous phase

d - Dispersed phase

e - Extraction run value

ei - Transfer in by the eddy mechanism

eo - Transfer out by the eddy mechanism

fi - Transfer in by bulk flow

fo - Transfer out by bulk flow

l - Longitudinal

t - Non-extraction run value

ti - Transfer into a phase, across a liquid interface

to - Transfer out of a phase, across a liquid interface

x - Raffinate phase

y - Extract phase

oe - Over-all, based on the extract phase

APPENDIX B

EXPERIMENTAL AND CALCULATED DATA FOR EDDY DIFFUSIVITY MEASUREMENTS

TABLE IV

EDDY DIFFUSIVITY DETERMINATIONS

MIBK - WATER SYSTEM

Run No. z, cm.	Reduced Tracer Concentrations, c/c_o				
	T-5	T-6	T-7	T-8	T-10
0	0.805		1.15		1.025
3	0.322	0.608	0.702	0.695	
5					0.945
6	0.207	0.409	0.586		
7				0.338	
9	0.081	0.342	0.285		0.795
10					
11				0.083	
12	0.080	0.223			
15			0.151	0.151	0.610-0.612
20				0.041	
25					0.407
30					0.350

Run No.	Experimental and Calculated Data				
	T-5	T-6	T-7	T-8	T-10
f	64.5	171	114	228	171
$2V_p$	1450	3840	2560	5120	3840
G	260	250	250	258	120
L	250	250	250	247	100
G + L	510	500	500	505	220
G/L	1.04	1.00	1.00	1.04	1.20
F_h	0.041		0.067	0.092	0.080
L'	1.52	1.56	1.56	1.58	1.58
F_y	0.206	0.206	0.206	0.203	0.082
b	-0.1991	-0.1225	-0.1236	-0.1624	-0.0369
E_c	1.04	1.69	1.67	1.25	2.23

TABLE IV (Continued)

Run No. z, cm.	Reduced Tracer Concentrations, c/c_o				
	T-11	T-13	T-14	T-15	T-16
3		0.0153	0.159	1.260	0.1240
5	0.805	0.0170			
6			0.042	0.636	0.0680
8		0.0017	0.0065		
9				0.472	
10	0.486				0.0063
11			0.0042		
12				0.228	
15				0.148	
20	0.315				
25	0.210				
30	0.136				

Run No.	Experimental and Calculated Data				
	T-11	T-13	T-14	T-15	T-16
f	64.5	22.8	64.5	171	171
$2V_p$	1450	512	1450	3840	3840
G	717	245	510	125	712
L	120	240	500	375	700
G / L	137	495	1010	500	1412
G/L	0.975	1.020	1.020	0.333	1.020
F_h	0.013	0.143	0.041		0.132
L'	1.65	1.54	1.71		1.41
F_y	0.098	0.197	0.412	0.309	0.576
b	-0.649	-0.7450	-0.5253	-0.1766	-0.5217
E_c	1.53	0.27	0.78	1.75	1.10

TABLE IV (Continued)

Run No. z, cm.	Radial Position	Reduced Tracer Concentrations, c/c_o T-42	T-43	T-44	T-45	T-46
-5	1				1.187	
	3				1.211	
	5				1.160	
0	1	1.080	1.082			1.010
	2					0.998
	4					1.005
	5					1.036
5	1	0.896	0.748	0.770	0.130	0.821
10	1	0.617	0.590	0.368	0.0201	0.580
	1					0.654
15	1	0.426	0.483	0.170	0.0034	0.516
20	1	0.258	0.374	0.0646		0.294
	1			0.0710		0.339
25	1	0.137		0.0146		
30	1	0.115		0.0051		
				0.0121		

Run No.	Experimental and Calculated Data T-42	T-43	T-44	T-45	T-46
f					
$2V_p$	5100	2470	5100	5100	1450
G	117	113	250	520	112
L	126	120	250	505	110
G + L	243	233	500	1025	222
G/L	0.929	0.943	1.000	1.030	1.020
F_h	0.027	0.022	0.093	0.126	0.119
L'	1.55	1.63	1.56	1.49	0.79
F_y	0.104	0.098	0.206	0.415	0.091
b	-0.0873	-0.0458	-0.1880	-0.3684	-0.0554
E_c	1.19	2.15	1.10	1.13	1.64

TABLE V

EDDY DIFFUSIVITY DETERMINATIONS

TOLUENE - WATER SYSTEM

Run No. z, cm.	Reduced Tracer Concentration, c/c_o				
	T-17	T-23	T-24	T-25	T-26
1				0.970	
5	0.875	0.715	0.883	0.231	0.860
10	0.780	0.542	0.735	0.040	0.739
15	0.690	0.405	0.610	0.014	0.638
20	0.690	0.331	0.551	0.0032	0.582
25		0.245	0.478		0.452
30	0.492				0.430

Run No.	Experimental and Calculated Data				
	T-17	T-23	T-24	T-25	T-26
f	110	110	110	24.3	119
$2V_p$	2470	2470	2470	545	4460
G	435	885	226	450	445
L	47	100	27	52	48
G + L	482	985	253	502	493
G/L	9.25	8.85	8.38	8.66	9.28
F_h	0.058	0.175	0.065		0.101
L	1.45	1.54	1.45		1.50
F_y	0.0387	0.0824	0.0223	0.0429	0.0396
b	-0.0222	-0.0552	-0.0302	-0.3047	-0.0290
E_c	1.74	1.49	0.74	0.14	1.36

TABLE V (Continued)

Run No. z, cm.	Reduced Tracer Concentration, c/c_o T-18	T-19	T-20	T-21	T-22
1					
2	0.606		0.176	0.530	
4	0.278		0.0946	0.0368	
5		0.416			0.229
6			0.0164		
7	0.286			0.318	
8			0.0067		
9	0.119			0.0055	
10		0.184	0.0036		0.033
12	0.0657				
15	0.0316	0.0923			0.0081
20		0.0404			0.0019
25		0.0147			

Run No.	Experimental and Calculated Data T-18	T-19	T-20	T-21	T-22
f	110	110	110	24.3	199
$2V_p$	2470	2470	2470	545	4460
F_h	0.027	0.040	0.046	0.253	0.027
G	41	26	102	50	50
L	450	250	910	450	450
G + L	491	276	1012	500	500
G/L	0.091	0.104	0.112	0.111	0.111
F_Y	0.371	0.206	0.749	0.371	0.371
L^Y	1.54	1.57	1.52	1.51	1.55
b	-0.2220	-0.1626	-0.5662	-0.5647	-0.3172
E_c	1.67	1.27	1.32	0.65	1.17

TABLE VI

EDDY DIFFUSIVITY DETERMINATIONS

MIBK - 38% ETHYLENE

GLYCOL SYSTEM

Run No. z, cm.	Radial Position	Reduced Tracer Concentration, c/c_o T-31	T-32	T-33	T-34
-5	1		1.029		
	2		1.022		
	3		0.883		
	4	1.000	1.022		
	5		1.017		
5	1	0.900	0.776	0.523	0.860
10	1	0.824	0.585	0.314	0.795
15	1	0.622	0.473	0.215	0.588
	2	0.677			
	3	0.681			
	4	0.627			
	5	0.658			
20	1	0.588	0.354	0.148	0.485
25	1	0.431	0.237	0.0960	0.280
	5			0.114	
30	1	0.320	0.068	0.0599	0.236

Run No.	Experimental and Calculated Data T-31	T-32	T-33	T-34
f	133	99	64.5	167
$2V_p$	2980	2220	1450	3750
G	370	367	370	375
L	118	125	125	126
G + L	488	492	495	501
G/L	3.14	2.94	2.96	2.97
F_h	0.072	0.073	0.075	0.078
L'	1.70	1.56	1.52	1.56
F_y	0.097	0.103	0.103	0.104
b	-0.0414	-0.0546	-0.0833	-0.0503
E_c	2.35	1.89	1.24	2.06

TABLE VI (Continued)

Run No. z, cm.	Radial Position	Reduced Tracer Concentration, c/c_o T-35	T-41
-5	1		1.370
	2		1.210
	3		1.180
	4		1.023
	5		0.763
5	1	0.874	0.910
10	1	0.624	0.550
	4	0.583	
15	1	0.359	0.359
	4	0.368	
20	1	0.238	0.347
25	1	0.232	0.090
	5	0.280	
30	1	0.143	0.043
	4	0.161	

Run No.	Experimental and Calculated Data T-35	T-41
f	148.2	133
$2V_p$	3330	2980
G	426	220
L	119	245
G + L	545	465
G/L	3.59	0.899
F_h	0.097	0.039
L'	1.71	1.62
F_y	0.098	0.202
b	-0.0636	-0.1177
E_c	1.54	1.72

TABLE VII

EDDY DIFFUSIVITY DETERMINATIONS

MIBK - 62% ETHYLENE

GLYCOL SYSTEM

Run No. z, cm.	Radial Position	Reduced Tracer Concentration, c/c_o T-27	T-28	T-29	T-30
3		1.270/0.609	0.143	0.746	
4					0.582
5	1		0.221	0.884	
	3		0.220		
	5		0.214		
6		0.740			
8			0.0455		
9		0.275			
10				0.605	0.319
12		0.316	0.0322		
15	1			0.497	0.170
	3			0.465	0.317
	4			0.598	0.407
	5			0.519	0.331
16.5		0.107			
20			0.0059	0.384	0.110
21		0.215			
25				0.277	0.073
26.5		0.091			
30				0.239	0.072
31.5		0.048			

Run No.	Experimental and Calculated Data T-27	T-28	T-29	T-30
f	228	22.8	160	91.2
$2V_p$	5120	512	3590	2050
G	250	340	370	358
L	250	135	126	125
G + L	500	475	496	483
G/L	1.00	2.52	2.94	2.87
F_h	0.140	0.122	0.103	0.079
L'	1.58	1.48	1.71	1.62
F_y	0.206	0.111	0.104	0.103
b	-0.1150	-0.2438	-0.0477	-0.0919
E_c	1.79	0.44	2.17	1.12

TABLE VII (Continued)

Run No. z, cm.	Radial Position	Reduced Tracer Concentration, c/c_o T-39	T-40
-5	1		1.38
	2		0.790
	3		0.693
	4		0.785
	5		0.866
0	1	1.205	
	2	0.996	
	4	0.881	
	5	0.752	
5	1	0.890	0.591
10		0.705	0.298
15	1	0.528	0.254
20		0.413	0.194
25		0.235	0.108
30		0.155	

Run No.	Experimental and Calculated Data T-39	T-40
f	121.8	76.1
$2V_p$	2720	1615
G	355	380
L	130	125
G + L	485	505
G/L	273	3.04
F_h	0.086	0.067
L'	1.58	1.57
F_y	0.107	0.103
b	-0.0557	-0.0836
E_c	1.92	1.23

TABLE VIII

EDDY DIFFUSIVITY DETERMINATIONS

MIBK - 82% ETHYLENE

GLYCOL SYSTEM

Run No. z, cm.	Radial Position	Reduced Tracer Concentration, c/c_o T-36	T-37	T-38	*T-47
-5	1		1.020	1.200	
	2			1.127	
	3	1.247	1.035		
	4		1.040	1.090	
	5	1.110	0.975	0.866	
0					
5		0.870	0.579	0.664	
10		0.638	0.292	0.455	0.665
15		0.394	0.185	0.323	0.502
20		0.232	0.0669	0.161	0.460
25			0.0464	0.0974	0.426
30			0.0255	0.0560	0.346

Run No.	Experimental and Calculated Data T-36	T-37	T-38	*T-47
f	64.5	45.6	64.5	
$2V_p$	1450	1023	1450	5100
F_h	0.013	0.013	0.020	0.280*
G	126	125	112	395
L	111	125	115	130
G + L	237	250	227	525
G/L	1.13	1.00	0.975	2.89
F_y	0.092	0.122	0.101	0.107
L'	1.62	1.57	1.58	1.61
b	-0.0889	-0.1251	-0.0966	-0.0343
E_c	1.03	0.97	1.04	3.12

*Operation was in the Emulsion Flooding Region

TABLE IX

EXPERIMENTAL DATA OF SWIFT AND BURGER (39)

Pulse Column Description

Column Diameter	2.0 in.
Plate Diameter	1.988 in.
Hole Size	0.125 in.
Free Area	24.5 %
Packed Height	27.5 in.

Experimental Data

Run Number	$\frac{F_c}{F_d}$	G/L ml./min.	a in.	f cycles/min.	$2V_p$ ml./min.	I in.	E_{c_2} cm.²/sec.
BM-1	0.533	935	1.125	70	8120	2.0	10.41
BM-2	0.209	940	1.125	70	8120	2.0	11.20
BM-3	0.099	904	1.125	70	8120	2.0	10.57
BM-4	0.557	948	1.125	90	9041	2.0	10.17
BM-5	0.542	937	1.125	70	8120	1.0	10.65
BM-6	0.506	1175	1.125	70	8120	1.0	11.20
BM-7	0.504	935	0.500	70	5800	1.0	8.11

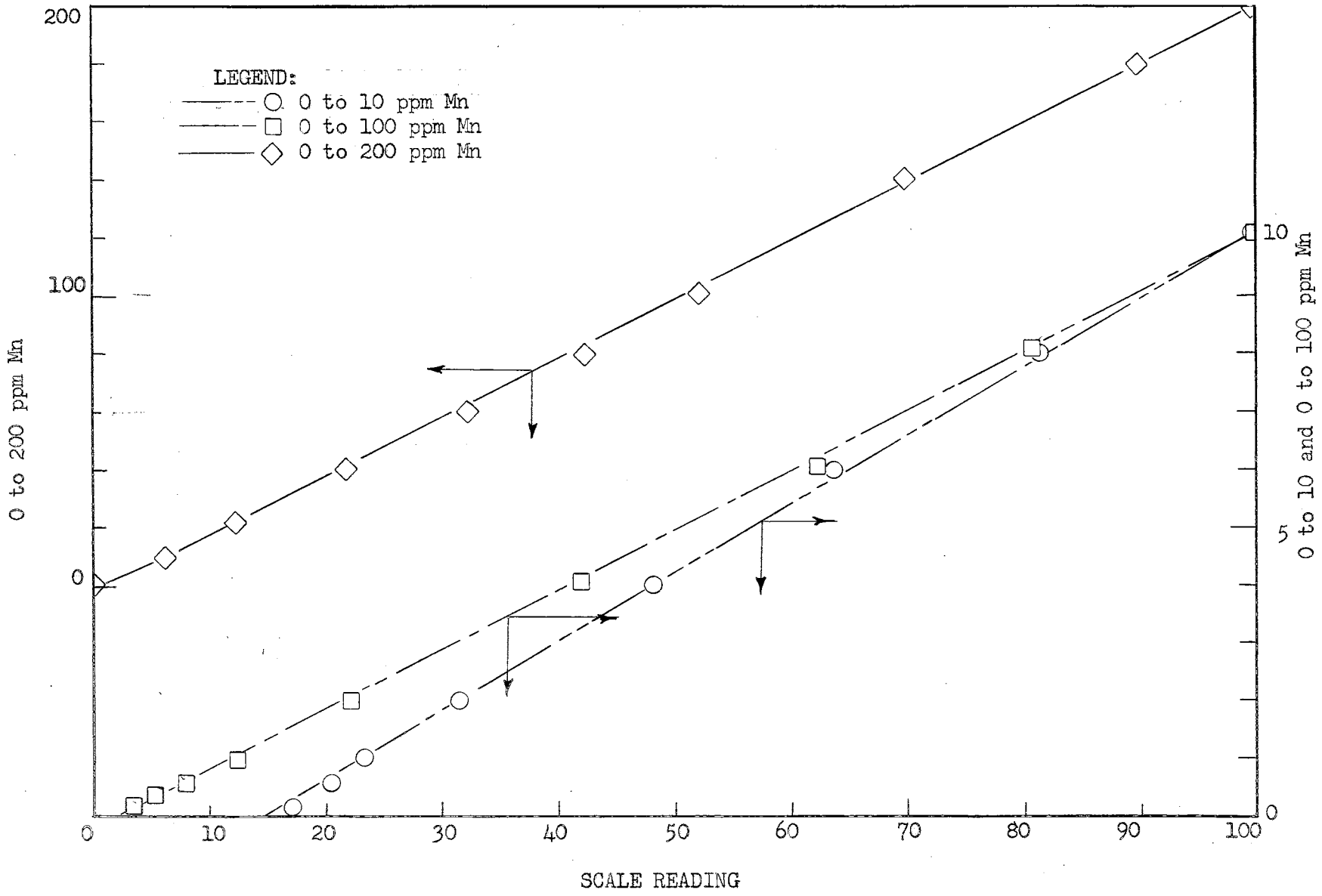

FIGURE 37. FLAME SPECTROPHOTOMETER CALIBRATION CURVES

APPENDIX C

OPERATING DATA AND CONCENTRATION PROFILES-

EXPERIMENTAL AND CALCULATED

TABLE X

OPERATING DATA FOR THE SYSTEM

MIBK - ACETIC ACID - WATER

Operating Condiditions

Run Number	E-9	E-10	E-11	E-12
f	171	171	64.5	228
$2V_p$	3840	3840	1450	5120
G	111	260	300	263
L	124	250	250	256
G+L	235	510	550	519
G/L	0.895	1.040	1.200	1.027
F_h	0.030	0.035	0.038	0.028
L', cm.	483	476	48.2	46.0

Calculated Data

R/E	0.981	1.130	1.320	1.115
R/E, graphical solution	0.885	1.022	1.285	1.091
F_y	0.102	0.206	0.206	0.211
G'	110	256	322	279
% error	+0.91	+2.34	-6.74	-5.74

TABLE XI

EXPERIMENTAL CONCENTRATION PROFILE DATA FOR

THE SYSTEM MIBK - ACETIC ACID - WATER

Run E-9

Sampling Position	Z	c_x	C_x	c_y	C_y
B	0.000	0.0447	1.000	0.0353	0.790
1	0.053	0.0397	0.889	0.0390	0.873
2	0.158	0.0335	0.750	0.0353	0.790
3	0.263	0.0264	0.581	0.0316	0.707
4	0.368	0.0256	0.573	0.0279	0.625
5	0.474	0.0211	0.473	0.0253	0.566
6	0.578	0.0169	0.379	0.0232	0.520
7	0.685	0.0191	0.428	0.0237	0.530
8	0.788	0.0141	0.316	0.0145	0.325
9	0.895	0.0096	0.216	0.0123	0.275
T	1.000	0.0086	0.194	(0.0080)	(0.180)

Run E-10

B	0.000	0.0397	1.000	0.0341	0.859
1	0.053	0.0333	0.839	0.0344	0.866
2	0.160	0.0216	0.545	0.0320	0.806
3	0.266	0.0242	0.610	0.0276	0.675
4	0.373	0.0232	0.585	0.0247	0.623
5	0.480	0.0167	0.421	0.0222	0.559
6	0.586	0.0161	0.407	0.0194	0.490
7	0.692	0.0157	0.397	0.0181	0.456
8	0.800	0.0115	0.291	0.0119	0.301
9	0.905	0.0106	0.268	0.0095	0.240
T	1.000	0.0094	0.238		(0.170)

TABLE XI (Continued)

Run E-11

Sampling Position	Z	c_x	C_x	c_y	C_y
B	0.000	0.0396	1.000	0.0364	0.920
1	0.053	0.0381	0.963	0.0384	0.970
2	0.158			0.0348	0.880
3	0.263	0.0305	0.770	0.0307	0.775
4	0.368	0.0264	0.667	0.0267	0.675
5	0.474	0.0212	0.535	0.0225	0.568
6	0.578	0.0212	0.535	0.0181	0.457
7	0.685	0.0175	0.442	0.0142	0.359
8	0.788	0.0149	0.376	0.0116	0.293
9	0.895	0.0138	0.348	0.0082	0.207
	0.968			0.0070	0.177
T	1.000	0.0120	0.303		(0.140)

Run E-12

B	0.000	0.0490	1.000	0.0435	0.889
1	0.055	0.0434	0.885	0.0469	0.957
2	0.165	0.0346	0.706	0.0427	0.872
3	0.276	0.0301	0.614	0.0386	0.787
4	0.386			0.0342	0.698
5	0.487	0.0213	0.435		
6	0.607	0.0198	0.404	0.0260	0.531
7	0.718			0.0221	0.451
8	0.828	0.0144	0.294	0.0162	0.331
9	0.938	0.0129	0.264	0.0127	0.259
T	1.000	0.0100	0.202		

TABLE XII

CALCULATED CONCENTRATION PROFILES, RUN E-9

Calculation Parameters

K	1.923	
E_c	2.23	(From Run E-10, with plate sealing)
P_yB	2.21	
E_c	2.97	(From Figure 16, no plate sealing)
P_yB	1.66	
F_x/F_y	0.980	
Λ	0.510	
D_b	0.21	

	With Plate Sealing				Without Plate Sealing	
	For Interface Mass Transfer		Miyauchi's Equation		For Interface Mass Transfer	
	N_{ox} = 4.23		N_{ox} = 3.85		N_{ox} = 6.12	
Z	C_x	C_y	C_x	C_y	C_x	C_y
0.0	1.000	0.783	1.000	0.746	1.000	0.814
0.1	0.793	0.763	0.793	0.763	0.737	0.802
0.2	0.655	0.712	0.655	0.690	0.588	0.745
0.4	0.470	0.584	0.470	0.566	0.417	0.625
0.6	0.353	0.456	0.353	0.437	0.322	0.495
0.8	0.267	0.341	0.267	0.317	0.253	0.389
1.0	0.196	0.239	0.196	0.216	0.195	0.295

TABLE XIII

CALCULATED CONCENTRATION PROFILES, RUN E-10

Calculation Parameters

K	1.923	
E_c	1.69	(From Run T-6, with plate sealing)
P_yB	5.82	
E_c'	2.48	(From Figure 15, no plate sealing)
P_yB	3.96	
F_x/F_y	1.130	
Λ	0.587	
D_b	0.21	

	With Plate Sealing				Without Plate Sealing	
	For Interface Mass Transfer		Miyauchi's Equation		For Interface Mass Transfer	
	$N_{ox} = 2.67$		$N_{ox} = 2.50$		$N_{ox} = 3.00$	
Z	C_x	C_y	C_x	C_y	C_x	C_y
0.0	1.000	0.880	1.000	0.855	1.000	0.890
0.05	0.935	0.875				
0.1	0.873	0.855	0.873	0.830	0.860	0.862
0.2	0.768	0.762	0.768	0.756	0.750	0.794
0.4	0.598	0.596	0.598	0.573	0.578	0.794
0.6	0.455	0.417	0.455	0.394	0.442	0.467
0.8	0.338	0.267	0.338	0.240	0.331	0.312
1.0	0.240	0.138	0.240	0.107	0.238	0.190

TABLE XIV

CALCULATED CONCENTRATION PROFILES, RUN E-11

Calculation Parameters

K	1.923	
E_c	1.035	(From run T-5, no plate sealing)
P_yB	9.60	
F_x/F_y	1.320	
Λ	0.687	
D_b	0.42	

For Interface Mass Transfer			Miyauchi's Equations	
	N_{ox} = 2.24		N_{ox} = 2.00	
Z	C_x	C_y	C_x	C_y
0.0	1.000	1.000	1.000	0.961
0.1	0.901	0.950	0.908	0.900
0.2	0.813	0.858	0.822	0.799
0.4	0.658	0.649	0.668	0.589
0.6	0.524	0.455	0.534	0.405
0.8	0.403	0.287	0.410	0.203
1.0	0.297	0.141	0.300	0.075

TABLE XV

CALCULATED CONCENTRATION PROFILES, RUN E-12

Calculation Parameters

K	1.923	
E_c	1.17	(From runs T-8 and T-44, with plate sealing)
P_yB	8.28	
E_c	3.12	(From Figure 15, no plate sealing)
P_yB	3.11	
F_x/F_y	1.115	
Λ	0.580	
D_b	0.22	

With Plate Sealing

For Interface Mass Transfer			Miyauchi's Equation	
	N_{ox} = 3.07		N_{ox} = 2.80	
Z	C_x	C_y	C_x	C_y
0.0	1.000	1.002	1.000	0.840
0.1	0.864	0.890	0.864	0.800
0.2	0.750	0.790	0.750	0.710
0.4	0.565	0.574	0.565	0.500
0.6	0.420	0.394	0.420	0.325
0.8	0.299	0.239	0.299	0.174
1.0	0.200	0.113	0.200	0.053

TABLE XV (Continued)

Without Plate Sealing

For Interface Mass Transfer			Miyauchi's Equation	
	$N_{ox} = 4.30$		$N_{ox} = 3.94$	
Z	C_x	C_y	C_x	C_y
0.0	1.000	0.915	1.000	0.888
0.1	0.810	0.885	0.823	0.861
0.2	0.682	0.823	0.695	0.797
0.4	0.501	0.654	0.519	0.640
0.6	0.381	0.496	0.370	0.477
0.8	0.283	0.352	0.289	0.332
1.0	0.203	0.228	0.205	0.205

TABLE XVI

OPERATING DATA FOR THE TOLUENE-BENZOIC

ACID-WATER SYSTEM

Operating Conditions

Run Number	E-6	E-7	E-8
f	110	110	110
$2V_p$	2470	2470	2470
G	50	101	27
L	450	905	228
G + L	500	1006	235
G/L	0.111	0.111	0.118
F_h	0.020	0.033	0.007
L', cm.	48.3	48.3	47.6

Calculated Data

R/E	9.11	0.1133	0.1370
F_x	0.370		
F_y		0.745	0.188
G	49.4	102.6	31.2
% error	+1.21	-1.56	-13.5

TABLE XVII

EXPERIMENTAL CONCENTRATION PROFILE

DATA FOR THE TOLUENE-BENZOIC

ACID WATER-SYSTEM

Run E-6

Sampling Position	Z	c_x	C_x	c_y	C_y
T	0.000	0.000720	1.000	0.001457	2.025
9	0.105	0.000609	0.846	0.001256	1.747
8	0.211	0.000660	0.927	0.001355	1.883
7	0.316	0.000665	0.910		
6	0.422	0.000605	0.831	0.000843	1.172
5	0.527	0.000620	0.861	0.000800	1.112
4	0.632	0.000615	0.855	0.000592	0.823
3	0.738	0.000585	0.813	0.000466	0.648
2	0.844	0.000557	0.774	0.000496	0.690
1	0.950	0.000563	0.783	0.000280	0.389
B	1.000	(0.000560)			

Run E-7

B	0.000	0.01240	1.000	0.000262	0.0211
1	0.0527	0.01238	0.999	0.000330	0.0266
2	0.158	0.01226	0.990	0.000405	0.0327
3	0.263	0.01185	0.957	0.000506	0.0408
4	0.368	0.01175	0.948	0.000407	0.0328
5	0.474	0.01165	0.940		
6	0.578	0.01125	0.908	0.000417	0.0336
7	0.685	0.01132	0.915	0.000359	0.0289
8	0.788	0.01105	0.892	0.000281	0.0227
9	0.895	0.01056	0.852	0.000306	0.0247
T	1.000	0.01009	0.814		

TABLE XVII (Continued)

Run E-8

Sampling Position	Z	c_x	C_x	c_y	C_y
					(0.0325)
B	0.000	0.01180	1.000	0.000288	0.0244
1	0.053	0.01365	1.157	0.000381	0.0323
2	0.160	0.01181	1.000		
3	0.266	0.01180	1.000	0.000358	0.0303
4	0.373	0.01175	0.996	0.000296	0.0251
5	0.480	0.01127	0.955		
6	0.586	0.01140	0.967	0.000317	0.0269
7	0.692	0.01150	0.975	0.000247	0.0209
8	0.800			0.000280	0.0237
9	0.905	0.00963	0.816	0.000338	0.0288
T	1.000	0.00987	0.837		(0.0200)

TABLE XVIII

CALCULATED CONCENTRATION PROFILES, RUN E-6

Calculation Parameters

K	7.19	
E_c	1.67	(From Run T-18, no plate sealing)
P_yB	0.370	
F_x/F_y	9.11	
Λ	1.270	
D_b	0.30	

For Interface Mass Transfer			Miyauchi's Equation	
	$N_{ox} = 0.27$		$N_{ox} = 0.30$	
Z	C_x	C_y	C_x	C_y
0.0	0.954	1.810	0.978	2.04
0.2	0.920	1.502	0.936	1.70
0.4	0.871	1.061	0.896	1.31
0.6	0.842	0.825	0.850	0.870
0.8	0.797	0.382	0.803	0.404
1.0	0.774	0.0	0.780	0.0

TABLE XIX

CALCULATED CONCENTRATION PROFILES, RUN E-7

Calculation Parameters

K	0.139	
E_c	1.32	(From Run T-20, no plate sealing)
P_yB	27.0	
F_x/F_y	0.113	
Λ	0.802	
D_b	0.25	

For Interface Mass Transfer			Miyauchi's Equation	
	$N_{ox} = 0.23$		$N_{ox} = 0.23$	
Z	C_x	C_y	C_x	C_y
0.0	1.0	0.0225	1.0	0.0225
0.2	0.966	0.0195	0.966	0.0195
0.4	0.924	0.0148	0.924	0.0148
0.6	0.887	0.0106	0.887	0.0106
0.8	0.850	0.0064	0.850	0.0064
1.0	0.812	0.0023	0.812	0.0023

TABLE XX

CALCULATED CONCENTRATION PROFILES, RUN E-8

Calculated Parameters

K	0.139
E_c	2.12* (From Figure 16, no plate sealing)
P_yB	4.22
F_x/F_y	0.137
Λ	0.852
D_b	0.21

For Interface Mass Transfer			Miyauchi's Equation	
	$N_{ox} = 0.29$		$N_{ox} = 0.26$	
Z	C_x	C_y	C_x	C_y
0.0	1.00	0.0322	1.000	0.0250
0.2	0.954	0.0308	0.950	0.0227
0.4	0.910	0.0265	0.920	0.0209
0.6	0.873	0.0236	0.880	0.0162
0.8	0.840	0.0181	0.842	0.0130
1.0	0.794	0.0135	0.796	0.0065

*The backmixing run at similar operating conditions, T-19, was in the mixer-settler region of operation where plate sealing was prevalent, $E_c = 1.27$.

TABLE XXI

OPERATING DATA FOR THE TOLUENE-ACETIC ACID-WATER SYSTEM

Operating Conditions

Run Number	E-3	E-4	E-5
f	110	24.3	199
$2V_p$	2470	545	4460
G	450	450	450
L	50.0	52	53
G + L	500	502	503
G/L	9.00	8.65	8.50
F_h	0.050	0.115	0.060
L', cm.	48.3	49.5	47.6

Calculated Data

R/E	7.30	8.26	8.19
F_y	0.051	0.045	0.045
L'	61.6	54.5	55.0
% error	-18.8	-4.60	-3.64

TABLE XXII

EXPERIMENTAL CONCENTRATION PROFILE

DATA FOR THE TOLUENE-ACETIC

ACID-WATER SYSTEM

Run E-3

Sampling Position	Z	c_x	C_x	c_y	C_y
B	0.000	0.03000	1.000	0.1670	5.56
1	0.0527	0.02480	0.826	0.1681	5.61
2	0.158	0.01970	0.656		
3	0.263	0.01770	0.590	0.1642	5.47
4	0.369				
5	0.474	0.02430	0.810	0.1382	4.61
6	0.580				
7	0.685	0.00821	0.276	0.1182	3.94
8	0.790				
9	0.895	0.00674	0.225	0.0946	3.15
T	1.000	0.00716	0.239	(0.0827)	(2.76)

Run E-5

B	0.000	0.0283	1.000	0.1690	5.96
1	0.053	0.0221	0.780	0.1640	5.78
2	0.160	0.0163	0.575	0.1682	5.94
3	0.267	0.0157	0.555		
4	0.374	0.01342	0.473	0.1550	5.49
5	0.480	0.01075	0.380		
6	0.586	0.01085	0.383	0.1420	5.01
7	0.693	0.00985	0.344	0.1320	4.67
8	0.800	0.00590	0.208	0.1155	4.08
9	0.907	0.00845	0.299	0.1132	4.00
T	1.000	0.00765	0.270	(0.1040)	(3.68)

TABLE XXII (continued)

Run E-4

Sampling Position	Z	c_x	C_x	Z	c_y	C_y
B	0.000	0.0302	1.000	0.00	0.1940	6.42
1	0.103	0.0156	0.516			
2				0.154	0.1830	6.06
3	0.308	0.0128	0.424	0.256	0.1582	5.24
4						
5	0.513	0.00785	0.260	0.461	0.1175	3.89
6	0.615	0.01375	0.455			
7	0.717	0.00861	0.285	0.666	0.0773	2.56
8	0.820	0.00567	0.094			
9	0.922	0.00286	0.094	0.872	0.0294	0.974
T	1.000	0.00674	0.223	1.000	(0.000)	(0.000)

TABLE XXIII

CALCULATED CONCENTRATION PROFILES, RUN E-3

Calculated Parameters

K	76.52	
q	0.048	
E_c	1.74	(From Run T-17, no plate sealing)
P_yB	1.408	
F_x/F_y	7.30	
Λ	0.442	
D_b	0.38	

For Interface Mass Transfer			Miyauchi's Equation	
	$N_{ox} = 2.13$		$N_{ox} = 2.13$	
Z	C_x	C_y	C_x	C_y
0.0	1.000	5.60	1.000	5.60
0.1	0.855	5.53	0.855	5.53
0.2	0.734	5.37	0.734	5.37
0.4	0.553	4.75	0.553	4.75
0.6	0.419	4.03	0.419	4.03
0.8	0.317	3.29	0.317	3.29
1.0	0.235	2.55	0.235	2.55

TABLE XXIV

CALCULATED CONCENTRATION PROFILES, RUN-4

Calculated Parameters

K	25.0	
E_c	0.141	(From Run T-25, no plate sealing)
P_yB	15.80	
F_x/F_y	8.26	
λ	0.331	
D_b	0.51	

For Interface Mass Transfer

N_{ox} = 1.86

Z	C_x	C_y
0.0	1.000	6.48
0.05	0.935	6.30
0.1	0.873	6.15
0.2	0.762	5.05
0.4	0.578	3.43
0.6	0.432	2.11
0.8	0.317	1.08
1.0	0.226	0.27

Miyauchi's Equation

N_{ox} = 1.86

C_x	C_y
1.000	6.48
0.935	6.30
0.873	6.15
0.762	5.05
0.578	3.43
0.432	2.11
0.317	1.08
0.226	0.27

TABLE XXV

CALCULATED CONCENTRATION PROFILES RUN E-5

Calculated Parameters

K	16.52	
q	0.048	
E_c	1.36	(From Run T-26, with plate sealing)
P_yB	1.59	
E_c	2.80	(From Figure 15, no plate sealing)
P_yB	0.765	
F_y/F_x	8.19	
Λ	0.495	
D_b	0.33	

For Interface Mass Transfer and for Miyauchi's Equations

	With Plate Sealing		Without Plate Sealing	
	N_{ox} = 1.90		N_{ox} = 2.36	
Z	C_x	C_y	C_x	C_y
0.0	1.000	5.96	1.000	6.11
0.1	0.870	5.87	0.852	6.05
0.2	0.762	5.68	0.731	5.90
0.4	0.591	4.95	0.552	5.56
0.6	0.461	4.20	0.433	5.08
0.8	0.353	3.35	0.330	4.60
1.0	0.266	2.55	0.273	4.02

TABLE XXVI

PULSE COLUMN STABILITY DATA

Effluent Stream Concentrations

Run E-10 Time, min.	c_{xi} lb. moles./ft.^{3}	c_{yo} lb. moles./ft.^{3}
0	0.0	0.0
7	0.0083	0.0254
14	0.0099	0.0824
23	0.0100	0.0344
56	0.0094	0.0341
65	0.0095	0.0338
Run E-11		
0	0.0	0.0
1	0.0044	0.0
10	0.0113	0.0346
20	0.0123	0.0356
30	0.0129	0.0363
41	0.0122	0.0364
60	0.0115	0.0375
Run E-12		
0	0.0	0.0
2	0.0015	0.0019
9	0.0108	0.0501
24	0.0116	0.0510
39	0.0112	0.0473
52	0.0104	0.0448
64	0.0101	0.0422

APPENDIX D

SAMPLE CALCULATIONS

SAMPLE CALCULATION

Estimation of Average Droplet Diameter, Run E-12

Initial Calculation

X Measured Droplet Diameter, mm.	f Frequency of Occurrence	fX^3
1	26	26
2	16	128
3	15	404
4	12	767
5	9	1130
6	2	432
7	2	694
8	0	0
	82	3581

$$\bar{x} = (\Sigma fX^3/\Sigma f)^{1/3} = (3581/82)^{1/3} = 3.52 \text{ mm.}$$

Correction for Photograph Enlargement

1/16 inch rod = 2.5 mm., 0.0250 in./mm.

2.33 inch column = 92 mm., 0.0253 in./mm.

$D_b = (3.53 \text{ mm.})(0.0251 \text{ in./mm.})(2.54 \text{ cm./in.}) = 0.22 \text{ cm.}$

PLATE II. DISPERSED PHASE DROPLETS, TYPICAL PHOTOGRAPH

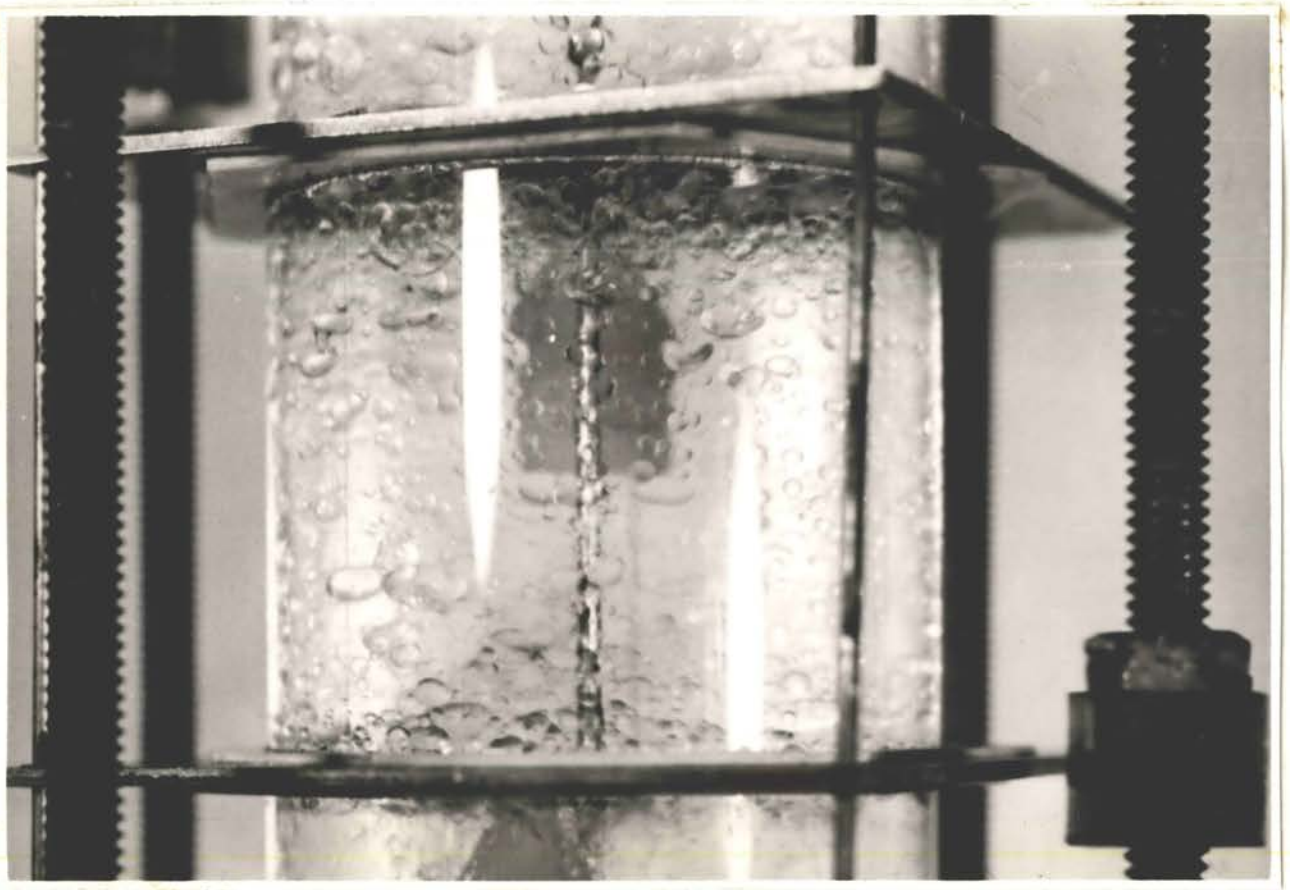

SAMPLE CALCULATION

Calculation of the Eddy Diffusion Coefficient

For run number T-19, the following tracer concentration profile data were obtained.

z cm.	c/c_o
0	1.00
5	0.416
10	0.184
15	0.0923
20	0.0404
25	0.0147

Also $F_y = L/A = (250 \text{ cm.}^3/\text{min.})(\text{min.}/60 \text{ sec.})[1/\pi(2.54)^2 \text{ cm.}^2]$

$= 0.206 \text{ cm.}^3/\text{sec. cm.}^2$

Equation (3) may be written

$$Y = bX + a$$

where $Y = \ln c/c_o$

$b = -F_y/E_c$

$X = z$

$a = B$

The "method of least squares" calculation technique of Snedecor (35) is given below.

$\Sigma X = 75$	$\Sigma Y = -12.2699$	$n = 6$
$\bar{x} = 12.5$	$\bar{y} = 2.0450$	
$\Sigma X^2 = 1375$	$\Sigma Y^2 = 36.7177$	$XY = -224.5135$
$(\Sigma X)^2/n = 937.5$	$(\Sigma Y)^2/n = 25.0921$	$(\Sigma X \Sigma Y)/n = -153.3738$
$\Sigma x^2 = 437.5$	$\Sigma y^2 = 11.6276$	$\Sigma xy = -71.1397$

$$b = \sum xy / \Sigma x^2 = -0.1626$$

$$a = \bar{y} - b\bar{x} = 0.0025$$

Thus $E_c = -F_y/b = -(0.206)/(-0.1262) = 1.27$

and $B = 1.00$

SAMPLE CALCULATION

Calculation of the Concentration Profiles During Extraction

The following calculations are for run E-9 for the case of interface mass transfer but for no plate sealing. The calculation parameters are given in Table XII and the applicable equations are given in Chapter III. The raffinate phase is assumed to be in slug flow and the extract (continuous) phase is undergoing a finite amount of backmixing. Values of N_{ox} will be assumed and values of ϕ_1 will be calculated until ϕ_1-calculated approximates ϕ_1-experimental (0.194).

Assume $N_{ox} = 6.14$

$$h = N_{ox} \neq P_y B = 6.14 \neq 1.66 = 7.80$$

$$k = N_{ox} P_y B (1 - \Lambda) = (6.14)(1.66)(1 - 0.51) = 4.99$$

$$\lambda_2 = -(h/2) \neq \sqrt{(h/2)^2 - k} = -3.90 \neq \sqrt{15.21 - 4.99} = -0.70$$

$$\lambda_3 = -(h/2) - \sqrt{(h/2)^2 - k} = -3.90 - 3.20 = -7.10$$

$$h_2 = 1 - \lambda_2/N_{ox} = 1 - (-0.70/6.14) = 0.886$$

$$h_3 = 1 \neq \lambda_3/N_{ox} = 1 \neq (-7.10/6.14) = -0.158$$

$$D_{H2} = h_3 \lambda_3 = (-0.158)(-7.10) = 1.121$$

$$D_{H3} = -h_2 \lambda_2 = -(0.886)(-0.70) = 0.620$$

$$J' = \pi N_{ox} \Lambda D_b / 3\sqrt{3} F_h L' = \pi(6.14)(0.51)(0.21) / 3\sqrt{3} (0.03)(48.3)$$
$$= 0.273$$

$$D_{H1} = -\left[D_{H3}\ (1-\lambda_3/P_yB)e^{\lambda 3}\ h_3 + D_{H3}\ J'\ (1-h_3)e^{\lambda 3}\right] -$$

$$\left[D_{H2}\ (1-\lambda_2/P_yB)e^{\lambda 2}\ h_2 - D_{H2}\ J'\ (1-h_2)e^{\lambda 2}\right]$$

$$= -\left[(0.620)(1+7.10/1.66)(0.008)(-0.158) + (0.620)(0.273)(1.158)(0.0008)\right] - \left[(1.121)(1-0.422)(0.497)(0.886) - (1.121)(0.273)(0.114)(0.497)\right] = -0.269$$

$$D_H = D_{H1} + D_{H2} + D_{H3} = -0.269 + 1.121 + 0.620 = 1.472$$

$$\phi_1 = H_1 + H_2e^{\lambda 2Z} + H_3e^{\lambda 3Z}$$

$$= (1/1.472)\left[-0.269 + (1.121)(0.497) + (0.620)(0.0008)\right] = 0.195$$

$$C_{x1} = \phi_1 = 0.195$$

$$\Upsilon_1 = H_1 + h_2\ H_2e^{\lambda 2Z} + h_3\ H_3e^{\lambda 3Z}$$

$$= (1/1.472)\left[-0.269 + (0.886)(1.121)(0.497) + (-0.158)(0.620)(0.0008)\right] = 0.154$$

$$C_{y1} = \Upsilon_1\ K = (0.154)(1.923) = 0.296$$

At other values of Z, we have

Z	$\phi = C_x$	Υ	C_y
0.0	1.000	0.423	0.814
0.1	0.737	0.416	0.802
0.2	0.588	0.387	0.745
0.4	0.417	0.325	0.625
0.6	0.322	0.259	0.498
0.8	0.253	0.202	0.389
1.0	0.195	0.154	0.295

VITA

Bill Edward Claybaugh

Candidate for the Degree of

Doctor of Philosophy

Thesis: EFFECTS OF BACKMIXING ON CONCENTRATION PROFILES IN A PULSE COLUMN

Major Field: Chemical Engineering

Biographical:

Personal data: Born in Tulsa, Oklahoma, August 10, 1931, the son of Charles E. and Ruth D. Claybaugh; married to Marian R. Brandon, Garber, Oklahoma, in May, 1952; two daughters, Jeanette R. and Louise A.

Education: Attended grade and high schools in Tulsa, Oklahoma; graduated from Tulsa Will Rogers High School in May, 1949; attended the University of Tulsa, Tulsa Oklahoma, 1949 to 1953; received the degree of Bachelor of Science in Petroleum Engineering, June 1, 1953; attended Oklahoma State University, Stillwater, Oklahoma, 1957 to 1960; received the degree of Master of Science in Chemical Engineering, August, 1959; completed the requirements for the Doctor of Philosophy degree in August, 1961.

Professional experience: Employed as a Chemical Engineer with Continental Oil Company, Research and Development Department, 1953; served two years as an Armament Officer, United States Air Force, 1954 to 1956; employed as a Teaching Assistant, Chemical Engineering Department, Oklahoma State University, during the 1957-1958 school year; presently employed by Humble Oil and Refining Company, Research and Development Department, Baytown, Texas.

Professional societies: Associate Member, American Institute of Chemical Engineers.